

Anette Vartdal

Modelling of a Combined Infiltration and Detention Solution with Investigation of System Performance

Master's thesis in Civil and Environmental Engineering

Supervisor: Tone Merete Muthanna

Co-supervisor: Birgitte Gisvold Johannessen

June 2021

Anette Vartdal

Modelling of a Combined Infiltration and Detention Solution with Investigation of System Performance

Master's thesis in Civil and Environmental Engineering
Supervisor: Tone Merete Muthanna
Co-supervisor: Birgitte Gisvold Johannessen
June 2021

Norwegian University of Science and Technology
Faculty of Engineering
Department of Civil and Environmental Engineering



Abstract

Population growth and urbanization in combination with global warming are driving factors for the development of a new mindset within the field of stormwater management. The existing conventional drainage systems are inadequate in handling the expected increased stormwater amounts, potentially resulting in combined sewer overflows (CSOs) and urban flooding. Low impact developments (LIDs) have gained increased attention as they are found to restore pre-developed hydrological processes by delaying and reducing the stormwater peak flows. However, LIDs are found not to be sufficient in handling the largest precipitation events. To create a stormwater management solution adequate in handling all storm events, and at the same time have a resilience factor against global warming and urbanization, the phenomenon of combining LIDs and conventional detention-based solution has risen. However, knowledge in regard to the long-term performance of combined systems is lacking.

This master thesis studied the performance of a full-scale combined infiltration and detention solution in the city center of Trondheim, Norway. A model of the stormwater facility was developed in SWMM, including the sub-catchments draining to the upstream storm inlets. Further, the developed SWMM model evaluated through calibration and validation using Nash-Sutcliffe Efficiency (NSE). Based on the calibrated model, five model scenarios were created to assess the performance of the combined system against the performance of infiltration and detention in separate processes. Both event-based and long-term continuous simulations were run on the model scenarios. The long-term simulations of the scenarios were investigated using flow duration curves (FDCs).

The event-based simulations showed the interaction between infiltration and detention. The infiltration process showed to retain stormwater, hence delaying the start of outflow generation until infiltration capacity was reached. Exceeded infiltration capacity led to activation of the detention basins, which ensured the release of stormwater at a lower rate over a longer time span. The FDCs for long-term simulations showed that the combined system of infiltration and detention was a successful implementation as it benefited from both processes. Detention ensured reduction of peak outflow, and infiltration ensured reduction of time generating outflow. Implementation of the combined system reduced peak outflow with 45.6% and 37.4% for respectively without and with climate factor. Further, the number of hours simulating outflow was reduced with 99.96% and 99.91% for respectively without and with climate factor.

Combined stormwater systems are not yet widely implemented, especially combinations using infiltration pipes. A design guideline regarding infiltration pipe design was created based on the developed SWMM model to increase the applicability of combined stormwater systems for municipalities and consultants. This thesis concludes that combining infiltration and detention is a successful modern stormwater management strategy as it increases the resilience against global warming and urbanization by reducing peak outflow and outflow duration.

Preface

This thesis is performed as a part of the Civil and Environmental Engineering program at the Norwegian University of Science and Technology (NTNU). Further, is the thesis the final product of the course TVM4905 Water Supply and Wastewater Systems, Master's Thesis. The master's thesis is based on preliminary work done by Sagli (2020) and my student thesis, "Performance of combined infiltration and detention solution with measurement uncertainty analysis" (Vartdal 2020).

This master's thesis revolves around modelling and investing the performance of a full-scale combined infiltration and detention system located in the city center of Trondheim, Norway. To develop the model, SWMM was used for modelling and ArcMap for input generation. New knowledge was required to get familiar with both programs. The thesis is performed in cooperation with Trondheim Municipality, which assisted with supervision, data, and materials.

I would like to thank my supervisor, Professor Tone Merete Muthanna, for all guidance, inspiring conversations, and suggestions through the process of model development and writing process. Further, I want to thank my secondary supervisor Birgitte Gisvold Johannessen at Trondheim Municipality for all helpful advice and answers to my questions regarding the stormwater facility. Further, for all the great assistance during fieldwork and data collection.

Lastly, I would also like to thank the following:

- PhD candidate at NTNU, Elhadi Mohsen Hassan Abdalla, for learning and assisting me with programming in R.
- PhD candidate at NTNU, Vincent Ponds, for interesting discussion of model development in SWMM.
- Trondheim Bydrift, for assistance during fieldwork.
- Bendik Øverhus Hassel at Trondheim Municipality for advice on GIS functions.
- Klima 2050, for the opportunity to write this thesis on one of your pilot projects.

Trondheim, June 16th, 2021



Anette Vartdal

Table of Contents

List of Figures	xii
List of Tables	xiii
List of Abbreviations	xiv
1 Introduction	1
1.1 Description and objectives of thesis	3
1.2 Structure of thesis	3
2 Background theory	4
2.1.1 Modern stormwater management	4
2.1.2 Retrofitting of stormwater structures	5
2.1.3 Stormwater modelling.....	6
2.1.4 Calibration and validation of models	9
3 Methodology.....	11
3.1 Study area, stormwater pilot and data collection.....	11
3.1.1 Site description.....	11
3.1.2 Stormwater pilot description.....	13
3.1.3 Data collection	14
3.2 Analysis of Digital Elevation Model (DEM) in ArcMap	17
3.2.1 Procedure for sub-catchment delineation.....	18
3.2.2 Sub-catchment attributes for SWMM input.....	21
3.3 Model setup in SWMM	23
3.3.1 Sub-catchments	24
3.3.2 Drainage system.....	25
3.3.3 Detention basins.....	26
3.3.4 Infiltration pipes.....	27
3.3.5 Trench and native soil.....	30
3.3.6 Swirl chamber	32
3.3.7 Model simulation settings	34
3.4 Calibration and Validation.....	34
3.4.1 Defining calibration and validation periods.....	35
3.4.2 Parameter calibration for the sub-catchments.....	35
3.4.3 Parameter calibration for the stormwater pilot	37
3.5 Performed simulations for combined system evaluation.....	38

3.5.1	Developed simulation scenarios	38
3.5.2	Event-based simulations	40
3.5.3	Long-term simulations	41
4	Results and discussion	43
4.1	Calibration	43
4.2	Validation	46
4.3	Evaluation of design precipitation events.....	47
4.4	Evaluation of long-term system performance	51
4.4.1	Detention basins activations	51
4.4.2	Evaluation of combining infiltration and detention	53
4.4.3	Threshold for system outflow	57
4.5	Design guideline for design exfiltration flow	60
5	Conclusion.....	63
5.1	Further work	64
	References	65
	Appendices	71

List of Figures

Figure 1: The change in hydrology as a consequence of urbanization turning previous area into impervious (FISRWG, 1998).....	1
Figure 2: An illustration of the stormwater 3-step-approach inspired by Lindholm et al. (2008, pp. 37) modified by the author.	4
Figure 3: Illustration of the ESS (Li et al., 2015).....	6
Figure 4: Illustration of a black-box model transforming input to output (Killingtveit et al., 1995).....	7
Figure 5: Model classification depending on randomness, spatial variation, and time variation (Killingtveit et al., 1995).	8
Figure 6: The location of stormwater facility showed on the orthophoto of the city square received by Trondheim Municipality. The air photo of Trondheim city center is from (Kartverket 2021).	12
Figure 7: Photo of a part of a long gutter stretching across the square.	13
Figure 8: Flow chart of the combined infiltration and detention solution inspired by Sagli (2020), modified by the author. Water depth in manhole x is given as y_x . IC is infiltration capacity in native soil.	14
Figure 9: Visualisation of a) installation of the tipping bucket and the logger on the roof of Trondheim Torg and b) location of the precipitation station in relation to the stormwater facility.....	17
Figure 10: The steps of sub-catchment delineation in ArcMap. The following figures show a) orthophoto of the city square, b) DEM of the city square, c) Modified DEM, d) surface runoff stream lines, e) polygons of the drainage inlets for subcatchment delineation and f) sub-catchments draining to stormwater facility and flowerbeds.....	19
Figure 11: Visualization and numeration of the generated sub-catchments draining to the stormwater facility through drainage inlets.....	21
Figure 12: Developed SWMM model.	23
Figure 13: Sketch of the cross-section of the trench with the three detention basins and infiltration pipes inspired by dimensional drawing developed by Multiconsult, Appendix 2. Dimensions are given in mm.....	26
Figure 14: Sketch of one detention basin with sloped sides in lower half assumed to be cords, inspired by the drawing developed by Multiconsult, Appendix 2.	27
Figure 15: Sketch of the cross-section of one of the perforated pipes illustrating the locations of the perforation. Diameters given in m.	28
Figure 16: A sketch of the trench cross-section inspired by the dimensional drawing by Multiconsult (2018), Appendix 2. All dimensions given in mm.	30
Figure 17: A sketch illustrating the trench where the chosen water depths for surface area calculation are highlighted as red dotted lines. The sketch is inspired by the drawing by Multiconsult (2018), Appendix 2.	31
Figure 18: Rating curve uploaded to SWMM simulating the characteristics of the installed swirl chamber.	33
Figure 19: The developed model scenarios, a) scenario 0, b) originally combined infiltration and detention, c) only detention, d) only infiltration and, e) half exfiltration capacity.	40

Figure 20: Result of calibration against observed outflow. Observed outflow in green and simulated outflow from calibrated model in dotted red plotted against the left axis. Precipitation in blue plotted against the right axis.	43
Figure 21: Result of validation period against observed outflow. Observed outflow in green and simulated outflow from calibrated model in dotted red plotted against the left axis. Precipitation in blue plotted against the right axis.	46
Figure 22: Simulated outflows for design events of a) 20-year return period with dry soil, b) 20-year return period with wet soil, c) 100-year return period with dry soil, d) 100-year return period with wet soil, e) 200-year return period with dry soil and f) 200-year return period with wet soil.	48
Figure 23: Water depths from result of continuous simulation in a) manhole O8 for simulation without climate factor, b) manhole O8 for simulation with climate factor, c) detention basin for simulation without climate factor and d) detention basin for simulation with climate factor.	52
Figure 24: Continuous simulated outflows from the swirl chamber for the five scenarios presented as flow duration curves for simulation a) without climate factor and b) with climate factor.....	54
Figure 25: Continuous simulated outflows from the swirl chamber for the five scenarios presented as flow duration curves compared with a threshold for pre-developed surface runoff for simulation a) without climate factor and b) with climate factor.....	58
Figure 26: Continuous simulated outflows from the swirl chamber for the five scenarios presented as flow duration curves compared with a threshold for downstream pump capacity for simulation a) without climate factor and b) with climate factor.....	59
Figure 27: Illustration of the three developed perforations alternatives used for guideline development.	62

List of Tables

Table 1: Comparison of stormwater models.	8
Table 2: Table describes where the sensors are located in the stormwater pilot and which parameters measured at each location are marked with ●.....	15
Table 3: Sub-catchment properties generated from ArcMap.	21
Table 4: Runoff coefficients suggestions from Trondheim municipality associated with different surface type (Trondheim Municipality, 2020).....	25
Table 5: The chosen five depth and their corresponding surface area [m2].	32
Table 6: The input parameters for sub-catchments set for calibration with corresponding calibration intervals and source.	36
Table 7: The input parameters for the stormwater pilot set for calibration with corresponding calibration intervals and source.	37
Table 8: Description of the fives developed model scenarios.....	39
Table 9: Overview of the performed event-based simulations. The model scenarios used for the stated simulations are marked with ●.....	41

Table 10: Overview of the performed long-term simulations. The model scenario used for the stated simulations are marked with ●.....	42
Table 11: Optimized parameter values for the calibrated parameters after calibration.	45
Table 12: Percent reduction in peak flow for the event-based simulations of scenarios compared to scenario 0.....	49
Table 13: Percent reduction in peak flow for the long-term simulations of scenarios compared to scenario 0.	55
Table 14: Percent reduction in hours simulating outflow for the long-term simulations of scenarios compared to scenario 0.....	55
Table 15: Percent reduction in the number of hours generating outflow above pre-developed threshold compared to scenario 0.....	58
Table 16: Percent reduction in the number of hours generating outflow above the pump capacity threshold compared to scenario 0.	59
Table 17: Developed design guideline relating design exfiltration flow to pipe lengths depending on the number of perforations per meter.	61

List of Abbreviations

BMP	Best Management Practice
CSO	Combined Sewer Overflow
DEM	Digital Elevation Model
FDC	Flow duration curve
GI	Green Infrastructure
GIS	Geographic Information System
IDF	Intensity-Duration-Frequency
ITAS	Scanmatic Instrument Technology AS
LID	Low impact development
MOUSE	Model of urban sewers
NSE	Nash-Sutcliffe Efficiency
PP	Polypropylene
RMSE	Root Mean Square Error
SUDS	Sustainable Urban Drainage System
SWMM	Storm Water Management Model

1 Introduction

Population growth and urbanization in combination with global warming are driving factors for the development of a new mindset within the field of stormwater management. The challenges revolve around the overload of the existing pipe networks and further the risk of flooding and combined sewer overflows (CSOs) (Stovin et al. 2012). Urbanization causes disturbance of the natural hydrological balance and hydrograph by turning the pervious area into impervious area (Wong and Eadie 2000). Consequently, precipitation occurring in urbanized areas is to a higher degree turned into direct runoff, whereas it would have been infiltrated in pre-developed areas, illustrated in Figure 1. Additional consequences of urban development are soil compaction reducing the infiltration rates, and reduction in groundwater recharge. The overall result is increased amounts and intensified stormwater runoff (Butler and Davies 2010; Chen et al. 2016; Wong and Eadie 2000). The occurrence of global warming is expected to increase both the intensity and frequency of high-intensity precipitation events. Further, is the total volume of annual precipitation expected to rise (Hirabayashi et al. 2013). The magnitude and intensity of stormwater amounts are further increased as global warming is combined with urbanization and population growth, enhancing the stress on the existing pipe networks (Wong and Eadie 2000).

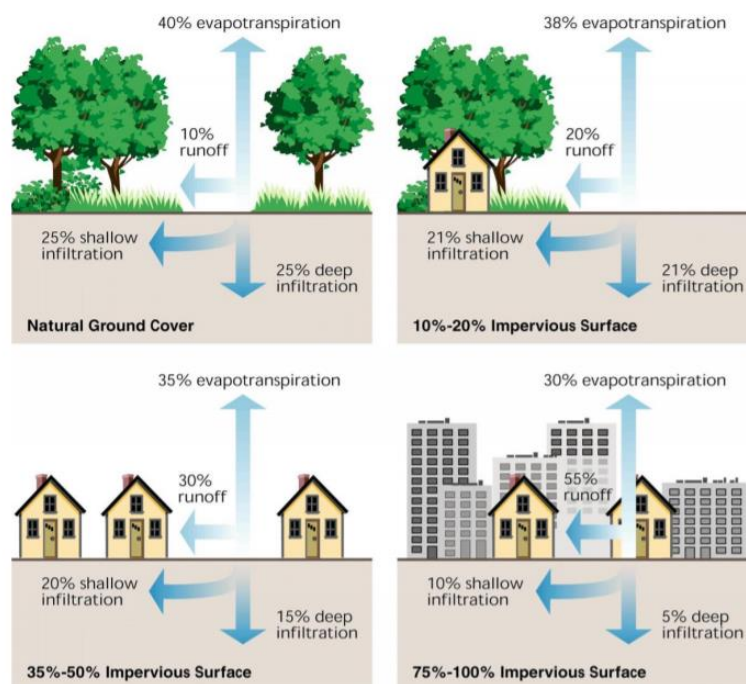


Figure 1: The change in hydrology as a consequence of urbanization turning previous area into impervious (FISRWG, 1998)

The existing pipe networks are based on conventional methods that aim to convey stormwater away for urban areas in the most effectively and safely way possible to avoid urban damages. However, the method of rapid conveyance in combination with urbanization and global warming strengthens the flow peaks even more (Wong and Eadie 2000). Therefore, it can be concluded that the conventional methods alone are not sustainable urban development, as they contain limitations regarding drainage capacity and lack of pollution control (Chen et al. 2016; Eckart et al. 2017). Hence, the need for a more sustainable approach in stormwater management has risen.

Nature-based solutions, decentralized designs and local handling of stormwater are put on the agenda with increased attention. These are measures aiming to locally reducing the stormwater amounts and increasing the runoff time. Multiple terms for nature-based solutions have been used in literature. Among them are Low Impact Development (LID), Green Infrastructure (GI) and Sustainable Urban Drainage System (SUDS) (Fletcher et al. 2015). In this thesis, the term LID will be the term describing nature-based solutions. Damodaram et al. (2010) described LIDs to have the goal to restore pre-developed hydrological functions through mimicking natural water cycles. LIDs typically include the processes of infiltration and evaporating. Among the developed LIDs are permeable pavements, infiltration trenches, bio-retention cells, and green roofs. Damodaram et al. (2010) found that LIDs perform efficiently for small precipitation events. However, for precipitation events of higher intensity, LIDs are not adequate in reducing the highest peaks. Nevertheless, conventional detention-based solutions are shown to perform well during high-intensity precipitation events. Combined solutions of LIDs and conventional detention-based solutions are suggested to achieve both resilience and flood control (Damodaram et al. 2010; Eckart et al. 2017; Kristvik et al. 2019; Xian et al. 2021).

Urbanization increases the radius around the city centers. Resulting in challenging and limited possibilities for stormwater management implementation in the city centers as most surface areas are developed. Projects mainly revolve around retrofitting existing stormwater structures and seldom developing new measures in pre-developed sites. Retrofitting projects are limited in terms of area and possibilities. Surface areas may already have needed functions, forcing the retrofitting to be implemented underground or to use creativity to create more surface area. Efficient retrofitting measures for implementing LIDs in urbanized cities are gaining increased focus. The concept “Sponge cities” was developed in China in 2015 with the aim to retrofit the existing drainage systems in developed cities with LIDs to increase resilience against urbanization (Li et al. 2017).

The development of combined solutions of LIDs and conventional measures through retrofitting is a relatively new phenomenon. Consequently, the performance of combined systems is not comprehensive evaluated, especially in regard of long-term. Stormwater modelling is a handy tool for performance prediction. Multiple stormwater models modelling of both conventional methods and LIDs are on the market (Elliott and Trowsdale 2007). The incorporation of models can enable the long-term evaluation of combined systems.

1.1 Description and objectives of thesis

A combined infiltration and detention stormwater solution has been built in the city center of Trondheim, Norway. The stormwater facility was built by Trondheim Municipality and constructed by Multiconsult. With the goal to monitor and assess the performance of the system, the stormwater facility has been established as a pilot project within Klima 2050 with Trondheim Municipality and Multiconsult as partners. Klima 2050 is a Centre for Research-based Innovation (SFI), aiming to reduce societal risks associated with climate change in Norway. Through collaboration with the public and private sector, novel pilot projects are being demonstrated in Norway (Klima 2050 n.d.).

The performance of combined stormwater management systems, as the combined infiltration and detention system, is valuable information for both municipalities and consultants regarding future projects and decision-making processes. With that in mind, the main objective of this thesis is to develop a model of the full-scale combined infiltration and detention solution located in the city center of Trondheim. Further, to evaluate the performance of the stormwater facility based on model simulations for both continuous and event-based time series. Especially are the interaction between the processes of infiltration and detention in the combined system compared to infiltration and detention as separate processes of interest. Furthermore, as combined stormwater management systems gain growing attention, a guideline demonstration in terms of design and applicability is relevant. Investigation of pollutant removal and sedimentation are not in the scope of this study.

To specify the aim of the thesis, the following objectives were stated:

1. How can the full-scale combined infiltration and detention solution be modelled in a suitable stormwater model? Verify the developed model against observed data.
2. How does the coupled infiltration-detention system perform during event-based and long-term continuous time series for current and future climate? Specifically investigating the robustness of each of the separate components (infiltration and detention) and the combined solution.
3. Based on the developed model, how can the applicability of coupled infiltration-detention systems be demonstrated in terms of design?

1.2 Structure of thesis

Background theory is present in Section 2 of modern stormwater management, retrofitting of stormwater management, stormwater modelling, and modelling calibration and validation. Section 3 is the methodology of the thesis, including system description, available data, work in ArcMap, model development in SWMM, the method for calibration and validation, and description of the performed model simulations. The results and discussion of model calibration and validation, and system performance and applicability are presented in Section 4. Lastly, the conclusion and further work stated in Section 5.

2 Background theory

2.1.1 Modern stormwater management

Modern stormwater management focuses on local handling of stormwater rather than effective conveyance from site. Due to urbanization and increased transformation of permeable areas to impermeable areas, the conventional management approach of fast conveyance through pipes experiences increased stress. Something leading to an increase in the frequency of CSO emissions into natural water resources. Local stormwater handling includes handling through natural processes as infiltration and runoff to open streams and dams. Depending on local climate and variations, the most suited stormwater management solutions should be implemented (Ødegaard et al. 2014:352).

The stormwater 3-step-approach is a modern stormwater strategy developed by Lindholm et al. (2008), shown in Figure 2. Depending on the magnitude of precipitation and generated stormwater amounts, the different steps are activated. The first step aims to manage stormwater from the most frequent precipitation events, < 20 mm, through retaining and infiltrating stormwater. For precipitation events larger than 20 mm but less than 40 mm, step one is no longer sufficient, and step two is activated. Step two manages stormwater by delaying and detaining the runoff. Step three is activated when the capacity of step one and two are exceeded. This is likely to occur during precipitation events of large magnitude, > 40 mm. The purpose of step three is to safely lead stormwater away by securing safe floodways (Lindholm et al. 2008:37; Ødegaard et al. 2014:353).

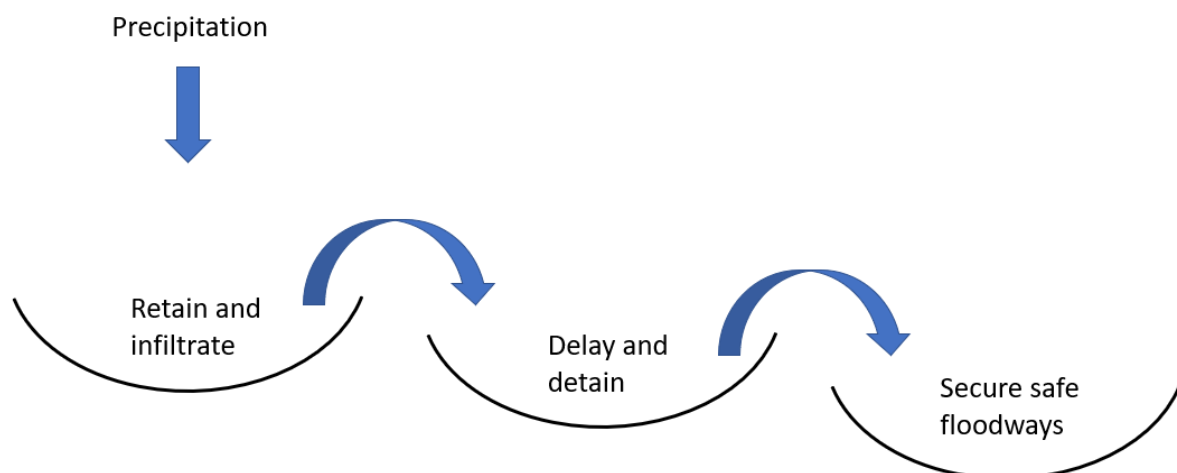


Figure 2: An illustration of the stormwater 3-step-approach inspired by Lindholm et al. (2008, pp. 37) modified by the author.

The most frequent occurring precipitation events are of lower intensity. Infiltration-based stormwater solutions are found to be most efficient for these frequent smaller precipitation events, whereas conventional detention-based solutions are most efficient for the larger storm events. The reduction in peak flow from infiltration-based solutions is higher during smaller

storm events compared to the reduction from conventional detention-based solution. During the larger storm events, the conventional detention-based solutions are proved to have a significantly higher reduction in peak flow compared to infiltration solutions (Damodaram et al. 2010; Xian et al. 2021). Even though infiltration solutions are not as efficient in reducing the peak flow from large storm events, they achieve to preserve the hydrograph and the timing of flows of a pre-developed system better than conventional detention-based solutions (Damodaram et al. 2010; Xian et al. 2021).

LIDs are found to reduce stormwater runoff and be a positive contribution to the urban environment (Semadeni-Davies et al. 2008). Combining multiple LIDs proved to be a more effective strategy in reducing peak flow for a wider range of precipitation events. However, the conventional urban drainage system cannot be substituted by LIDs, as LIDs alone are not sufficient in managing the largest precipitation events (Damodaram et al. 2010; Qin et al. 2013).

Xian et al. (2021) modelled a hypothetical study area in SWMM to evaluate the effectiveness of a LID, BMP (Best Management Practice), and the LID and BMP combined. The studied LID was a vegetative infiltration swale, whereas the BMP was a detention pond. The results indicated that both the LID and the BMP alone managed to reduce the peak flow, however, the combination of the two gave the highest reduction in peak flow. Implementing LID alone or in combination with a conventional detention measure showed to extend the time to peak flow occurrence. For simulations with wet soil, the time before peak flow occurrence was reduced for infiltration solutions, additionally an increase in the peak flow was observed (Xian et al. 2021). Combining LIDs with conventional detention-based solutions is found to reduce peak flow from both small and large precipitation events (Damodaram et al. 2010; Eckart et al. 2017; Kristvik et al. 2019; Xian et al. 2021).

2.1.2 Retrofitting of stormwater structures

The phenomenon of retrofitting has raised as the sufficiency of existing stormwater management decreases with increased urbanization and climate change. Especially in the city centers, there are limited surface areas available for new stormwater structures as most of the surface area is efficiently utilized. Kristvik et al. (2019) address that there is potential to increase the resilience against climate change by combining LIDs to existing conventional stormwater structures designed for the present climate. The approach can be converting an already existing rooftop to a green roof and combining it to an already existing downstream detention basin (Kristvik et al. 2019).

Kristvik et al. (2019) investigated LID performance in three cities in Norway (Oslo, Bergen, and Trondheim) under the effect of developed IDF-curves (Intensity-Duration-Frequency-curves) describing future precipitation based on temporal downscaling. The investigated LIDs were green roofs, bioretention cells, and detention basins. By combining detention basin with green roof or bioretention cell, the required detention basin volume was reduced. Further, combining detention basin in a series with both green roof and bioretention cell, the required volume was even more reduced. In the study case in Trondheim, the required detention basin volume was equal to zero when combined with both green roof and bioretention cell. Studying scenarios of detention basin performance alone, it was found that all future scenarios gave an

increase in required detention basin volumes. For the maximum future scenario in Trondheim the required detention volume increased by 100% (Kristvik et al. 2019).

In conjunction with a road reconstruction in the City of Etobicoke, Canada, in 1993, a LID technology was implemented as a retrofitting measure called the Etobicoke Exfiltration System (EES). The aim was to restore the natural hydrological cycle in an urbanized area. Hence, two perforated pipes with a diameter equal to 200 mm were installed below the conventional storm sewer. The two perforated pipes exfiltrate stormwater to the trench, and further to the surrounding native soil, creating reproduction of infiltration and groundwater recharge. Further, as system inflow exceeds the exfiltration rate the conventional storm sewer is activated. The built system is illustrated in Figure 3. ESS showed to reduce both the runoff volumes and peak flow, and for small and medium precipitation events EES was found to exfiltrate most of the incoming water (Li et al. 2015).

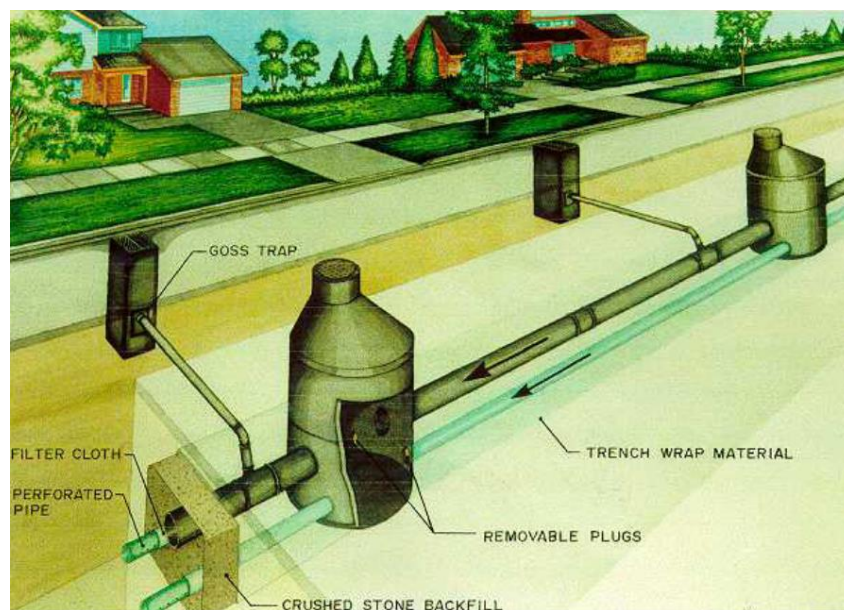


Figure 3: Illustration of the ESS (Li et al., 2015).

Liu (2016) and McBean et al. (2019) both modelled EES in SWMM and achieved a reduction in the outflow of respectively 77% and 71%. Retrofitting with EES is relevant in urbanized areas as it does not require surface area. Additionally, it utilizes the already existing trench by using the voids between the crushed stones as storage volume (McBean et al. 2019).

Modelling of retrofitting existing drainage systems with LID implementation was also performed by Stovin et al. (2012). By implementing LIDs on surface area and combining them with existing drainage systems in London the number of CSOs was reduced, and in some cases eliminated (Stovin et al. 2012).

2.1.3 Stormwater modelling

Modelling is a simplification and an approximation of reality. The benefit of modelling is to analyze operations and predict the performance of modelled systems. Models have a structure of equations that links input and output together, where input and output are measurable variables (Chow et al. 1988). Models that simply find the regression between input and output

data are known as black-box models, shown in Figure 4. In modelling of complex systems as the hydrological cycle, the system can be assumed to have simplified subsystems. Where the full system can be analyzed by the combined result of the separately treated subsystems. These models are called conceptual models and represent the modelled system in a mathematical form.

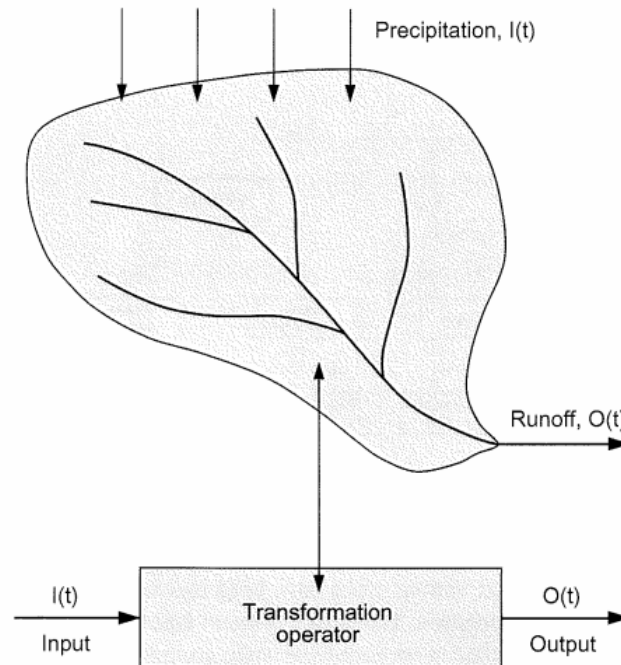


Figure 4: Illustration of a black-box model transforming input to output (Killingtveit et al., 1995).

Depending on how the models are built, they can be categorized. Three main categories are randomness, spatial variation, and time variability. The system classification is shown in Figure 5. Randomness is defined by whether the model is deterministic or stochastic. A deterministic model does always produce the same output for a given input, hence deterministic models do not consider randomness. Stochastic models on the other hand consider randomness as multiple output generations from a given input are not identical.

Models can further be categorized depending on the spatial variation into lumped, semi-distributed, and distributed. In a lumped model, the system is spatially averaged, hence it does not consider spatial variability, resulting in a less complex model requiring less input data. In contrast, does distributed models include spatial variability at various points in space, often in the form of cells or regions. A semi-distributed model is a combination of lumped and distributed models. It offers subsystems for modelling spatial variability, but where each subsystem is a lumped system.

The last criteria consider time variability. In deterministic models, it is defined as steady flow or unsteady flow depending on whether the flow, respectively, varies with time or not. For stochastic models, it is expressed as time-independent or time-correlated. In a time-independent model, the different events do not influence each other. While the presented result in a time-correlated model is influenced by the previous one (Chow et al. 1988; Killingtveit et al. 1995).

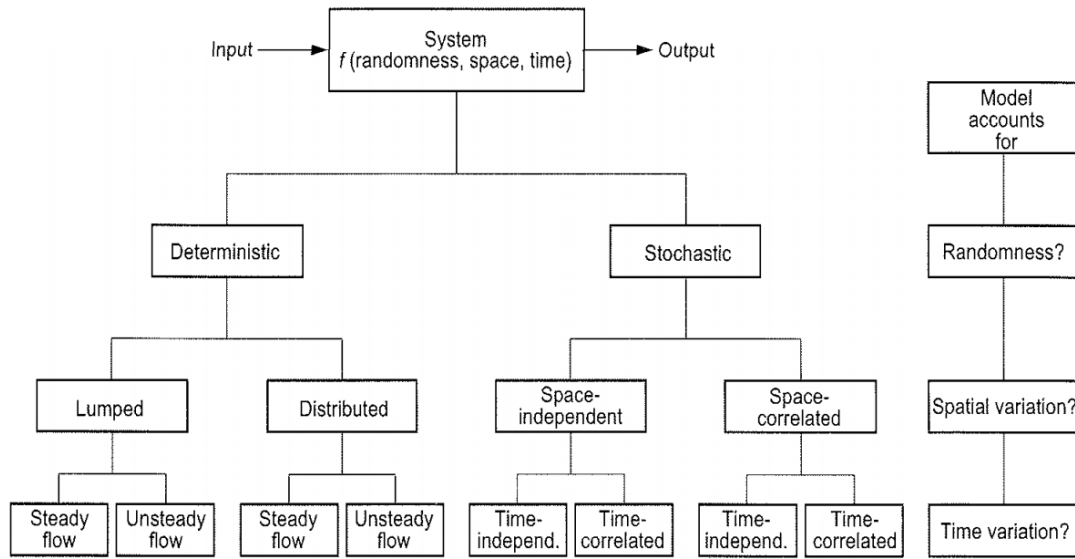


Figure 5: Model classification depending on randomness, spatial variation, and time variation (Killingtveit et al., 1995).

Stormwater and hydrological models are often precipitation-runoff models. These are models receiving precipitation data as input and generating runoff as output. In the field of stormwater modelling there are many models on the market. Multiple of these combines hydrological modelling of runoff generation from catchments with hydraulic modelling through stormwater structures. This combination is essential for stormwater modeling in urban areas. The characteristics of surfaces in urban areas have different properties than of pre-developed areas. Stormwater structures as drainage inlets in urban areas change the flow accumulation compared to pre-developed areas.

Table 1: Comparison of stormwater models.

Model	Primary function	Developer	Open-source?
MIKE Urban	Modeling of water distribution systems and collection systems for stormwater and sewer.	DHI (DHI Inc. 2017a)	No
MOUSE (Model of urban sewers)	Detailed modelling of urban drainage.	DHI (DHI Inc. 2017b)	No
SWMM (Storm Water Management Model)	Dynamic rainfall-modelling of event or continuous simulation of runoff quality and quantity in urban areas.	U.S. EPA (Rossman 2015)	Yes

SWMM, MIKE Urban, and MOUSE are well-known stormwater models. An overview of the three models is shown in Table 1. The three stormwater models are deterministic models with semi-distributed spatial variation. It is possible to model the combination of catchments and drainage systems where stormwater runoff from catchments enters stormwater drainage systems using each of the three models. Hence, they are all suitable for modelling the combined infiltration and detention solution in this thesis. MIKE Urban is a model based on SWMM and MOUSE (DHI Inc. 2017a). Consequently, do the three models contain similar characteristics. SWMM is the chosen stormwater model for this thesis as it is a widely used stormwater model (Elliott and Trowsdale 2007), additionally, since it has been used for modelling of similar retrofitting systems containing exfiltration (Liu 2016; McBean et al. 2019). Additionally, SWMM is the only one of the three models that is an open-source software, which is beneficial.

2.1.4 Calibration and validation of models

The process of model calibration is the process of aiming to increase the agreement between the observed data and the simulated output from a model. Model calibration is performed by comparing the observed data to simulated outputs computed using multiple sets of input parameter values. The objective is to find the set of input parameter values that gives a simulated output as close as possible to the observed data (Killingtveit et al. 1995:114). Calibration can be performed through trial and error and automatic optimization. The method of trial and error depends on manually testing different values for the input parameters. This is a subjective method enabling the modeler to address for subjective observations from the field or by visually comparing the observed against the simulated data. The method of automatic optimization is a mathematical method aiming to minimize the difference between the observed and simulated data. Objective functions are used in automatic optimization. Objective functions are functions describing the goodness-of-fit between the measured data and the simulated output from the model (Dongquan et al. 2009). There exist multiple objective functions, among them are root mean square error (RMSE), the coefficient of determination R^2 , and Nash-Sutcliffe Efficiency (NSE).

The formula of RMSE is shown in Equation (1). A RMSE equal to 0 indicates a perfect fit. Further, is R^2 given in Equation (2), and ranges from 0 to 1 where a R^2 closer to 1 indicates a better agreement between observed and simulated (Legates and McCabe 1999). Nash-Sutcliffe Efficiency (NSE) is an objective function defined in Equation (3) (Nash and Sutcliffe 1970). The NSE can range between $-\infty$ to +1, where +1 describes perfect fit. A NSE below zero indicates that the mean of the observed data is a better estimate than the simulated data. The Nash-Sutcliffe Efficiency is sensitive to extreme data, and is likely to overestimate peaks and underestimate lower values (Krause et al. 2005). Dongquan et al. (2009) found that a NSE above 0.5 indicates an acceptable model performance.

$$RMSE = \sqrt{\frac{1}{n} \sum_{i=1}^n (Q_{sim,i} - Q_{obs,i})^2} \quad (1)$$

$$R^2 = \left\{ \frac{\sum_{i=1}^n (Q_{obs,i} - \bar{Q}_{obs})(Q_{sim,i} - \bar{Q}_{sim})}{\sqrt{\sum_{i=1}^n (Q_{obs,i} - \bar{Q}_{obs})^2} \sqrt{\sum_{i=1}^n (Q_{sim,i} - \bar{Q}_{sim})^2}} \right\}^2 \quad (2)$$

$$NSE = 1 - \frac{\sum_{i=1}^n (Q_{sim,i} - Q_{obs,i})^2}{\sum_{i=1}^n (Q_{obs,i} - \bar{Q}_{obs})^2} \quad (3)$$

Where,

$Q_{sim,i}$ = Simulated discharge [l/s] at time step i

$Q_{obs,i}$ = Observed discharge [l/s] at time step i

\bar{Q}_{obs} = The mean of the observed discharge [l/s]

\bar{Q}_{sim} = The mean of the simulated discharge [l/s]

n = Total number of timesteps

RMSE = Root Mean Square Error

R² = Coefficient of determination

NSE = Nash Sutcliffe Efficiency

Equifinality is a term describing that the same model prediction can be achieved through the use of multiple sets of values for the calibrated parameters (Beven 1993). Equifinality creates a challenge in how to decide which set of parameter values that is the most correct for the calibrated parameters.

NSE is widely used as objective function for stormwater model calibration (Dongquan et al. 2009; Lim et al. 2020; Rosa et al. 2015). Peak modelling is of importance in stormwater modelling, hence the sensitivity to extremes is therefore a positive contribution by using NSE. Consequently, is NSE used as the objective function in calibration and validation in this thesis.

3 Methodology

This thesis aimed to evaluate the performance of the full-scale combined infiltration and detention solution located in the city center of Trondheim. In order to do so, a model of the system was developed in SWMM. The characteristics of the sub-catchments draining stormwater to the facility were generated in ArcMap based on a DEM received from Trondheim Municipality. The model was calibrated against available data collected through sensors monitoring the stormwater system.

The calibrated SWMM model was further used in simulations aiming to investigate the performance of the combined system. The main focus was on performance in terms of generated system outflow, hence detention basin activations. To evaluate the interaction between detention and infiltration, five model scenarios were developed illustrating combined and separate stormwater strategies. Both event-based simulations using design precipitation events and long-term simulations using historical data were performed. To address possible future system performance, simulations using a climate factor of 1.4 were performed and evaluated.

3.1 Study area, stormwater pilot and data collection

3.1.1 Site description

The studied stormwater pilot is stationed in Trondheim, a city located in mid-Norway. Trondheim is a city experiencing a coastal climate as it is located in the Trondheim fjord. The annual average precipitation is 950 mm and the annual average temperature is 5.5 °C (Norsk Klimaservicesenter 2021a).

Trondheim is an urbanized city and is the fourth biggest city in Norway with a population of 207 595 (Statistics Norway 2020). The stormwater pilot is located in the densely urbanized city center in the northwest end of an open city square, shown in Figure 6. During the renovation of the city square, the stormwater pilot was built in 2019. The square is decorated with a statue in the middle, a stage, and permanently placed benches. The square is surrounded by buildings with restaurants, stores, and cafes. The city square is created to function as a meeting point in the city and was built to have a lifetime of 100 years (Multiconsult 2018). In total, 21 elevated flowerbeds are built framing the city square. Many of these elevated flowerbeds have their own drainage inlets leading water to storage spaces under each flowerbed for plant irrigation and not further transportation to drainage systems. The surface of the city square consists of large densely paved slate flagstones (Trondheim Municipality n.d.). The gaps between the flagstones are cemented.

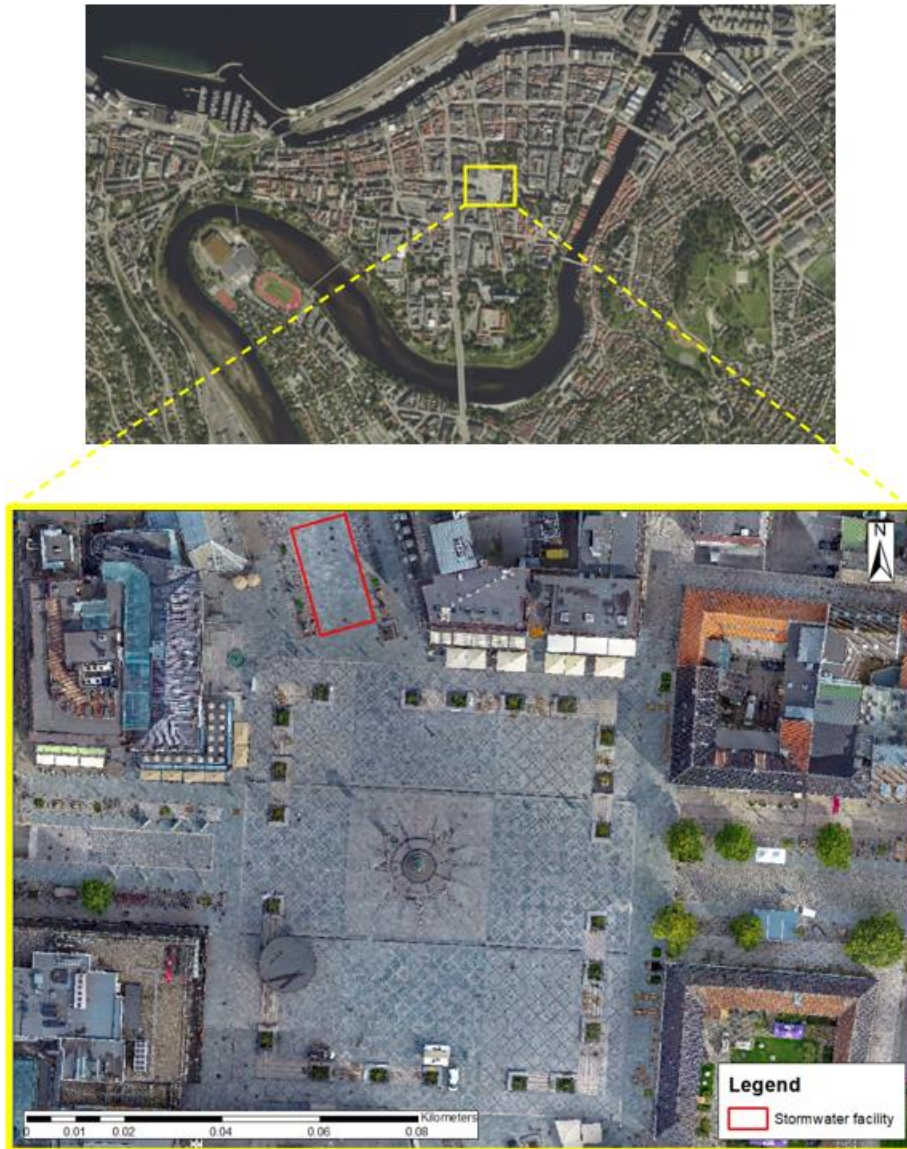


Figure 6: The location of stormwater facility showed on the orthophoto of the city square received by Trondheim Municipality. The air photo of Trondheim city center is from (Kartverket 2021).

The knowledge regarding local soil and infiltration characteristics are uncertain as no infiltrometer tests have been conducted on the site in conjunction with the construction of the stormwater pilot. A review of prior core drillings at the city square was performed by Sagli (2020). The overall conclusion was that the soil is likely to consist of homogenous materials of sand and silt. At 1-2.5 m depth the soil consists of backfill and cultural layers. Below 2.5 m, stratified layers of sand and silt are located. Sand was found in the depth of 3-4 m, and silt containing fine sand and clay was found in between 4-10 m depth. Below 10 m, the soil consists of silty and clay sand (Sagli 2020). Multiconsult (2018) assumed the soil to be homogenous sand with an infiltration rate equal to 0.001 m/s (Multiconsult 2018). Based on the previous assumptions the native soil can be assumed to have properties somewhere in the range of sandy loam, loamy sand, and sand.

The groundwater table is assumed to be at 3.8 masl (meters above sea level) (Multiconsult 2018). Further, based on a digital elevation model received by Trondheim Municipality, the surface elevation of the city square varies between 8 and 9 masl.

3.1.2 Stormwater pilot description

The studied stormwater pilot receives stormwater from the upstream city square through 11 drainage inlets. No other upstream pipe networks are connected to the combined system. Consequently, the stormwater pilot does only manage water draining from the city square into the 11 inlets. Appendix 1 shows a planer view of the pipe network in the city square. Two of the inlets are long gutters stretching across the square, shown in Figure 7. Additionally, are four out of the 11 inlets identical, but shorter, gutter on the sides. The remaining three inlets are conventional drainage inlets.



Figure 7: Photo of a part of a long gutter stretching across the square.

The stormwater pilot combines the process of infiltration and detention. Appendix 2 shows a detailed constructional design of the combined system. The system consists of three detention basins with a diameter of 2000 mm, in addition to four infiltration pipes with a diameter of 160 mm. The infiltration pipes are of type PP SN16 with 300 perforations per meter, where each perforation has a diameter of 8 mm (Multiconsult 2018). During a precipitation event, the idea of the combined system is for the infiltration system to first be activated. Further, if the infiltration alone is not sufficient in managing the incoming stormwater amounts, then the detention basins are activated.

Figure 8 shows a flow chart of the combined infiltration and detention solution. Stormwater from the drainage inlets is led to manhole O17. Further, stormwater is led to manhole O8, which is the upstream manhole of the stormwater pilot. From O8, stormwater is distributed into the infiltration pipes and the detention basins depending on the water level in the manhole. During a precipitation event, stormwater enters manhole O8 and activates the infiltration system. Due to a vertical extension of the infiltration pipes at the pipe end in downstream manhole O1, water pressure is created, and stormwater exfiltrates through the perforations into the voids of the

trench. Further, the stormwater infiltrates into native soil from the trench. If the incoming stormwater to manhole O8 exceeds the exfiltration rate through the perforations, water starts to accumulate in manhole O8. Inlets to the detention basins are located 2.34 m above manhole bottom and 1.19 m above bottom inlet infiltration pipes. As the water depth equals 2.34 m, the detention basins are activated. Detention basins activation is the only way outflow is generated from the combined system. Stormwater from the detention basins is led to downstream manhole O1 where the stormwater is discharged onto the downstream combined sewer system through a swirl chamber. The swirl chamber regulates the outflow depending on the water depth above the centerline of its outlet orifice and has a dimensioning outflow of 25 l/s (MFT 2018). The master's thesis of Sagli (2020) is recommended for a detailed description of the swirl chamber.

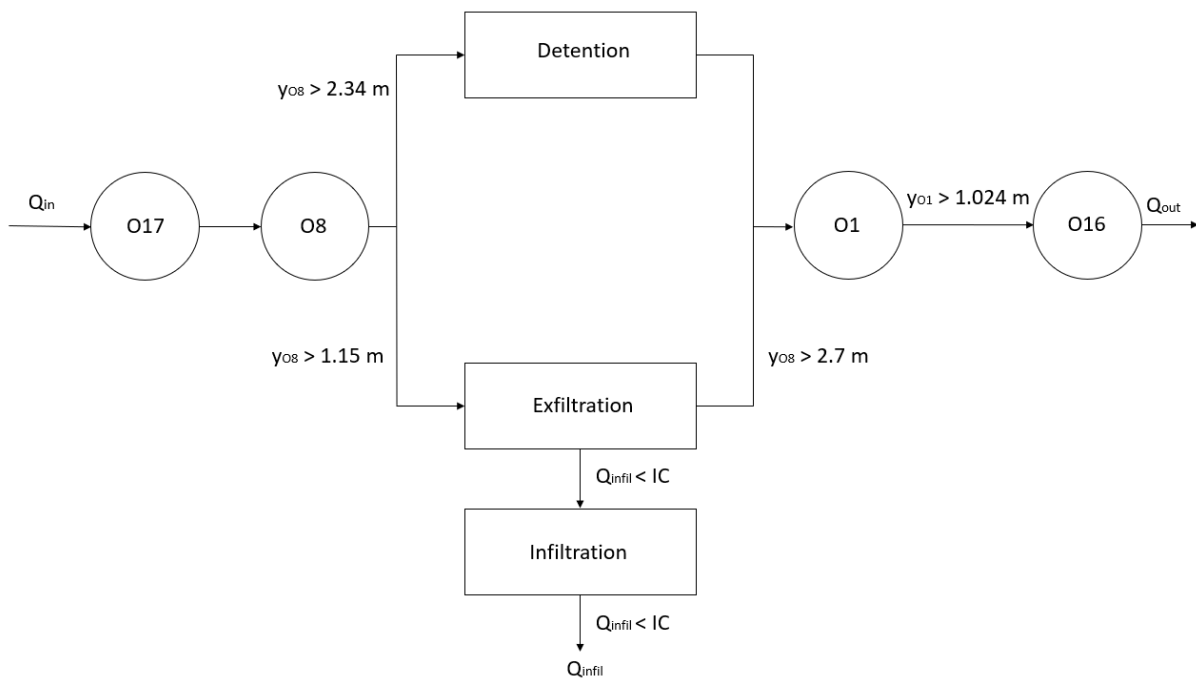


Figure 8: Flow chart of the combined infiltration and detention solution inspired by Sagli (2020), modified by the author. Water depth in manhole x is given as y_x . IC is infiltration capacity in native soil.

Through the downstream combined sewer system, the stormwater is led to a pumping station at Frostakaia (PA34) pumping stormwater and sewer to the treatment plant at Høvringen.

Even though the detention basins are the main source for inflow to manhole O1, stormwater can also be discharged from the infiltration pipes to manhole O1. Stormwater is discharged from the vertical infiltration pipes extensions in manhole O1 if the water level in manhole O8 exceeds the elevation of top vertical extensions. The vertical extension had an elevation of 6.75 masl, equaling a water depth of 2.7 m manhole O8. If water depth in manhole O8 equals 2.7 m, the detention basins are full, and the capacity of the system is reached.

3.1.3 Data collection

Monitoring of the stormwater pilot started preliminary of this study, more specifically June 26th, 2020. Installations had been performed by ITAS (Scanmatic Instrument Technology AS), Trondheim Municipality, and Sagli (2020). Measurements from the installations of ITAS were

available for downloading through Vista Data Vision online. The data was mainly collected with minute resolution. Trondheim Municipality and Sagli (2020) installed CTD-divers at additional measuring locations in the pilot. Data from the CTD-divers needed to be collected manually regularly. Based on recommendation from Sagli (2020), a precipitation gauge was installed near the stormwater pilot as a part of the study of Vartdal (2020). Further, CTD-divers were installed in an exfiltration system separate from the stormwater pilot for future research. This second exfiltration system is not in the scope of this thesis and is therefore not further discussed.

Multiple sensors have been placed out at different locations in the stormwater facility. The measured parameters depend on the specific sensors. Among the measured parameters are water pressure, conductivity, and flow. Table 2 shows an overview of the sensor locations and which parameters they measure.

Table 2: Table describes where the sensors are located in the stormwater pilot and which parameters measured at each location are marked with ●.

Sensor location	Water pressure	Atmospheric pressure	Conductivity	Temperature	Groundwater level	Flow
Manhole						
O17	●			●		
O8	●	●	●	●		
O1	●			●		
O16				●	●	
Detention basin						
O2	●		●	●		
Pipe						
O17-O8						●

Measurements of water depths and temperature in manhole O17 and O1 were measured by Seametric water level sensors called PT12 (Seametrics n.d.). The sensors in the detention basin and manhole O8 are CTD-divers of model DI27 measuring water pressure, conductivity, and temperature (Van Essen Instruments 2016a). An additional sensor was located in manhole O8, called Baro-diver, which measures atmospheric pressure and temperature (Van Essen Instruments 2016a). Flow in the pipe between manhole O17 and O8 was measured using a Viatronics AVSS Waterflow sensor (Viatronics n.d.).

A detailed description of the installed sensors and the processing of the monitored data can be found in the master’s thesis of Sagli (2020) and the student thesis of Vartdal (2020). Water depths above the CTD-divers measuring water pressure were found using the barometric compensation function in the Diver-Office software (Van Essen Instruments 2016b). By addressing water pressure in a manhole and the air pressure in the system, the water column above the sensor was computed. Further, as the water depths during precipitation events were of interest, the stable water depth through dry periods was subtracted from the measured water

depths, Equation (4). The stable water depths were assumed to equal the median of all measured water depths. By doing so, noise in measurement occurring during dry periods was neglected.

$$h_{adjusted} = h_{measured} - h_{median} \quad (4)$$

The system inflow was directly measured by the sensor in the pipe between manhole O17 and O8. Noise in inflow measurements was addressed by subtracting the inflow during dry periods, which was assumed to be the median inflow measured, shown in Equation (5).

$$Q_{adjusted} = Q_{measured} - Q_{median} \quad (5)$$

Further, was the system outflow indirectly measured based on the water depth above the sensor in manhole O1. The swirl chamber in O1 generated the system outflow based on the water depth above its outlet orifice. The measured water depth was also here adjusted by subtracting the water depth during dry periods, assumed to be the median water depth. The median water depth was assumed to reach the bottom of the outlet orifice of the swirl chamber, hence the adjusted water depth was the one outflow generation was based on. By using a table describing the characteristic of the swirl chamber developed by its operator MFT (2018), the corresponding outflow was found.

There is a gap in measured data from November 20th, 2020, until February 10th, 2021. Due to an unannounced reconstruction of the pipe through manhole O17, the sensor measuring flow in between manhole O17 and O8 was removed in addition to the sensor located in manhole O1. The specific date of reconstruction is unknown, however, an abrupt change in measured data was observed November 20th, 2020, at time 08:43. Consequently, are the reconstruction assumed to have taken place on November 20th, 2020. As this was an unannounced intervention it was not noticed until January 20th, 2021. The sensors were reinstalled on February 10th, 2021, resulting in a gap in measured inflow and outflow data from November 20th, 2020, until February 10th, 2021.

An installation of a precipitation gauge close to the studied stormwater facility was performed as a preliminary study by Vartdal (2020) to obtain high accuracy precipitation data for the facility. On December 18th, 2020, a tipping bucket was installed on the roof of a building named Trondheim Torg with a resolution of 1-minute intervals. Trondheim Torg is located within 100 m away from the facility. In comparison, the closest already existing precipitation gauges were Lade and Risvollan located respectively 2.73 km and 3.85 km away from the facility. As local variations are expected for the climate Trondheim experiences (Norsk Klimaservicesenter 2021a), the installation of a closer located precipitation measurement station was suggested for further work by (Sagli 2020). Figure 9 shows in figure a) a photo of the installation of the tipping bucket and the logger with the city square in the background, further, figure b) shows the location of the precipitation station in relation to the stormwater facility.

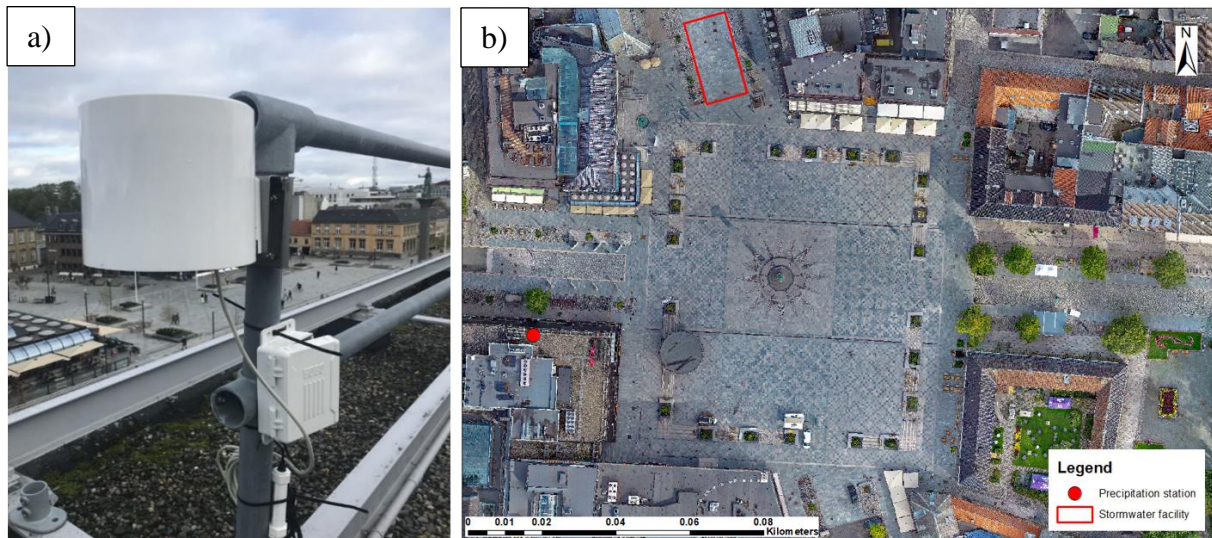


Figure 9: Visualisation of a) installation of the tipping bucket and the logger on the roof of Trondheim Torg and b) location of the precipitation station in relation to the stormwater facility.

The installed tipping bucket was of model ECRN-100 with a resolution of 0.2 mm per tip (METER, 2020). A waterproof data logger called HOBO Micro Station (H21-USB) was installed together with the tipping bucket. The measured data was manually collected through a USB-port on the HOBO Micro Station on a regular basis (Onset Computer Corporation, 2016). The software HOBOWare was used to set up the desired measurement timestep and read out data from the HOBO logger (Onset Computer Corporation, 2010) (Vartdal 2020).

3.2 Analysis of Digital Elevation Model (DEM) in ArcMap

Trondheim Municipality developed a digital elevation model (DEM) of Trondheim city square for the project. The DEM was of high resolution with cell size 5 cm x 5 cm. The method used for developing the DEM was photogrammetry. Additionally, a high-resolution orthophoto of the city square was made. The orthophoto is shown in Figure 10 a) and the DEM with its elevation distributions above mean sea level can be seen in Figure 10 b). The DEM shows that the square decrease in elevation in the north direction, hence the runoff flows from south to north. Consequently, a big fraction of the stormwater in the city square flows against the stormwater facility in the northwest.

ArcMap was chosen as the preferable GIS-tool for analyzing the DEM. It was chosen as it was well known in the community of the university and has been commonly used in research. Additionally, that help regarding functions, tools, and procedures in ArcMap was easily available online. ArcMap does have a license, but as the license is covered by the university this was not an issue in the choice of GIS-tool. An alternative would have been the open-source GID-tool QGIS.

Esri's ArcMap Desktop 10.8.1 in combination with the extension ArcHydro toolbox (ESRI 2011) was used to study the elevation data received by Trondheim Municipality. The main goal was to generate information needed as input to model the city square in SWMM. Sub-catchments with the characteristics of area, average slope, and width were generated for drainage inlets leading water to the stormwater facility. In total were 11 drainage inlets leading

stormwater to the facility. 9 out of the total 11 were chosen for sub-catchment delineation as three inlets were closely located. Sub-catchment delineation in urban areas can be challenging compared to delineation in undeveloped areas as the urban areas contains city interior and stormwater management elements as drainage inlets. If the inlets are not addressed, their effect would not be included in the ArcMap analyses. As a part of a study performed by Hosseiny et al. (2020), ArcMap was used to delineate sub-catchments to each drainage inlet in Philadelphia. The delineation was done after modification of the original DEM, where the drainage inlets were sunk into the DEM by 1.5 m (Hosseiny et al. 2020). Inspired by the work of Hosseiny et al. (2020), the original DEM received by Trondheim Municipality was modified before sub-catchment delineations were performed.

3.2.1 Procedure for sub-catchment delineation

To be able to reflect the true flow accumulation and sub-catchments taking place at the city square, the drainage inlets must be taken into account. The solution was to make a modified DEM where all inlets were lowered as sinks. Figure 10 shows figures of the procedure step by step.

The following steps were followed to achieve the modified DEM:

1. Firstly, to make a depressionless DEM the tool “Fill sinks” was used. This tool fills sinks in the DEM that are likely to be errors due to the resolution of the data. A DEM with incorrect sinks will result in incorrect flow directions and accumulations.
2. All inlets located within the area of the DEM were mapped out. In addition to studying the orthophoto received by Trondheim Municipality, a field trip was necessary to inspect locations of inlets. Further, the inlets were drawn as polygons in a shapefile. A total number of 56 drainage inlets was found within the area of the DEM. However, only 11 of these were connected to the studied stormwater facility. It was favorable to modify the DEM for all 56 inlets as upstream inlets will reduce the area draining stormwater to downstream inlets.
3. The “Clip” tool was used on the DEM and the shapefile containing the total number of inlets. Resulting in a raster with elevation data in the inlet polygons.
4. Next, the “Raster Calculator” tool was used on the inlet raster to lower the elevation of the inlet polygons. In the “Raster Calculator” tool 12 m was subtracted from the actual elevation. The value of 12 m was chosen to make sure that the inlets were lowered some meters without having a negative elevation value in the mosaiced raster (described in step 5.).
5. Lastly, the tool “Mosaic to new raster” was used to mosaic the depressionless DEM with the inlet raster having lowered elevation. “Sum” was chosen as the “Mosaic Operator” enabling summation of the elevations of the two input rasters. Output was a modified DEM with sinks at the locations of all drawn inlet polygons, Figure 10 c).

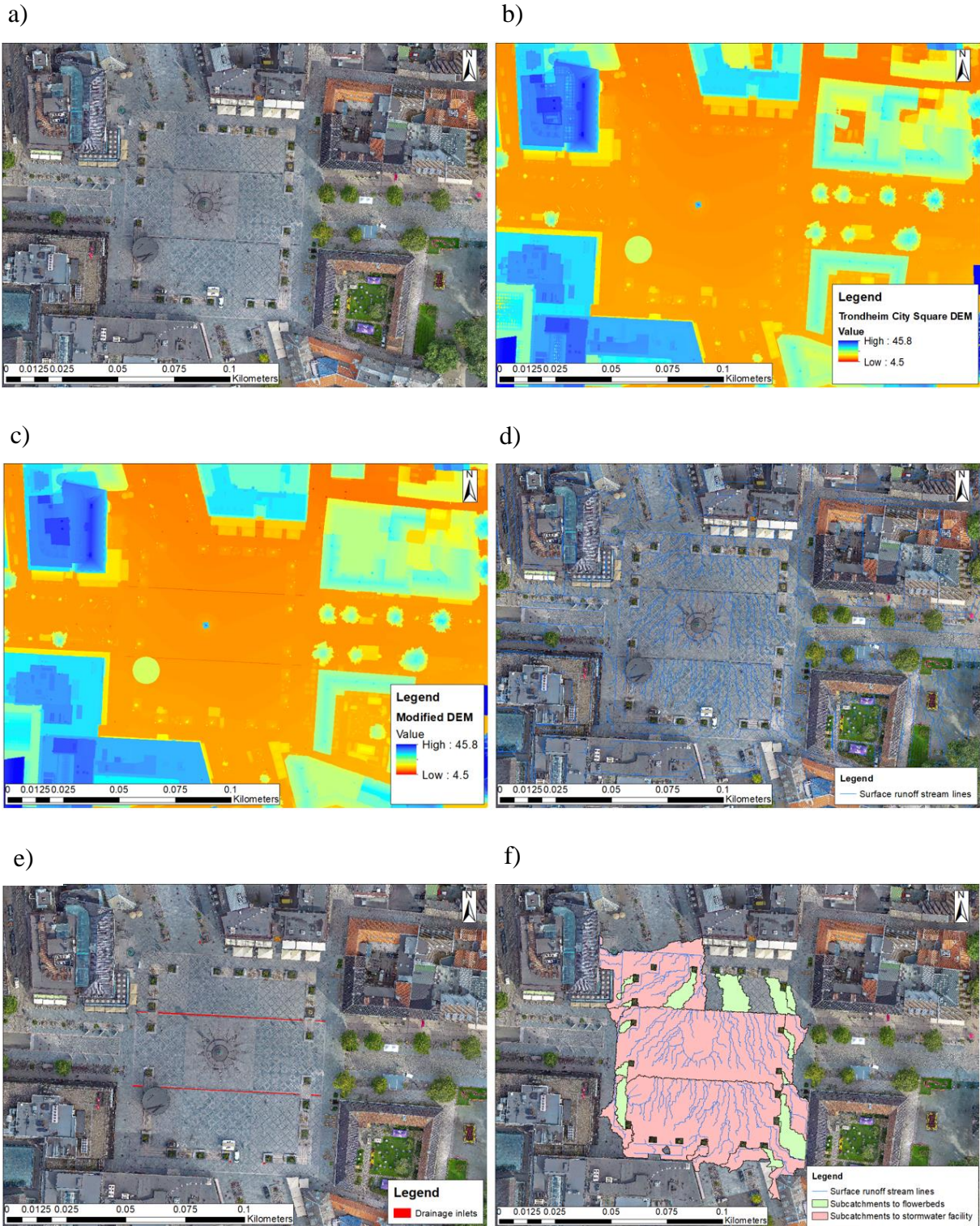


Figure 10: The steps of sub-catchment delineation in ArcMap. The following figures show a) orthophoto of the city square, b) DEM of the city square, c) Modified DEM, d) surface runoff stream lines, e) polygons of the drainage inlets for subcatchment delineation and f) sub-catchments draining to stormwater facility and flowerbeds.

ArcMap in combination with the extension ArcHydro toolbox was used for the process of sub-catchment delineation. A challenge in sub-catchment delineation occurred as two of the drain inlets to the stormwater facility are long and thin stretching across the city square. The tool “Watershed” in ArcMap, under “Spatial Analyst Tools”, was in this case not sufficient as it only generates sub-catchment to one specific point. After research and testing of multiple methods and tools, the tool “Batch watershed delineation for polygons” under “Watershed processing” in ArcHydro toolbox was found to work as desired. By using this tool, it was possible to generate sub-catchments to self-designed polygons. The focus was on generating sub-catchments to the inlets leading stormwater to the studied stormwater facility, but sub-catchments for surrounding drain inlets were also generated to get an overview. For example, were sub-catchments delineated for the inlets draining to the flowerbeds in the city square.

1. To visualize the flow paths, the flow direction was first generated based on the modified DEM using the tool “Flow direction”. Further, the tool “Flow Accumulation” was used with the calculated flow direction as input. The main flow paths were better visualized by modifying the flow accumulation with the tool “Raster Calculator” and converted to a shapefile, shown in Figure 10 d).
2. The tool in ArchHydro toolbox used for sub-catchment delineation was called “Batch watershed delineation for polygons”, found under “Watershed processing”. The required inputs were a flow direction raster and a shapefile containing the polygons of interest. Flow direction was calculated by using the tool “Flow Direction” on the modified DEM. A shapefile with polygons of the drainage inlets of interest was made, Figure 10 e). The generated output was a shapefile including sub-catchments for each of the input polygons.
3. The generated sub-catchments needed to be modified with respect to roofs and flowerbeds. Stormwater from the roofs of the buildings surrounding the city square was connected to gutters leading water to other drainage systems than the one leading to the studied stormwater facility. Further, some flowerbeds are located in the city square enabling infiltration, hence these are areas assumed to not contribute to the sub-catchments draining to the stormwater facility. Therefore, the area of roofs and flowerbeds that overlap with the generated sub-catchments were erased from the sub-catchments. The modification of sub-catchments was done by using the tool “Erase” under “Overlay” underneath “Analysis Tools”. Figure 10 f) shows the generated sub-catchments for the drainage inlets to the stormwater facility in addition to the sub-catchments draining water to the inlets connected to the flowerbeds. Figure 11 shows the sub-catchments draining water to the stormwater facility identified with numbers which they are referred to throughout the modelling.

Some small holes occurred in sub-catchments number 2 and 5. These were assumed to be obvious errors as stormwater in these spots had nowhere else to go. The errors were corrected by using the Editor toolbar in ArcMap.

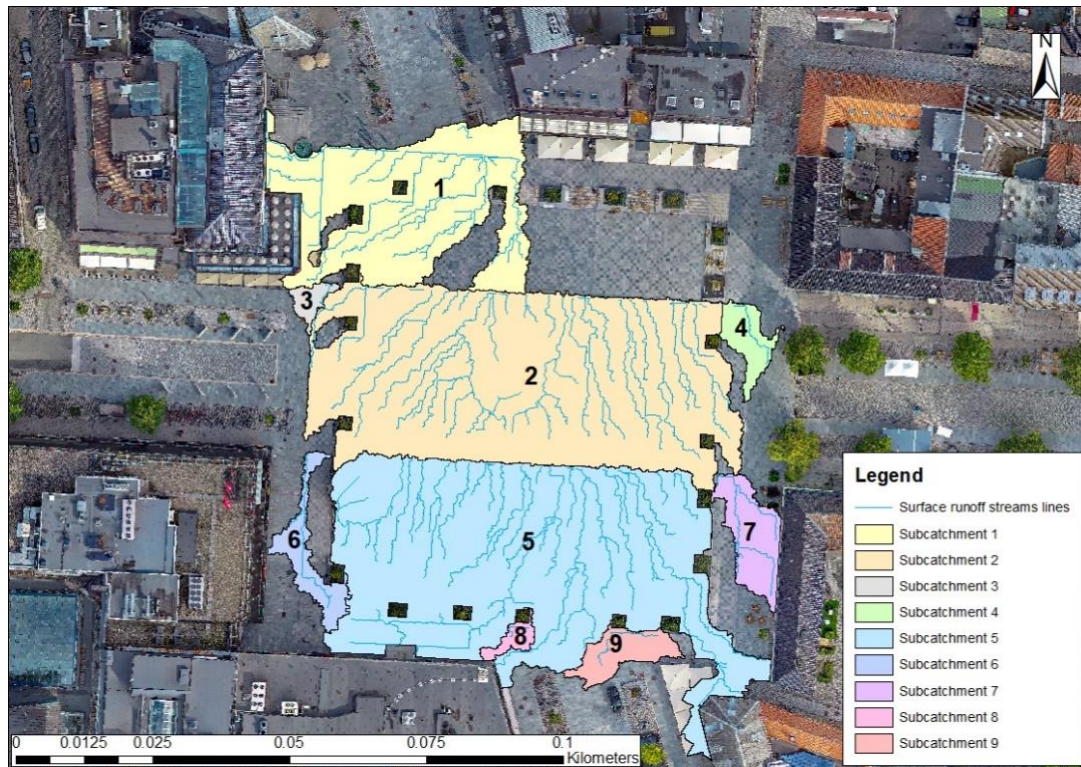


Figure 11: Visualization and numeration of the generated sub-catchments draining to the stormwater facility through drainage inlets.

3.2.2 Sub-catchment attributes for SWMM input

When modelling sub-catchments in SWMM, a collection of attributes was required as input. The attribute inputs “Area”, “Average slope”, and “Width” were computed in ArcMap. The computed attribute values for each sub-catchment are shown in Table 3.

Table 3: Sub-catchment properties generated from ArcMap.

SWMM required sub-catchment properties			
Sub-catchments	Area [ha]	Width [m]	Slope [%]
1	0.1018	19.15	3.84
2	0.2336	66.44	3.52
3	0.0038	3.94	3.31
4	0.0094	5.28	3.50
5	0.2378	56.45	3.39
6	0.0129	3.33	4.35
7	0.0174	4.65	3.70
8	0.0035	3.43	4.45
9	0.0116	9.95	4.10

The different attributes were computed following the procedures below:

Area (ha):

1. The areas of the different sub-catchments were computed by using the “Calculate Geometry” option in the attribute table of the shapefile containing the sub-catchments.
2. The areas obtained from ArcMap was given in square meter, but SWMM require hectare, consequently, a conversion was performed.

Slope (%):

1. The slope in each raster cell was calculated using the tool “Slope” with the DEM as input data. The “Slope” tool is located under “Surface” underneath “Spatial Analyst”. The slope was chosen to be calculated in percent as SWMM require slope in percent. Further, the “planar” method was selected as slope calculation method since the DEM is in projected coordinate system.
2. The slope input to SWMM is described as the average slope of the surface within the specific sub-catchment (Rossman 2015). The generated sub-catchments have city and portable interior as cars, railings, statues, and parasols, causing bias in the average slope calculation. The sub-catchments have similar surfaces with constant low slope values. Consequently, the city and portable interior results in unrealistically high average slope values. To avoid this, a shapefile was made where a polyline was generated within each sub-catchment, including the difference in surface elevation and excluding city and portable interior. The average slope for each polyline in each of the sub-catchments was found using the tool “Zonal Statistics to Table function”.

Width (m):

1. SWMM describes the attribute “Width” as the sub-catchment area divided by the average maximum overland flow length, Equation (6). The area of each sub-catchment has already been obtained. The average maximum overland flow length is the length of the flow path from the furthest drainage point in the sub-catchment to where the flow is channelized (Rossman 2015). This length was found manually using the measuring tool in ArcMap on the longest flow path in each sub-catchment computed by the “Flow Accumulation” tool.

$$Width = \frac{A_{Subcatchment}}{Average\ maximum\ overland\ flow\ length} [m] \quad (6)$$

2. The widths were calculated in excel by dividing the obtained sub-catchment areas over average maximum overland flow lengths.

3.3 Model setup in SWMM

The developed SWMM model consisted of sub-catchments draining stormwater runoff into inlets transporting water through the drainage system until it reached the combined infiltration and detention solution. As the performance of this specific facility was of interest, the model was limited to generate water coming into the system and simulate the flow out of the system. Hence, the downstream drainage system was not included in the model. Outflow from the facility was modelled to an outlet node, where the flow to the outlet node was the simulated flow to the downstream combined sewer system. Figure 12 shows the developed SWMM model.

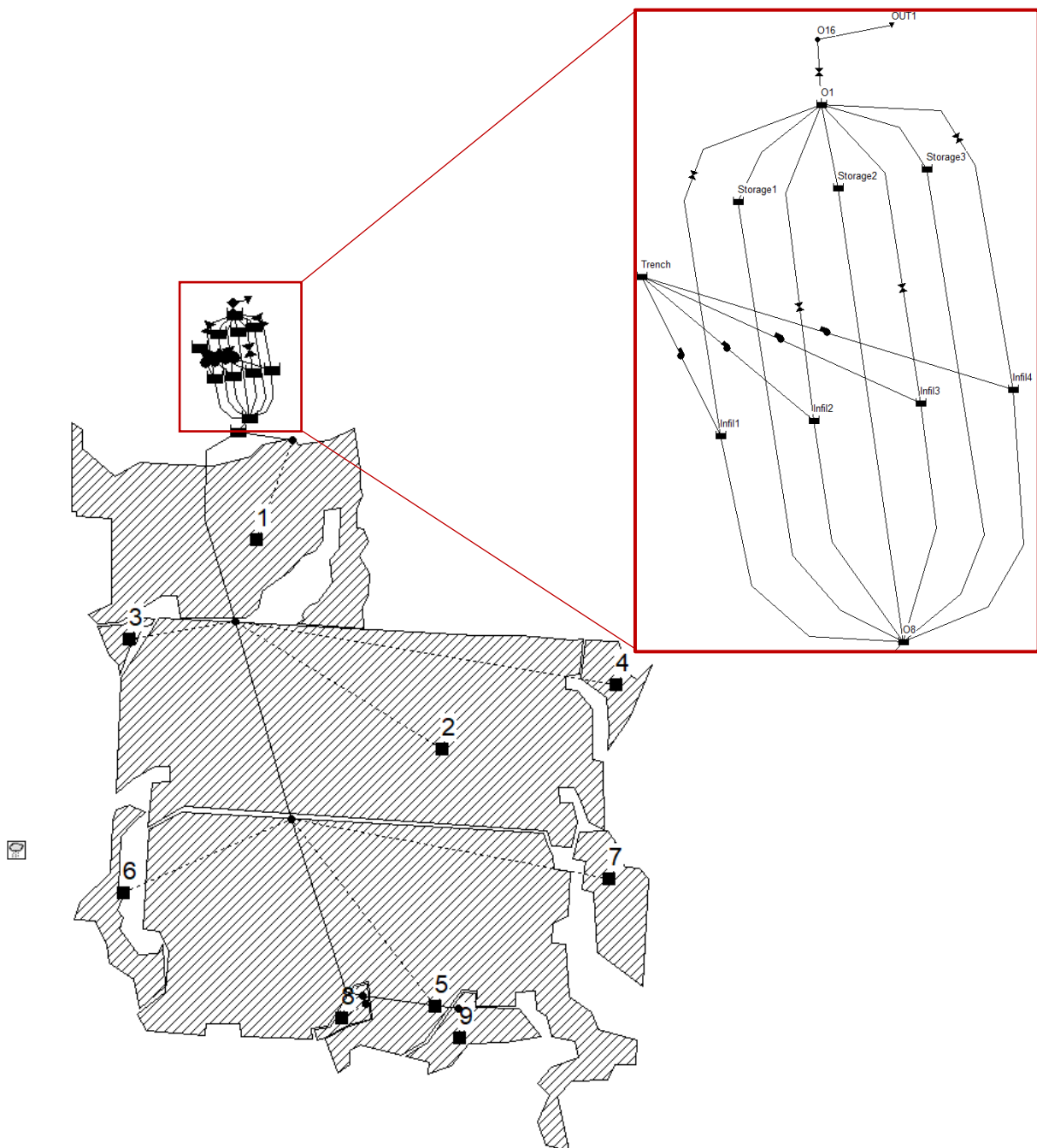


Figure 12: Developed SWMM model.

The conventional stormwater elements, as the detention basins, pipes, and manholes, were modelled using incorporated functions in SWMM. The challenge was to find a suitable method to model the infiltration system, as there was no explicit function in SWMM to model exfiltration from perforated pipes. Consequently, research was done on the functions in SWMM to understand how the desired effect could be modelled.

Input values were found based on DEM analysis in ArcMap, constructional dimensions designed by Multiconsult or measurements and data obtained by Trondheim Municipality. The input parameters of uncertainty were set for calibration with calibration ranges based on estimates from the SWMM manuals (Rossman 2015, 2017; Rossman and Huber 2016). The final input values for the modelled structures, and their sources, are found in Appendix 3-7.

The following subsections states how the different parts of the stormwater facility were modelled and the performed assumptions.

3.3.1 Sub-catchments

Using ArcMap, nine sub-catchments draining stormwater to the facility were generated. The generated input parameters for SWMM were area, average slope, and width, shown in Table 3. The total area of the catchments draining stormwater to the stormwater facility was 6319.2 m². Sagli (2020) found a total area of 6024 m² using a simplified method only delineating a catchment to the inlet located furthest downstream. Consequently, a total drainage area of 6319.2 m² is reasonable.

Sub-catchments are modelled in SWMM using the tool “Sub-catchment”. Sub-catchments receive precipitation, and according to parameters of topography, surface and soil characteristics, surface runoff was generated. The runoff can be drained to one specific node or to another sub-catchment. A sub-catchment consisted of the following three subareas; pervious area, impervious area with depression storage and impervious areas without depression storage. Runoff in the pervious subareas could infiltrate, whereas runoff in impervious subareas had no infiltration. The fraction of different subareas could be determined in each sub-catchment. This function enabled spatial variability as bigger catchments could be divided into smaller homogeneous sub-catchments containing different ratios of pervious and impervious areas. How runoff was routed within the sub-catchment could further be determined, runoff could either be routed from one subarea to another or runoff from all subareas could be routed directly to the outlet of the sub-catchment (Rossman 2015).

In the developed SWMM model, the nine sub-catchments were modelled draining surface runoff to junction nodes simulating the drainage inlets. Inside each sub-catchment, stormwater from the different subareas are assumed to be routed directly to the outlet.

The percent of impervious area are assumed to be equal for all sub-catchments as their surface characteristics are assumed to be identical. Moreover, was the percent of impervious area assumed to be high since the surface consists of densely paved flagstones. Trondheim Municipality had developed suggestions for runoff coefficients associated with different surface types, shown in Table 4 (Trondheim Municipality 2020). The sub-catchments were assumed to fall under the category of impermeable surfaces as the flagstones does not enable

infiltration. The gaps between the flagstone are assumed to have low infiltration as they are cemented. Consequently, the percent of impervious area was assumed to be 95% for all sub-catchments.

Table 4: Runoff coefficients suggestions from Trondheim municipality associated with different surface type (Trondheim Municipality, 2020).

Surface type	Runoff coefficient, ϕ
Impermeable surfaces (Roofs, asphalted surfaces/roads etc.)	0.85-0.95
City center	0.70-0.90
Dense residential areas (apartments)	0.60-0.80
Residential area (single houses)	0.50-0.70
Graveled surface	0.60-0.80
Industrial areas	0.50-0.90
Parks, lawn, forest, cropland	0.30-0.50

The roughness of the flag stones is a parameter of uncertainty. The Manning's roughness coefficients for impervious and pervious areas were therefore set for calibration. As the surface of the paved flagstones was smooth, the depression storages for both pervious and impervious were assumed to equal 0.05 mm. However, the percent of impervious area with no depression storage was also set for calibration.

3.3.2 Drainage system

The upstream drainage system transporting stormwater to the stormwater facility was modelled using junctions and conduits. The drainage inlets were modelled as junctions with its corresponding sub-catchment connected to it. The lengths and diameters of the drainage pipes were available data from Trondheim Municipality. However, the invert elevations of the drainage inlets and the slopes of the pipes were unknown. The drainage inlets were assumed to have a depth equal to 1 m, and as the surface elevations were known based on the DEM, the invert elevations could be estimated. It was also assumed that the inlet and outlet offsets equaled to zero for all pipes upstream the stormwater facility. Further, it was ensured that all pipes had a slope of at least 10 ‰, by adjusting the depths of the drainage inlets. The Manning's roughness coefficient of the pipes was assumed to be low as the pipes was only one year old, consequently it was set equal to the default-value of 0.01 for all pipes.

It was important to model the storage in manhole O8 and O1 correctly as their storage, respectively, affects the frequency of detention basin activations and outflow generation from the swirl chamber. Consequently, manhole O8 and O1 were modelled as storage units instead of junctions. By modelling the manholes as storage units, their storage capacity could be use-defined. This was beneficial as the diameters of manhole O8 and O1 was bigger than the other manholes. The dimensions and invert elevations of the stormwater structures in the stormwater facility were available through constructional drawings by Multiconsult, Appendix 1 and 2.

3.3.3 Detention basins

The stormwater facility had three identical circular detention basins with inside diameter equal to 2 m, length equal to 11.85 m and with a slope of 0.0084 m/m. The cross-section of the detention basins and the trench are visualized in Figure 13.

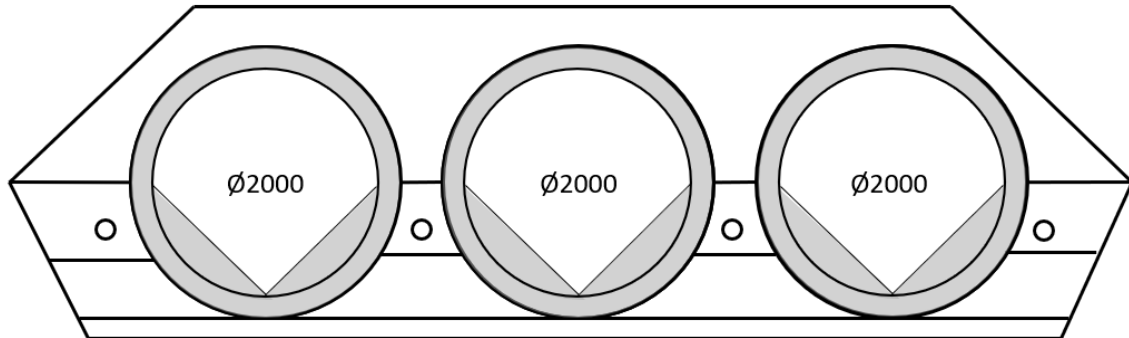


Figure 13: Sketch of the cross-section of the trench with the three detention basins and infiltration pipes inspired by dimensional drawing developed by Multiconsult, Appendix 2. Dimensions are given in mm.

The detention basins were modelled in SWMM using storage units. Modelling of storage units requires a describing storage curve. The storage curve was a method for describing the geometric shape of the storage unit by finding the relation between water depth and water surface area (Rossman 2015). The storage curve could either be expressed as a functional curve or as a tabular curve. Surface areas at water depths that were not explicitly addressed in the storage curve were found by interpolation. Further, determination of storage volume at a given depth y corresponded to finding the area under the storage curve from depth 0 m to y (Rossman 2017). In this thesis, a tabular curve was chosen as it was the easiest way to address the relationship between depth and surface area of the basins. The detention basins did not have a constant surface area but had surface areas varying with depth. The variations were due to the circular cross-sections with the sloped sides in the lower half, and the slope of the basins.

In modelling, the sloped sides in the lower half of the basins were assumed to be cords. The endpoints of the cords were located at the lowest point in the basin and at the point on the arc reached when water depth was equal to the radius. The assumption is illustrated in Figure 14.

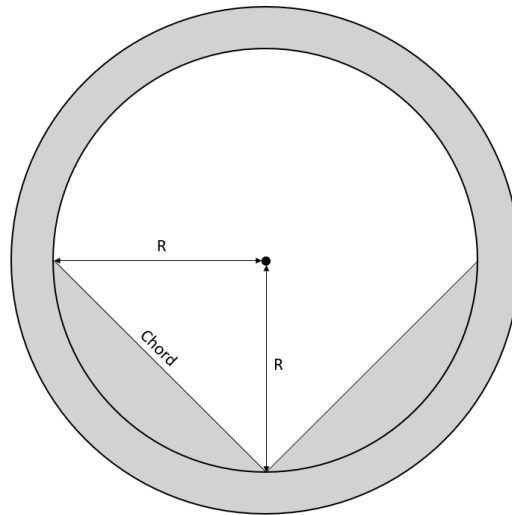


Figure 14: Sketch of one detention basin with sloped sides in lower half assumed to be chords, inspired by the drawing developed by Multiconsult, Appendix 2.

The water surface area was calculated differently for water levels below and above center of the circular cross-section. Based on the geometry of the cross-section of the detention basins, the corresponding surface areas for different water depths were calculated. A detailed calculation description with illustration and equations can be found in Appendix 8.

The tabular curve was made for water depths ranging from 0-2 m in 0.025 m increments. A csv-file with the depths and the corresponding water surfaces areas was developed. Python was used to convert the csv-file to a dat-file with data in the correct format SWMM requires. Furthermore, the dat-file was uploaded to SWMM and chosen to be the storage curve for the three detention basins. The developed detention basin storage curve is shown in Appendix 9.

3.3.4 Infiltration pipes

The infiltration pipes used in the facility were made of PP SN16 with 300 holes per meter. Figure 15 illustrates the cross-section of an infiltration pipe, showing the locations of the holes in addition to diameters of the pipe and the holes. Four holes are located in one cross-section, of which top, bottom, and sides.

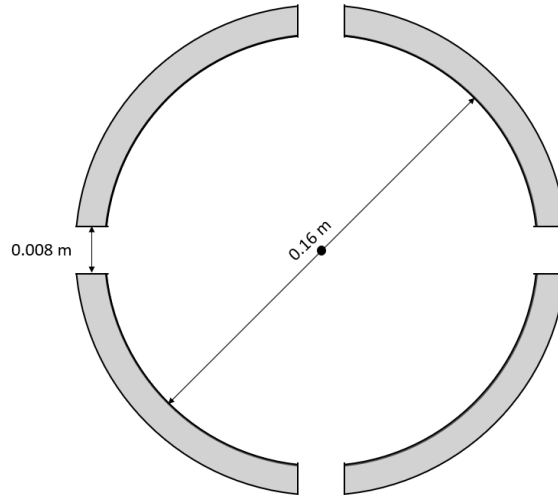


Figure 15: Sketch of the cross-section of one of the perforated pipes illustrating the locations of the perforation. Diameters given in m.

The originally planned length of the trench was 23 m (Multiconsult 2018). Infiltration used in combination with detention storage was assumed to reduce the needed storage volume. As a result, the size of the detention basins was decided to be reduced to 72 % of the original size by reducing its lengths (Multiconsult 2018). Consequently, the length of the trench and the infiltration capacity were reduced to 72 % of its original designs. As shown in Equation (7), the reduced length of the trench equaled 16.6 m.

$$L_{Reduced} = 23 \text{ m} * 0.72 = 16.6 \text{ m} \quad (7)$$

As a result of reducing the length of the trench, the lengths of the infiltration pipes were also reduced. Based on data regarding the pipe network received by the Trondheim Municipality, the lengths of the infiltration pipes are 16 m for the two infiltration pipes in the middle and 24 m for the outer infiltration pipes. A simplification was done in modelling by assuming the length of all four pipes to be 20 m each. Even though the simplification was performed, the total storage volume inside the pipes and the number of perforations remained unchanged.

There was no explicit function in SWMM to model perforated pipes. Consequently, research on the existing functions and possible methods were performed. Liu (2016) modelled an EES system in SWMM by combining the SWMM functions orifices, storage units and pumps. Inspired by conceptual modelling of desired functions through combined existing SWMM functions, the infiltration pipes were modelled as storage units. Since the infiltration pipes had a vertical extension at the pipe end, water will not flow straight through but be stored in the pipes before it exfiltrates to the trench. The storage capacity in the pipes was modelled by developing a storage curve describing the relationship between water depth and water surface area. The calculation of the storage curve was based on the geometric properties of the cross-sections and are detailed described in Appendix 10, and the developed storage curve describing the infiltration pipes are in Appendix 11.

Further, were pumps used to model the effect of exfiltration from the infiltration pipes. The idea was to simulate the exfiltrated flow into the voids of the trench by pumping flows depending on the number of perforations covered with water. A pump curve was developed relating outflow to water depth in the storage unit. The rate at which water moves through the trench was assumed to be described by a saturated hydraulic conductivity of the trench. Outflow was calculated by multiplying the saturated hydraulic conductivity of the trench with the total wetted area. The wetted area was assumed to be the sum of the areas of the number of perforations covered with water. Hence, the wetted area depended on the water depth in the infiltration pipes. There were 300 perforations per meter, where every meter had 75 perforations in the bottom location, 150 perforations located on the sides, and 75 perforations situated in the top. When the water depth equaled the diameter, 0.16 m, all perforations were covered. For water depths below mid-point, $y < 0.08$ m, 75 perforations were covered per meter. Further, were 225 perforations per meter covered for water depths in between 0.08 m and 0.16 m. Equation (8) shows the calculation of wetted area depending on the water depth. Furthermore, Equation (9) shows calculation of exfiltration flow used in the pump curve.

$$A_{wetted} = \left\{ \begin{array}{ll} 75 * \pi * \left(\frac{D_{hole}}{2}\right)^2 * L, & \text{for } y < 0.08 \text{ m} \\ 225 * \pi * \left(\frac{D_{hole}}{2}\right)^2 * L, & \text{for } 0.08 \leq y < 0.16 \text{ m} \\ 300 * \pi * \left(\frac{D_{hole}}{2}\right)^2 * L, & \text{for } y = 0.16 \text{ m} \end{array} \right\} \quad (8)$$

$$Q_{Exfiltration} = K_{sat_trench} * A_{wetted} \quad (9)$$

Where,

A_{wetted} = Total wetted area [m²]

D_{hole} = Diameter of the holes in the infiltration pipe [m]

y = Water depth in pipe [m]

L = Pipe length [m]

$Q_{Exfiltration}$ = Exfiltration flow to trench [l/s]

K_{sat_trench} = Hydraulic conductivity to trench [mm/hr]

The value of the assumed parameter of saturated hydraulic conductivity in the trench was uncertain as it was unknown. Hence, it was set for calibration.

A tabular pump curve was made for water depths ranging from 0-0.16 m in 0.0025 m increments. The developed pumping curve was uploaded to the SWMM model as a dat-file in

the required format and connected to the pumps between the storage units simulating the infiltration pipes and the trench. Appendix 12 shows the calibrated pumping curve.

A control rule was developed to control the behavior of the pumps in relation to the water depth in the trench. It was assumed that the water level in the trench could not be higher than the water level in the upstream manhole O8. The trench and the upstream manhole O8 were modelled to have the same invert elevation meaning that their water depths could be directly compared. Thus, a control rule was made saying that the pump status for all the pumps equaled OFF when the water depth in the trench was \geq than the water depth in the upstream manhole O8, else the pump statuses equaled ON. The structure and design of the developed control rule can be found in Appendix 15.

In the physical pilot, the vertical extensions of each infiltration pipes were located in downstream manhole O1. In the SWMM model, the vertical extensions were modelled as orifices between the storage units simulating the infiltration pipes and the storage unit simulating manhole O1. No water exited the raised extensions in the physical pilot unless the water depth in upstream manhole O8 was ≥ 2.7 m. Hence, the modelled orifices from the infiltration pipes were included in a control rule saying that the fraction of the orifice openings was equal to 1 when the water depth in upstream manhole O8 ≥ 2.7 m, else the fraction of orifice openings was equal to 0. The structure and design of the developed control rule can be found in Appendix 15.

3.3.5 Trench and native soil

The cross-section of the trench with its dimensions is shown in Figure 16. The length of the trench were originally planned to 23 m, but as the volume of the detention storage was reduced, the built trench length was 16.6 m, see Section 3.3.4, (Multiconsult 2018). The combined stormwater facility was embedded in washed crushed stones in the range of 16-64 mm. The trench is separated from the native soil with a filter fabric.

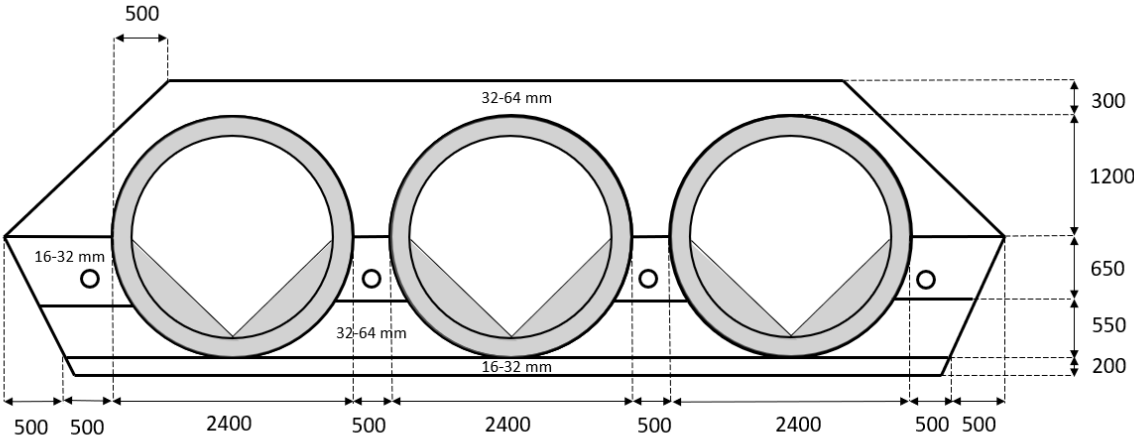


Figure 16: A sketch of the trench cross-section inspired by the dimensional drawing by Multiconsult (2018), Appendix 2. All dimensions given in mm.

Stormwater was stored in the voids of the trench after exfiltrating the infiltration pipes. The total volume of voids was therefore modelled as a storage unit. Crushed stones in the range of 16-64 mm were assumed to have a void ratio of 0.4. To obtain the correct storage volume of the trench, the volume of the pipes needed to be subtracted. The shape of a storage unit in SWMM was described through a storage curve relating water depths and surface areas.

The length of the detention basins does not equal the length of the whole trench. Consequently, the trench cross-sections before and after the start and end of the detention basin length will have more available storage volume. Hence, the total surface area was calculated in two steps. Step one was calculation of the surface area for the length where the detention basins are located, and step two was calculation of the surface area for the length without detention basins. The total surface area of the trench were the surface areas from step one and two summarized.

As the diameter of the infiltration pipes were much smaller than the diameter of the detention basins, the area of the infiltration pipes was neglected in the calculation of the trench surface area. The surface area available for storage varied with depth due to the shape of the trench, the circular shape of the detention basins and their location in the trench. To address for the circular shape of the basins a simplification was performed using interpolation. Based to the known dimensions of the trench, Figure 16, the surface areas at five chosen depths were calculated. As SWMM models water depths in storage units, the bottom trench was set to equal water depth of 0 m. The chosen depths, from bottom trench, were 0 m, 0.2 m, 1.4 m, 2.5 m and 2.9 m, visualized in Figure 17. Further, were the surface areas for depths in between the chosen depths found by interpolation.

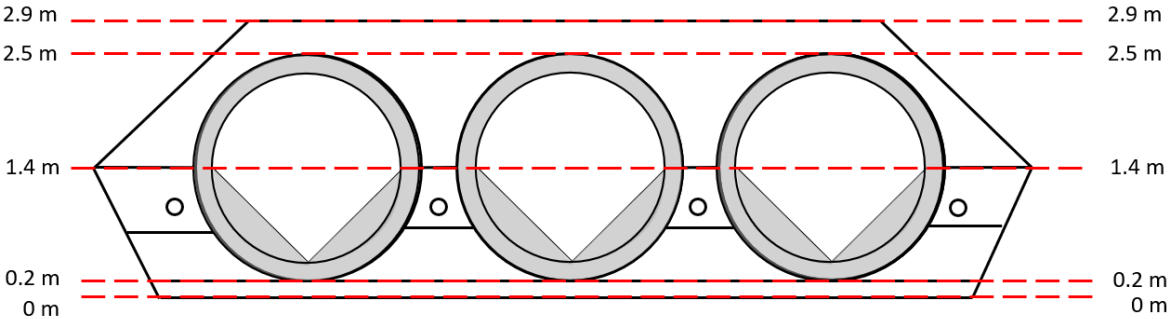


Figure 17: A sketch illustrating the trench where the chosen water depths for surface area calculation are highlighted as red dotted lines. The sketch is inspired by the drawing by Multiconsult (2018), Appendix 2.

To find the surface area of the voids, and not the full trench, the computed surface areas were multiplied with the void ratio of 0.4. The equation for surface area calculation is shown in Equation (10).

$$A_{Surface} = w * L * void\ ratio \quad (10)$$

Where,

- $A_{Surface}$ = Surface area [m²]
 w = Width of trench [m]
 L = Length of trench [m]
void ratio = Void ratio for the crushed stones in the trench []

Surface area calculation for the length including the detention basins, needed modification at depth 1.4 m due to the area of the detention basins. Consequently, were the diameters of the three detention basins subtracted from the dimensioned trench width at depth 1.4 m. The surface areas for the five chosen depths are shown in Table 5. The full storage curve of the voids of the trench can be found in Appendix 13.

Table 5: The chosen five depth and their corresponding surface area [m²].

Depth [m]	Surface area [m ²]
0	59.43
0.2	61.09
1.4	33.60
2.5	54.45
2.9	47.81

Infiltration from the trench to the native soil was modelled by activating seepage in the storage unit simulating the voids of the trench. Seepage loss from a storage unit in SWMM works as infiltration of ponded water into the native soil. SWMM calculates seepage rate per unite area over time based on the given infiltration characteristics and the chosen infiltration method. Further, based on the developed storage curve of the trench, SWMM was able to account for seepage from sloped sides. Therefore, the total rate of seepage loss was computed as the rate of seepage loss from bottom storage unit summarized with the rate of seepage loss from the sloped sides (Rossman 2017). Green-Ampt was the chosen infiltration method, and its infiltration parameters were suction head, saturated hydraulic conductivity, and initial deficit. Suction head and initial deficit were set for calibration, whereas the saturated hydraulic conductivity of the trench was set to 3600 mm/hr based on assumptions by Multiconsult (2018).

3.3.6 Swirl chamber

The discharge from the stormwater facility to the downstream pipe network was regulated by a swirl chamber in manhole O1. The outflow was determined by the water level above the center of the outlet orifice of the swirl chamber. The relationship between water levels and outflow was given as a table by the operator MFT (2018). The outlet orifice had a diameter of 199 ± 1 mm, consequently the distance from bottom to center orifice equaled approximately 100 mm.

For a more detailed description of the characteristics of the swirl chamber in the stormwater facility, the master’s thesis of Sagli (2020) is recommended.

To model the effect of the swirl chamber, a conduit was not sufficient as it could not regulate water. Instead, an outlet link was implemented. An outlet link gave the opportunity to relate specific water depths or heads to specific outflows. The outflow could be set as a function of either the water depth above the inlet offset of the outlet link, or the head difference across the outlet (Rossman 2015). The relationship was defined as a user-defined rating curve, which could either be described through a functional curve or a tabular curve.

In this study, a tabular curve was developed based on the table developed by MFT (2018). The only modification was adjusting the water levels from being above orifice center line to be above bottom orifice, which was required for the outlet link in SWMM. The distance from bottom to center orifice was approximately 100 mm (MFT 2018). Consequently, the distance of 100 mm was added to the water levels measured from the center line of the orifice. Further, the table was converted into a dat-file with the format SWMM accepts and uploaded to the outlet link in SWMM. The rating curve uploaded for swirl chamber modelling are shown in Figure 18 and can be found in Appendix 14.

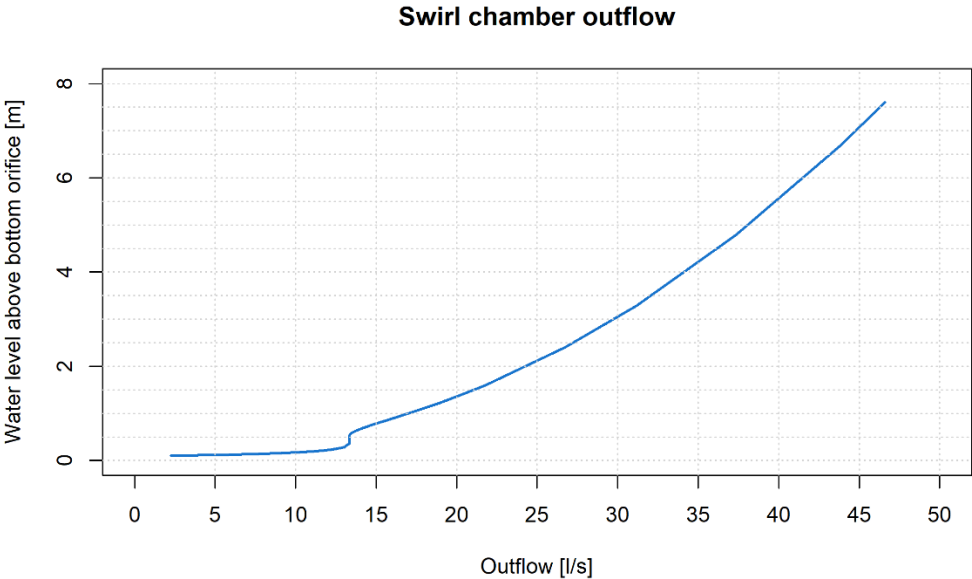


Figure 18: Rating curve uploaded to SWMM simulating the characteristics of the installed swirl chamber.

The maximum depth in manhole O1 was 5.082 m. As the swirl chamber was located 1.024 m above the manhole bottom, the maximum potential water depth above the swirl chamber was 4.058 m. The outflow generated from the swirl chamber at maximum water depth was according to the developed table equal to 34.33 l/s. Flooding occurred if the maximum depth was exceeded.

3.3.7 Model simulation settings

The developed SWMM model had a routing time step of 1 minute. Further with a runoff time step of 1 hour for dry weather and 1 minute for wet weather.

Green-Ampt was chosen as the infiltration method for the developed SWMM model. The processes included in the model were rainfall/runoff and flow routing. Groundwater was considered included but was decided excluded as it was assumed to not interfere with the performance of the stormwater facility. The groundwater table was at 3.8 masl, resulting in a distance of 1.4 m below the infiltration pipes. The distance of 1.4 m was assumed to be sufficient to avoid interference. Additionally, modelling of groundwater required multiple soil characteristics that were unknown in this thesis. Hence, it was concluded to be of higher uncertainty than of use.

To get the most theoretical accurate result, dynamic wave was chosen for the developed SWMM model. Dynamic wave combines water levels in nodes and flows in conduits, enabling pressurized flow in pipes as they became full (Rossman 2015).

In case of flooding during simulations, ponding of water was allowed. SWMM modelled flooding of nodes when their maximum water depths were reached. If no ponded area was allowed nor any surcharge depth was given, the flooded water would be lost to the system (Rossman 2017). The infiltration pipes and the trench were located underground in the physical system, whereas the manholes reached all the way to the surface elevation. In the model, the infiltration pipes and the trench were modelled as storage units with invert elevations similar to the manholes, but with significantly smaller maximum depths. Once the maximum depths of the storage units were reached, water continued to flow into the storage units and flooded the units. In order to not lose water from the system, but rather force the water to accumulate in the upstream manhole, surcharge depths were given to the storage units. The given surcharge depths were the distance from top storage units to surface elevation. When the water level in the upstream manhole O8 exceeded the maximum water level in the infiltration pipes, the infiltration pipes are surcharged, meaning that all connected conduits are full, and water accumulates in manhole O8 (Rossman 2017).

3.4 Calibration and Validation

Calibration of the SWMM model was performed for parameters affecting the water balance not known from DEM analysis in ArcMap, constructional dimensions designed by Multiconsult or measurements obtained by Trondheim Municipality. The calibration intervals for the calibrated parameters were mainly determined based on suggested parameter intervals in the SWMM manuals (Rossman 2015, 2017; Rossman and Huber 2016).

The calibration was performed by comparing observed and simulated system outflows for multiple combinations of parameter values. To address the goodness-of-fit, the objective function of NSE was chosen for calibration of the developed model, Section 2.1.4. Automatic optimization was the method used for calibration and was completed using an optimizer function to find the best NSE in the programming software R.

Validation was further performed on the calibrated SWMM model. A complete sensitivity analysis of the parameters was not performed due to the time limitations of the master's thesis. However, through trial and error the sensitivity of some of the parameters was evident.

3.4.1 Defining calibration and validation periods

During the one year of monitored data, two detention basin activations have been observed. The activations occurred on July 18th and August 8th, 2020. Thus, the system had outflow equal to zero throughout the rest of the monitored time, except for some small, unexpected outflow measurements likely to be measurement errors. The two monitored detention basin activations were desirable to have in the calibration period. As a result, the calibration period would be the summer of 2020. For this time period, local precipitation measurements were not available as the tipping bucket was installed six months post the activation occurrences. Precipitation data from the weather station at Lade was chosen for calibration as it was the closest station, 2.73 km east of the stormwater facility, with measured precipitation for the summer of 2020. Local variations in precipitation are expected, something giving uncertainty to the use of precipitation data from Lade for calibration. The calibration period was set to be July 1st to September 14th, 2020.

Since precipitation data from the weather station at Lade was chosen for the calibration period, it was also chosen for the validation period. When defining the validation period, it was favorable to choose a period without snow or snowmelt to avoid mismatch in volume of measured inflow and volume generated from measured precipitation. Further, the monitored data of the combined system was limited with only one year of data, and with a gap from November 20th to February 10th. The validation period was therefore chosen to be September 15th to November 15th, 2020.

3.4.2 Parameter calibration for the sub-catchments

The model contained in total nine sub-catchments. The characteristics of area, percent slope and width were found from DEM analysis in ArcMap. The parameter values were assumed to be correct and was therefore fixed values during calibration. The values for each of the sub-catchments are shown in Table 3.

As all sub-catchments had similar surface characteristics, they were assumed to have the same percent of impervious area. Moreover, as the sub-catchments had surfaces of densely paved flagstones, the amount of impervious area was assumed to be high. Consequently, the percent of impervious area (% Imperv) was assumed to be a fixed value equal to 95 % during calibration for all catchments. See Section 3.3.1 for further reasoning behind the choice of percent impervious area.

The main uncertainties in modelling of the sub-catchments were in regard of infiltration and characteristics of the flagstone surfaces. The roughness of the flagstone surface was unknown. Consequently, Manning's roughness coefficient for both impervious (n-imperv) and pervious area (n-perv) were calibrated. The surface of smooth flagstones was assumed to fit in the category of smooth impervious surface or smooth asphalt pavement. According to the Hydrology SWMM manual (Rossman and Huber 2016), the Manning's roughness for overland

flow was assumed in the range of 0.01-0.015. Further, the pervious areas of the catchments were assumed to be the gaps in between the flagstones. The gaps were filled with cement and were further assumed to have the characteristics in between concrete and graveled surface. According the Hydrology SWMM manual (Rossman and Huber 2016), graveled and concrete surface had a Manning`s roughness for overland flow estimated in the range of 0.012-0.045. The percent of impervious area with no depression storage were also unknown. It was set for calibration with a calibration interval from 25-100% as the flagstones had smooth surfaces.

Infiltration occurred in the pervious areas. The catchments consisted of 95 % impervious area, resulting in 5 % of the total area to be pervious. As previously mentioned, the pervious area was assumed to be the cement filled gaps between the flagstones. Consequently, the pervious area was assumed to have low infiltrated capacity. The chosen method for infiltration is Green-Ampt. Green-Ampt require three parameters, namely the suction head, saturated hydraulic conductivity and initial deficit. Based on the hydrology SWMM manual (Rossman and Huber 2016), suction head was calibrated in the range from 9-200 mm, saturated hydraulic conductivity from 0.2-20 mm/hr and the initial deficit was given the calibration interval from 0.21-0.34. Table 6 shows the parameters set for calibration regarding the properties of the sub-catchments and their corresponding calibration intervals and sources.

Table 6: The input parameters for sub-catchments set for calibration with corresponding calibration intervals and source.

Properties of the sub-catchments		
Parameter	Calibration interval	Source
n-Imperv	0.01-0.015 []	(Rossman and Huber 2016:75)
n-Perv	0.012-0.045 []	(Rossman and Huber 2016:75)
%Zero-Imperv	25-100 [%]	Assumed
Suction head	9-200 [mm]	(Rossman and Huber 2016:114)
Saturated hydraulic conductivity	0.2-20 [mm/hr]	(Rossman and Huber 2016:114)
Initial deficit	0.21-0.34 []	(Rossman and Huber 2016:116)

The remaining input parameters for the sub-catchments were depth of depression storage on impervious area (Dstor-Imperv) and pervious area (Dstor-Perv) in addition to the percent of routed runoff between sub-areas. Due to the smooth surface of the flagstones, depression storage for both impervious and pervious areas were set equal to 0.05 mm (Rossman and Huber 2016). Further, was the percent of routed runoff between the sub-areas set equal to 100%, as all stormwater was assumed to drain to the storm inlets. These input parameters were fixed values during calibration.

3.4.3 Parameter calibration for the stormwater pilot

The modelled stormwater pilot in SWMM consisted of multiple stormwater elements as manholes, pipes and detention basins with known dimensions. The dimensions are known due to insight in detailed dimensional drawings developed by Multiconsult, Appendix 1 and 2, in addition to measurements performed by Trondheim Municipality on the site after construction. The uncertainty of the model highly depended on the infiltration system. The characteristics of exfiltration to the trench and infiltration of the native soil were uncertain and therefore calibrated. Table 7 shows the parameters that were set for calibration for the stormwater pilot with corresponding calibration intervals and sources.

Table 7: The input parameters for the stormwater pilot set for calibration with corresponding calibration intervals and source.

Properties of native soil		
Parameter	Calibration interval	Source
Capillary suction head	10-454.66 [mm]	(Rossman and Huber 2016:114)
Initial deficit	0.31-0.34 []	(Rossman and Huber 2016:116)
Properties of the trench		
Parameter	Calibration interval	Source
Saturated hydraulic conductivity trench	20 000-200 000 [mm/hr]	Trial and error

The perforated pipes were not possible to model explicitly in SWMM, hence the chosen method for simulation of water exfiltrating through the perforated infiltration pipes contain uncertainty. A conceptual method was chosen where pumps were modelled to simulate the exfiltration. The pumping curve describing the relationship between the exfiltrated flow and the water depth in the infiltration pipes was calculated based on the wetted area and the saturated hydraulic conductivity of the trench. Whereas the wetted area, assumed to be the total area of perforations, was known, the saturated hydraulic conductivity of the trench was unknown and therefore set for calibration. Based on trial and error, the saturated hydraulic conductivity of the trench was assumed to be in the range of 20 000 to 200 000 mm/hr.

Green-Ampt is the infiltration method chosen in the model. The Green-Ampt method is based on three soil parameters, namely the saturated hydraulic conductivity, the capillary suction head and the initial deficit. There was uncertainty in the infiltration characteristics as no infiltrometer test had been conducted on the site. However, previous core drillings on the site have been reviewed by Sagli (2020), and the conclusion was a soil likely to consist of homogeneous material of sand and silt. A native soil consisting of sandy loam, loamy sand or sand was assumed.

Multiconsult designed the infiltration system based on the assumption that the native soil consisted of homogenic sand with saturated hydraulic conductivity of 3600 mm/hr (Multiconsult 2018). Based on the assumption that the soil was somewhere between sandy

loam, loamy sand or sand, the Hydrology SWMM manual estimated the saturated hydraulic conductivity to be in the range of 10.92 to 120.4 mm/hr. The deviation between the assumption of Multiconsult (2018) and the estimate from the SWMM manual was significant. As there is high uncertainty in regard of the infiltration characteristics, the assumption of Multiconsult (2018) was used as a fixed value during calibration.

The capillary suction head of the soil was assumed to have a calibration interval from 10 to 454.66 mm, including estimated suction heads for sand, loamy sand and sandy loam (Rossman and Huber 2016).

Initial deficit was described as the difference in soil moisture content at soil saturation and at the beginning of simulation (Rossman 2015; Rossman and Huber 2016). The hydrology SWMM manual contained estimates for initial deficit for a variation of soil types at dry condition. Since the soil in the studied area was assumed to consist of sand and silt, the calibration interval was assumed from 0.31-0.34 (Rossman and Huber 2016).

3.5 Performed simulations for combined system evaluation

The calibrated SWMM model was used in simulations aiming to investigate the performance of the combined system. Both event-based simulations using design precipitation events and long-term simulations using historical data were performed. Further, to evaluate the interaction between detention and infiltration, five model scenarios were developed illustrating different stormwater strategies. To address possible future system performance, simulations using a climate factor of 1.4 were performed and evaluated.

3.5.1 Developed simulation scenarios

To evaluate the performance of the combined infiltration and detention solution, five scenarios with different stormwater management strategies were developed for the purpose of comparison. All scenarios were developed based on the studied stormwater facility. Hence, all scenarios lead stormwater to manhole O1 where the stormwater was discharged downstream through the swirl chamber. Consequently, the outflow from the scenarios could be directly compared. The developed scenarios are shown in Table 8.

Table 8: Description of the fives developed model scenarios.

Scenario	Description
Scenario 0	Post-development with no stormwater management strategy. Inflow from the upstream sub-catchments equal the inflow to manhole O1.
Combined infil. and det.	Originally combined infiltration and detention solution.
Only detention	The infiltration pipes were neglected from the combined infiltration and detention solution. Hence, the model only contains the detention basins.
Only infiltration	The detention basins were neglected from the combined infiltration and detention solution. Hence, the model only contains the infiltration pipes.
Half exfil. capacity	Originally combined infiltration and detention solution, but with half exfiltration capacity.

One SWMM model was developed for each of the scenarios. One scenario was the calibrated version of the model developed in this thesis. Based on the calibrated model, all other scenarios were developed by only changing the model in between manhole O8 and O1. Figure 19 shows the SWMM model scenarios with their different build ups between manhole O8 and O1. A scenario 0 was developed to illustrate the consequence of no stormwater management, except for the swirl chamber. Inflow from the upstream sub-catchments equaled to the inflow to manhole O1. Further, to study the effect of the interaction between infiltration and detention, it was of interest to compare the combined performance with the performance of infiltration alone and detention alone. Consequently, one scenario of only detention and one scenario of only infiltration were developed. The scenario of only detention was developed to be a version of the original calibrated model without the infiltration pipes, hence only containing the detention basins. Further, the scenario of only infiltration was developed to only contain the infiltration pipes, where the detention basins were neglected from the original calibrated model. Lastly, a scenario identical to the originally combined infiltration and detention solution was developed but with half of its exfiltration capacity. Reducing the exfiltration to half is synonymous with reducing the pump capacity to half. Through reduced exfiltration, this scenario illustrates the performance of a combined infiltration and detention solution if clogging of perforations occurs or for a hypothetical system with half of the number of perforations.

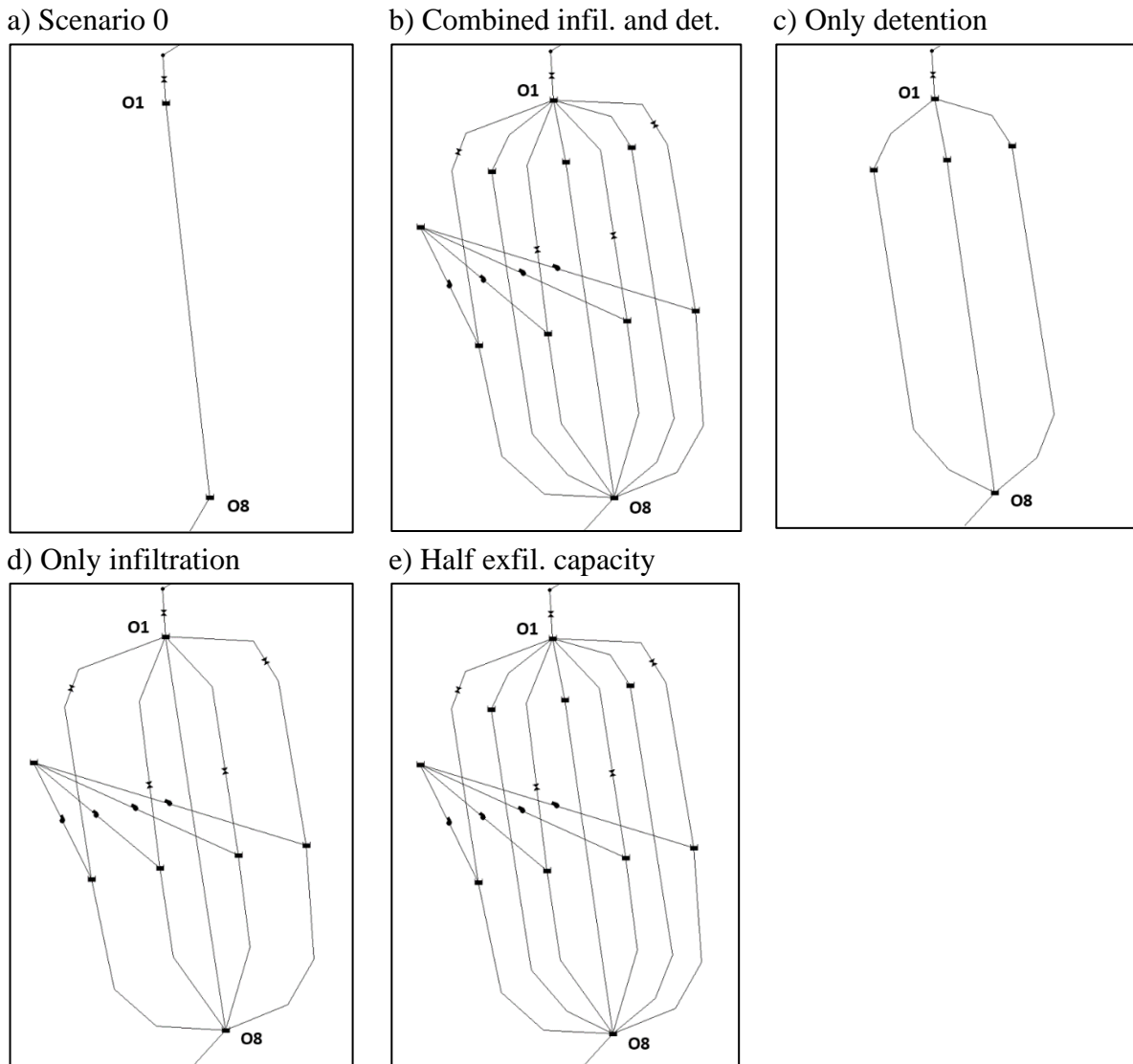


Figure 19: The developed model scenarios, a) scenario 0, b) originally combined infiltration and detention, c) only detention, d) only infiltration and, e) half exfiltration capacity.

3.5.2 Event-based simulations

The developed SWMM model of the stormwater facility was simulated against three design precipitation events. Return periods of 20, 100 and 200 years with duration of 60 minutes were chosen for simulations. A 20-year return period was chosen as it is often used as dimensional requirements for construction in developed areas. Further, were return period of 100 and 200 years chosen for simulations to get an indication of potential future system performance.

The design precipitation events were developed using the IDF-curve for Trondheim developed by Trondheim Municipality (Trondheim Municipality 2020). Further, development of the corresponding hyetographs was computed with 5 minutes time steps using the procedure described in Ødegaard et al. (2014:349–350). Appendix 16 shows the developed hyetographs. As the developed hyetographs were of 5 minutes time step, the recording time interval at the rain gage in the developed SWMM model was set to 5 minutes for the design events.

Table 9: Overview of the performed event-based simulations. The model scenarios used for the stated simulations are marked with ●.

Simulation	Soil condition	Scenarios				
		Scenario 0	Combined infil. and det.	Only det.	Only infil.	Half exfil. capacity
Design event 20-year return period.	Dry	●	●	●	●	
	Wet	●	●	●	●	
Design event 100-year return period.	Dry	●	●	●	●	
	Wet	●	●	●	●	
Design event 200-year return period.	Dry	●	●	●	●	
	Wet	●	●	●	●	

The main goal of the event-based simulations was to evaluate whether the developed model behaved as expected during precipitation events activation the detention basins. Especially in regard of the interaction between to the processes of infiltration and detention. The simulation results of the originally combined infiltration and detention solution was compared to results from model scenarios with only infiltration and only detention to investigate the effect of combining infiltration and detention. Further, were the simulated scenarios compared to the simulations results of scenario 0. Two simulations were run for each of the return periods per scenario. One for dry and one for wet soil. Wet soil was modelled as half exfiltration capacity through the infiltration pipes. Table 9 shows an overview of the performed simulations and which model scenarios included in simulations.

3.5.3 Long-term simulations

As the combined system was newly built, the long-term performance was unknown. Consequently, a long-term simulation was of interest as it could indicate system performance over time. Detention basin activations were the only way outflow could be generated from the system. The number of detention basin activations was therefore highly relevant, in addition to the generated outflow rates. This was especially relevant for Trondheim Municipality as the outflow from the combined system was discharged into the downstream combined sewer system. Comparing the long-term simulations for the five developed scenarios, the performance of the combined system regarding retention and detention of water could be evaluated. Long-term simulations with a climate factor of 1.4 were also performed to get an indication of future system performance. The climate factor was set equal to 1.4 as it is the recommended climate factor in Trondheim (Trondheim Municipality 2020). An overview of the performed long-term simulations is shown in Table 10.

Table 10: Overview of the performed long-term simulations. The model scenario used for the stated simulations are marked with ●.

Simulation	Scenarios				
	Scenario 0	Combined infil. and det.	Only det.	Only infil.	Half exfil. capacity
30 years of historical data	●	●	●	●	●
	●	●	●	●	●
30 years of historical data with climate factor 1.4	●	●	●	●	●
	●	●	●	●	●

Due to the newly installment of the tipping bucket close to the stormwater facility, local historical data at the city square was not available. However, the weather station a Risvollan contained long historical precipitation time series as it has measured since December 11th 1986 (Norsk Klimaservicesenter 2021b). Risvollan was located about 3.85 km away from the square, hence the climate at the two locations were assumed to be similar. From Risvollan, 30 years of precipitation data with 1 minute time step was used as input for the long-term simulations. Consequently, the recording time interval at the rain gage in the developed SWMM model was set to 1 minute for the long-term simulations. The 30 years were from January 1st, 1989, to January 1st, 2019. The precipitation during the 30 years, both without and with climate factor, are found in Appendix 17.

4 Results and discussion

This section presents and discusses the results of model calibration and validation. Further, the performance of the combined infiltration and detention system is evaluated based on the performed simulations. Lastly, a demonstration of the applicability of combined systems based on the developed SWMM model is stated.

4.1 Calibration

The model was calibrated against observed discharge in the period from July 1st to September 14th, 2020. The calibration result is shown in Figure 20, with a NSE equal to 0.41. The model underestimates the two observed outflow peaks. Further, the model simulates two outflow peaks when no outflows were observed.

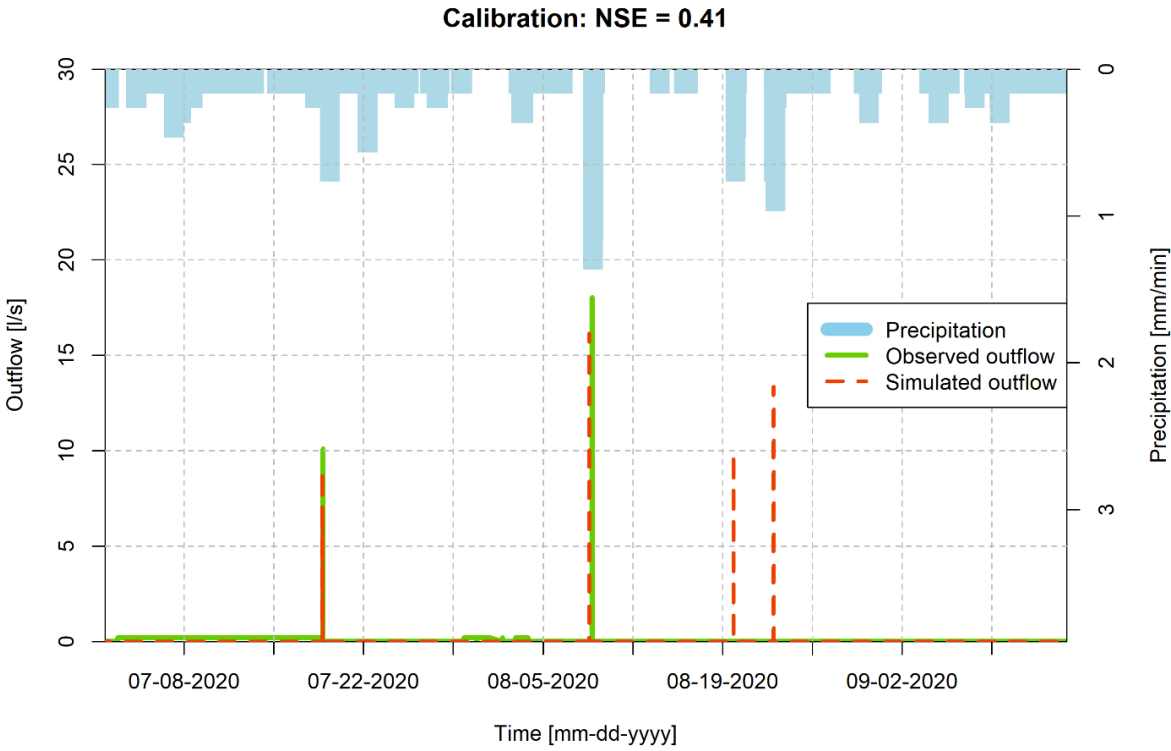


Figure 20: Result of calibration against observed outflow. Observed outflow in green and simulated outflow from calibrated model in dotted red plotted against the left axis. Precipitation in blue plotted against the right axis.

A NSE value of 0.5 is generally assumed to be acceptable (Dongquan et al. 2009). The obtained NSE of 0.41 is less than 0.5, hence the model cannot be assumed to be a well calibrated model. However, the model accomplishes to model the overall function of stormwater pilot. The main focus of this thesis in regard of modelling, is to model the performance of the combined system, hence the frequency and magnitude of detention basin activations. Figure 20 shows that smaller precipitation events are managed by exfiltration resulting in no system outflow, whereas only

the biggest precipitation events activate the detention basins and further lead to outflow. However, the model simulated 50 % more outflow occurrences than observed, in addition to underestimating the observed ones. The precipitation peaks occurring when outflow is simulated, but not observed, are equal or higher than the precipitation peak causing the first observed outflow. This might be because of reduced storage capacity in the trench and soil, due to more wet weather occurring before the precipitation peaks causing observed outflow compared to the ones only simulated. However, the deviation between simulated and observed outflows can also be explained by local variation in precipitation pattern between the city square and the weather station at Lade. Local variation can result in uncertainty in both time delay and magnitude. When looking at the precipitation peaks generating observed outflows, it is reasonable to predict outflow generation for the two precipitation peaks where the model simulated outflows. These two precipitation peaks might have been more intense at Lade than at the city square. Further, if the precipitation measured at Lade had occurred in the city square, four simulated outflow occurrences might have been observed.

The stormwater pilot is relatively newly constructed and has only one year of measured data. Hence, the available data for model calibration is limited. Through its lifetime, only two detention basin activations have been measured. The detention basin activations are the ones of interest as these are the ones generating outflow. Ideally, the developed SWMM model should have been calibrated against a period of several outflow occurrences. However, due to the absence of several detention basin activations, the calibration was performed on the available data. If the model had been calibrated against data including several outflow events in addition to the use of local precipitation, the preciseness of the detention activations is assumed to be better.

During the calibration process the challenge of equifinality was met as multiple sets of parameter value combinations gave the same NSE value. Equifinality gives uncertainty to the calibration and can be handled by reducing the parameter calibration ranges, for example through site measurements. Due to the time limitations of this thesis, site measurements have not been performed. The choice of parameter value combination focused on finding a combination not including extremes from the calibration ranges. The result of parameter calibration is shown in Table 11.

Table 11: Optimized parameter values for the calibrated parameters after calibration.

Result of parameter calibration	
Properties of the sub-catchments	
Parameter	Optimized value
n-imperv [-]	0.015
n-perv [-]	0.042
%Zero-Imperv [%]	52.32
Suction head [mm]	28.43
Saturated hydraulic conductivity [mm/hr]	2.57
Initial deficit [mm]	0.29
Properties of native soil	
Parameter	Optimized value
Suction head [mm]	223.63
Initial deficit [mm]	0.32
Properties of the trench	
Parameter	Optimized value
Saturated hydraulic conductivity [mm/hr]	70012.24

No complete sensitivity analysis has been performed. However, through trial and error the sensitivity of some of the parameters were evident. In regard of the sub-catchments, Manning roughness coefficient for both impervious and pervious area showed to be sensitive parameters in runoff generation. In regard of the stormwater pilot, the assumed saturated hydraulic conductivity of the trench showed to be highly sensitive for the amounts of water being exfiltrated, and further the system outflow. The saturated hydraulic conductivity of the native soil was seldom sensitive. Based in the incomplete sensitivity analyses, the saturated hydraulic conductivity showed to be sensitive for low values ranging from 1 to 20 mm/hr. Above 20 mm/hr the saturated hydraulic conductivity was of low sensitivity, and the saturated hydraulic conductivity of the trench was the sensitive factor in regard of system performance. As this study had the focus on detention basins activation, the saturated hydraulic conductivity of native soil was not highly prioritized as it seldom was the limiting factor of the model. Consequently, the saturated hydraulic conductivity of the native soil was not calibrated. Due to the low sensitivity, the assumed values by Multiconsult (2018) and the hydrology SWMM manual (Rossman and Huber 2016:114) of respectively, 3600 mm/hr and 120 mm/hr, both gave the same simulation results. Further, as no infiltrometer test has been performed and the uncertainty of the saturated hydraulic conductivity is high, the assumed value of 3600 mm/hr by Multiconsult (2018) was assumed in the model.

4.2 Validation

The calibrated model was validated from September 15th to November 15th, 2020. The validation resulted in a NSE equal to -0.64, shown in Figure 21. When NSE value is below zero, the mean of the observed data is a better estimate than the simulated data from the model (Krause et al. 2005), which is the case during the validation period.

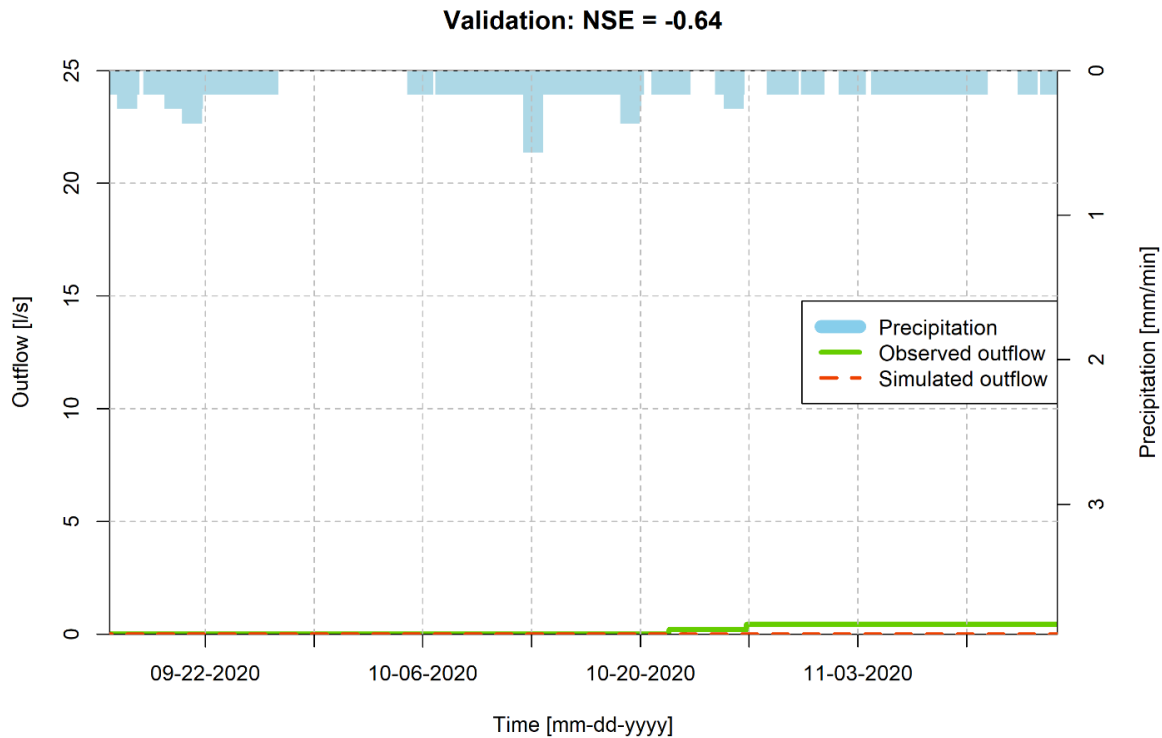


Figure 21: Result of validation period against observed outflow. Observed outflow in green and simulated outflow from calibrated model in dotted red plotted against the left axis. Precipitation in blue plotted against the right axis.

The model simulates no outflow, hence no detention basin activation, during the validation period. The reason behind the low NSE is the slight increase in observed outflow on October 21st which stays equal to 0.45 l/s until the end of the validation period. As the model simulates zero outflow throughout the validation period, once only some outflow is observed, the mean of the observed outflow is a better estimate than the simulated. The observed increase in outflow can be discussed. It is strange as no large precipitation event was measured on October 21st nor during the rest of the validation period, shown in Figure 21. Further, the fact that the observed outflow is constant equal to 0.45 l/s throughout the rest of the period is unexpected behavior. The increase might be due to error in outflow measurements, which can occur as a result of unintended movement of the sensor measuring water depth in manhole O1. Another explanation might be that the outflow did occur, but due to local variations, the precipitation initiating the outflow in the city square did not occur at the measurement station at Lade.

If the increase in observed outflow is due to error in data measurements, and the actual outflows were equal to zero throughout the validation period, the NSE from validation would have been equal to 1, which indicates perfect fit (Krause et al. 2005). Comparing the precipitation

occurring during the validation period and the calibration period, significantly fewer and smaller precipitation peaks occurred during the validation period. Based on the correspondence between precipitation peaks and observed outflow from the calibration period, the precipitation peaks in the validation period are not likely to cause system outflow.

Due to available data and the duration of this study, there was no other time period long enough to use for validation. Further, as uncertainty in data measurement is likely to be the reason for the low NSE value, not the model itself, the calibrated model is assumed to be good enough to simulate the overall function of the combined system. The calibrated model is therefore used for evaluation of the performance of the combined detention and infiltration solution. However, the model should be calibrated against more and local data in order to achieve a model to mirror the performance of the specific stormwater pilot located in the city center of Trondheim.

4.3 Evaluation of design precipitation events

Simulations of three design precipitation events were performed on the following scenarios:

- Scenario 0
- Originally combined infiltration and detention solution
- Only detention
- Only infiltration

The three design events were of 60 min duration for 20-, 100- and 200-year return periods. Simulations of the design precipitation events were run of both dry and wet soil. Figure 22 shows the simulated outflows from the performed simulations. The percent reduction in peak flow for each scenario compared to scenario 0 is showed in Table 12.

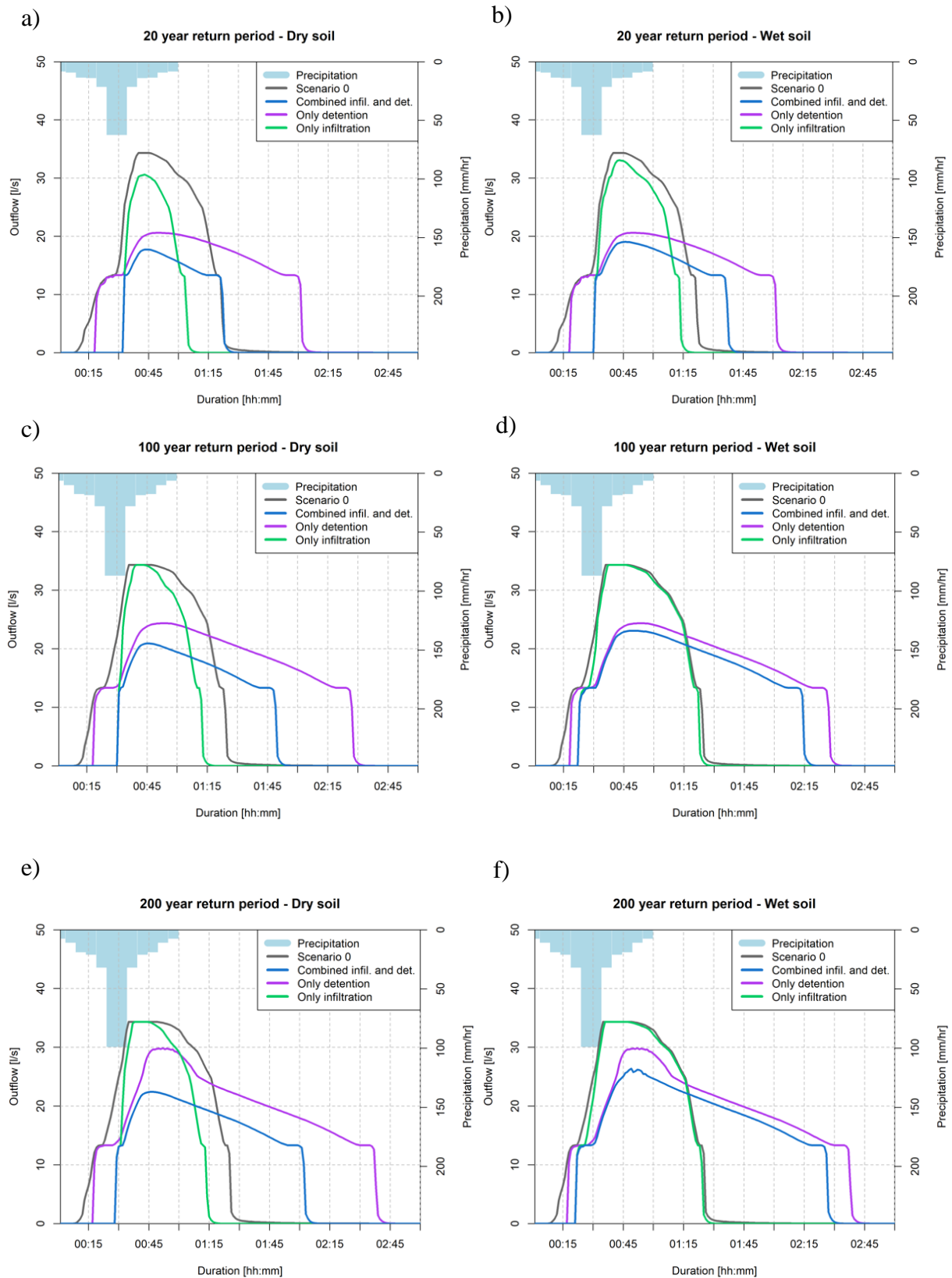


Figure 22: Simulated outflows for design events of a) 20-year return period with dry soil, b) 20-year return period with wet soil, c) 100-year return period with dry soil, d) 100-year return period with wet soil, e) 200-year return period with dry soil and f) 200-year return period with wet soil.

Table 12: Percent reduction in peak flow for the event-based simulations of scenarios compared to scenario 0.

Simulation	Soil condition	Reduction of peak outflow [%]		
		Combined infil. and det.	Only detention	Only infiltration
20-year return period	Dry	48.3	40.0	10.8
	Wet	44.5	40.0	3.6
100-year return period	Dry	39.0	29.0	0.0
	Wet	32.7	29.0	0.0
200-year return period	Dry	34.6	13.0	0.0
	Wet	23.1	13.0	0.0

The trends of the simulated outflows for each of the scenarios are evident during the three design precipitation events. The differences are in outflow magnitude and outflow duration. As the return period increases, increases both the outflow peak and the time of outflow generation.

Scenario 0 shows the simulated outflow if no stormwater managements are installed upstream of the swirl chamber. It is used for performance comparison of the other scenarios including stormwater management. As expected, scenario 0 is the first scenario to start outflow generation and does in all simulations reach the maximum outflow of 34.33 l/s.

Comparing the scenarios with stormwater management, the general trend is that outflow from the scenario of only detention is the first to start outflow generation. This is expected as the scenario of only detention is the only scenario without infiltration. Hence, the scenario of only detention starts outflow generating once it experiences inflow, no stormwater is retained. Further, does simulated outflow from the scenario of combined infiltration and detention system and the scenario of only infiltration equally start outflow generation sometime after precipitation start. The delay in outflow generation illustrates the effect of the infiltration process. The impact of the detention basins can be seen by studying the difference between the combined infiltration system and only infiltration. Stormwater starts to accumulate in the detention basins when outflow from the scenario of only infiltration exceeds the outflow from the combined system. This trend shows the 3-step-approach in practice. The combined infiltration and detention solution shows to include both step one and step two solutions. As incoming stormwater exceeds the infiltration capacity, step one, the detention basins, step two, are activated (Lindholm et al. 2008).

The effect of the detention basins is evident as the combined system delays the outflow and releases it at a lower rate over a longer time span. In comparison, does the scenario of only infiltration releases all incoming water directly after the exfiltration rate is exceeded. Consequently, a higher outflow rate and faster reaching of end of outflow generation are achieved. These results agree with the findings of Damodaram et al. (2010), where LIDs alone are not adequate in reducing the biggest flow peaks during larger precipitation events, but that conventional detention-based solutions manage to obtain a bigger reduction in peak flow for these larger events. Further, by comparing the simulations of the return periods, the shapes of

outflow curves from the combined system and the scenario of only detention have the same pattern. This is assumed to be the pattern of outflow generated from the detention basins. Another difference among the simulated scenarios is in regard to outflow volume. The scenario of only infiltration and the combined system are retaining water through infiltration, hence reducing outflow volume. The scenario of only detention, on the other hand, does only delay water, hence the total volume of the incoming water equals the volume of the generated outflow.

In regard of simulations with wet soil, it should be noted that the scenario of only detention and scenario 0 are unaffected by the soil moisture as they do not have any natural processes implemented. However, for the scenarios of only infiltration and the combined system, changes are observed as the soil moisture changes from dry to wet. Comparing simulations of dry and wet soil, the main difference is in regard of outflow volume. For wet soil, less water is retained through infiltration, leading to increased outflow volume compared to dry soil. Additionally, an increase of outflow peaks is simulated with wet soil. A further consequence of reduced infiltration through wet soil is that the time until the start of outflow generation for the scenarios including infiltration is reduced. Hence, less stormwater is needed before the infiltration capacity is exceeded.

The results of the event-based simulations show that the developed model behaves as expected. The infiltration system manages to retain stormwater until its capacity is exceeded. Through combining infiltration with the detention basins, the largest flood peaks are avoided, and stormwater is detained and released at a lower rate over a longer time span. Compared to scenario 0, the scenario of only detention reduces peak outflow, whereas only infiltration only achieves peak reduction for simulations with 20-year return period. For all simulated return period, the combined system gives the biggest reduction in peak outflow. The highest reduction was achieved for 20-year return period with dry soil equaling 48.3% compared to scenario 0. These results agree with the simulation results by Xian et al. (2021), which also found that combined solutions of LID and BMP gave the largest reduction in flow peak compared to LID and BMP separately. Reduction in peak flow due to combining LID with detention-based solution does also agree with the findings of (Damodaram et al. 2010; Eckart et al. 2017; Kristvik et al. 2019).

Flooding occurred for scenario 0 during all event-based simulations. The scenario for only infiltration flooded during simulation of 100- and 200-year return period, for both dry and wet soil. Flooding is indicated as the maximum outflow of 34.33 l/s is reached, shown in Figure 22. Flooding results in simulated outflow volumes that are less than the actual volume going out of the system. Directly comparing the outflow volumes between flooded and not flooded scenarios will not be directly comparable. However, the scenario of only detention nor the combined system flooded for any of the design events. The combined system reduced both the peak outflow and the duration of outflow more than the scenario of only detention. Thus, the combined system showed highest resilience against design events of increasing return period.

4.4 Evaluation of long-term system performance

For the long-term continuous simulations, a historical precipitation time series of 30 years from the weather station at Risvollan is used. The 30 years of data are from January 1st, 1989, to January 1st, 2019. Simulations were performed using the original historical precipitation data in addition to running simulations of the historical precipitation data with a climate factor of 1.4. Simulations are performed on the five developed model scenarios.

4.4.1 Detention basins activations

The occurrence of detention basin activation is necessary for outflow to be generated from the combined system. Consequently, the frequency of detention basin activations throughout a continuous simulation is relevant knowledge. It is especially relevant for the Trondheim Municipality regarding the discharge from the combined system onto the downstream combined sewer system.

The 30 years of historical precipitation data was given as input to the developed and calibrated SWMM model of the combined infiltration and detention system. Data from the continuous simulations of pure historical data are shown in Figure 23 plot a) and c). Figure 23 Plot a) shows the simulated water depth in manhole O8. The detention basins are activated as the water depth in manhole O8 exceeds 2.34 m, illustrated by the red dotted line in the plot. To better visualize the simulated detention basin activations throughout the 30 years, the water depth in one of the detention basins are showed in Figure 23 plot c). Through the continuous simulation the basins are activated in total 64 times, resulting in an average of 2.1 activations per year. The combined system has been monitored for about one year of which only two detention basins activations have been observed. Consequently, is the simulated average of 2.1 activation per year a reasonable result. Notice that the maximum depth of the detention basin, 2 m, is never reached. The largest measured water depth is only filling half of the detention basin equaling 1 m. Between the year 1995 and 2001, no detention basin activations occurred. This is a deviation from the rest of the simulated time period where activations occurred on a somewhat periodically term. The precipitation used for the continuous simulation can be found in Appendix 17. Less precipitation was measured in the years 1995-2001 compared to the rest of the data series, something that explains the lack of basin activation during these years.

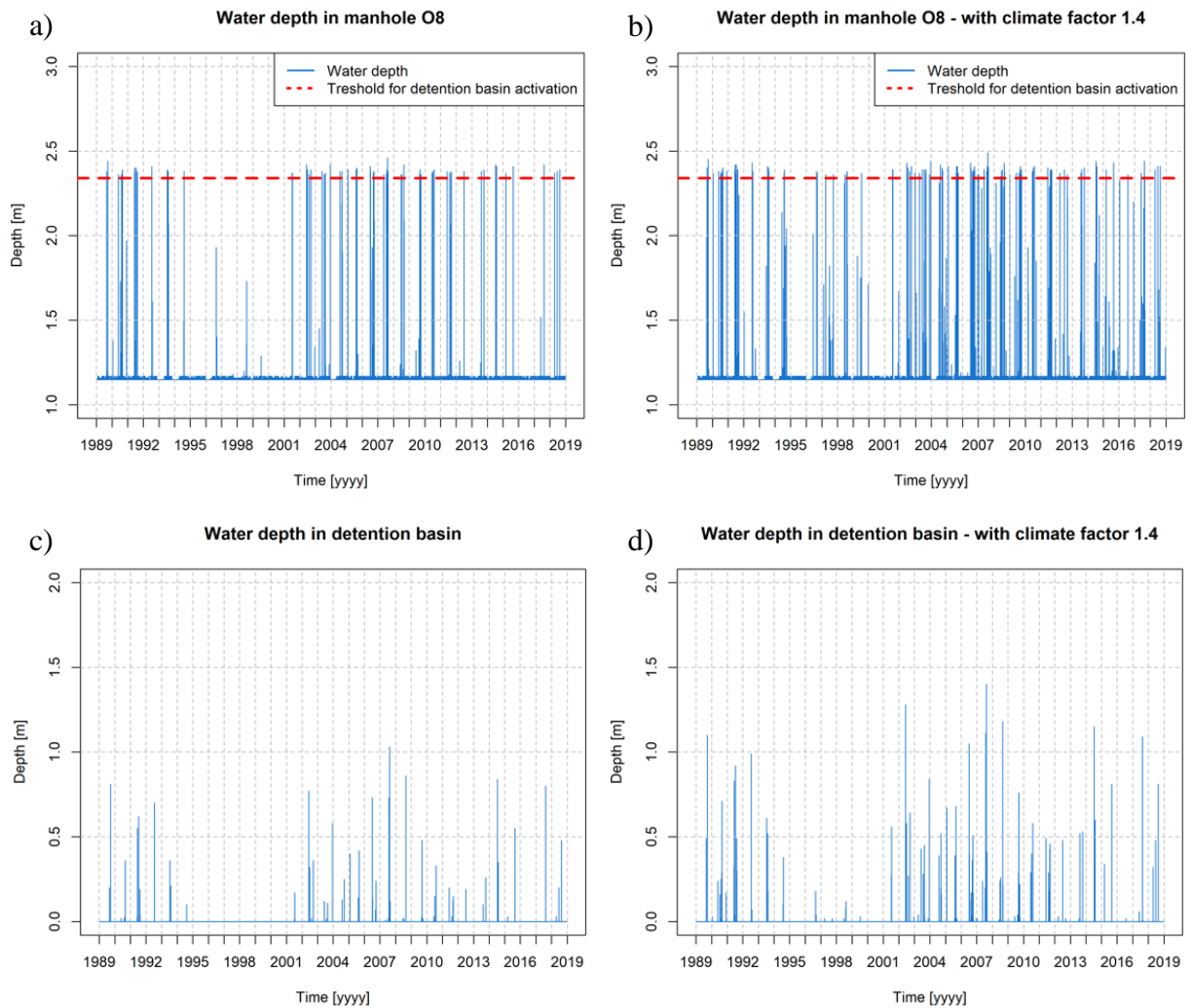


Figure 23: Water depths from result of continuous simulation in a) manhole O8 for simulation without climate factor, b) manhole O8 for simulation with climate factor, c) detention basin for simulation without climate factor and d) detention basin for simulation with climate factor.

Simulation result of the same 30 years but with a climate factor of 1.4 is also shown in Figure 23 plot b) and d). Plot b) shows the water depth in manhole O8, further does plot d) show water depth in one of the detention basins. Compared to the water depths simulated on pure historical precipitation data, the ones simulated with a climate factor have a higher frequency of water accumulating above the infiltration pipes in manhole O8, in addition to the number and intensity of detention basin activations. During the 30 years simulated with a climate factor, the detention basins were activated 90 times. Resulting in an annual average of 3 times. During both the simulations with and without climate factor the detention basins never reached the maximum depth of 2 m. Pure historical data gave the highest depth of just above 1 m, whereas the simulation with climate factor gave a maximum depth of 1.4 m.

Looking at Figure 23 plot c) and plot d), much of the detention basin volumes remains empty during the simulations. Thus, due to the capacity of the detention basins, the combined system was never flooded through the either the simulation with or without climate factor. The fact that the basins on average only are activated 2-3 times a year and never reaches maximum depth indicates conservative dimensions. However, if a conservative design can avoid downstream

damages, for example in the form of basement flooding, the additional cost of conservativity might be the cheapest solution in monetary terms. Further, as higher intensity precipitation events are expected due to climate change, the until now unused detention volume may be necessary in order to reduce or avoid downstream future floods. Through simulations of future climate scenarios Kristvik et al. (2019) found that all scenarios gave increase in required detention basin volumes. For a case study of a detention basin in Trondheim the needed volume increased with 100 % for the maximum future climate scenario (Kristvik et al. 2019). Based on this research, the dimensioned detention basin volume indicates to be needed in regard of future climate. However, the simulation result of using a climate factor of 1.4 on historical data in this thesis did not require 100 % increase in detention basin volume.

When designing a stormwater solution combining natural processes with conventional methods, the performance of the natural processes is often challenging to predict due to local variations. The characteristics of the soil must be well known in order to achieve a good prediction of infiltration. Combining LIDs with a detention basin can reduce the required detention basin volume (Kristvik et al. 2019), but to what degree is locally dependent. In the studied combined infiltration and detention system, the infiltration process performs successfully as it captures all frequent precipitation events whereas only the events of higher magnitude exceed the infiltration capacity (2-3 times per year). Thus, a possibility is that the characteristics of the local infiltration process was underestimated and reduces the required detention basin volume more than predicted.

4.4.2 Evaluation of combining infiltration and detention

All the developed model scenarios were run against the 30 years of historical precipitation data without and with climate factor. The model scenarios are the following:

- Scenario 0
- Originally combined infiltration and detention solution
- Only detention
- Only infiltration
- Half exfiltration capacity

The simulated outflows are shown in Figure 24 as flow duration curves. Figure 24 plot a) shows simulated outflow generated without climate factor and Figure 24 plot b) shows simulated outflow generated with climate factor. The flow duration curves show the number of hours throughout the 30 years that specific outflows were simulated. Table 13 and Table 14 show the percent reduction in peak outflow and the reduction in number of hours simulating outflow from the different stormwater management scenarios compared to scenario 0.

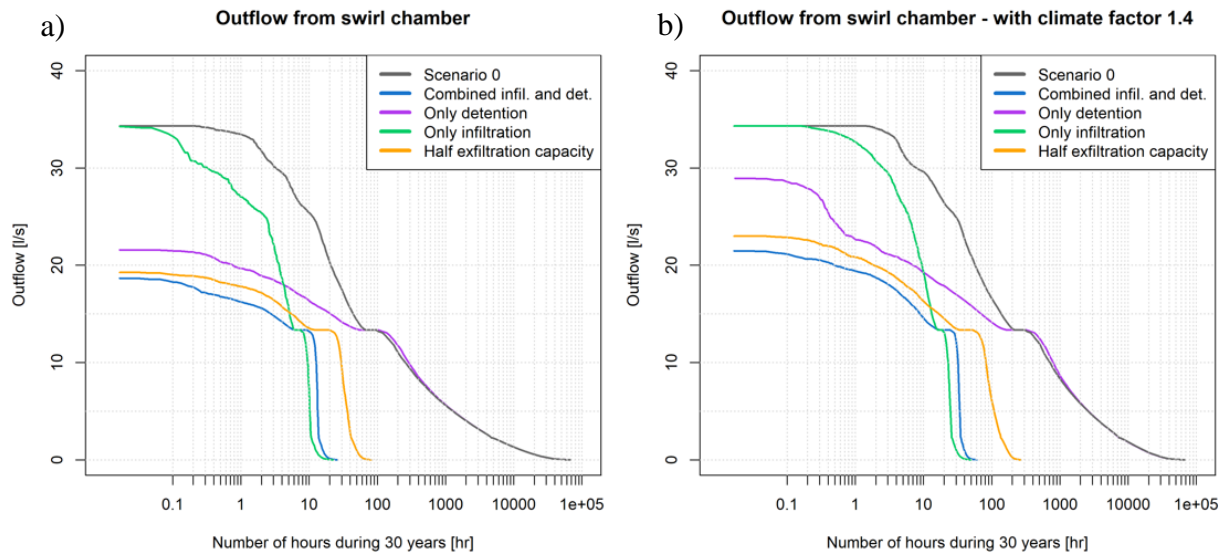


Figure 24: Continuous simulated outflows from the swirl chamber for the five scenarios presented as flow duration curves for simulation a) without climate factor and b) with climate factor.

Stormwater management aims to retain, delay and control stormwater (Ødegaard et al. 2014). Thus, as expected does scenario 0, with no stormwater management, generate the largest outflows for the highest number of hours throughout the 30 years compared to the other scenarios. Comparing the five flow duration curves, similar behavior is observed as they all flatten out around 13-14 l/s. Investigating the plotted data, the outflow simulated for the highest number of hours was for all scenarios equal to 13.35 l/s. The swirl chamber in manhole O1, which was included in all scenarios, is likely to be the cause of this. The aim of the swirl chamber is to regulate outflows. For water depths between 0.381 to 0.512 m above the outlet orifice of the swirl chamber, outflow equal to 13.35 l/s is generated, Appendix 14. The range of 0.381 to 0.512 m is the longest range generating the same outflow from the swirl chamber. Consequently, the trend of flattening out at 13.35 l/s is visible for both the simulation without and with climate factor. Further, is the cause likely to be due to the characteristics of the swirl chamber and not the size of the most frequent detention basin activation. If the size of the most frequent detention basin activation was the cause, the simulation with climate factor would have flattened out on a higher outflow value than for the simulation without climate factor. However, a water depth between 0.381 to 0.512 m above the outlet orifice is no significant water accumulation. It can be assumed to be caused by not only the largest detention basin activations, but also the more frequent ones. Hence, the trend of flattening out at outflow equal to 13.35 l/s is due to the characteristics of the swirl chamber, but also due to detention basin activations resulting in water levels in manhole O1 in the range of 0.381 to 0.512 m above outlet orifice of the swirl chamber.

Table 13: Percent reduction in peak flow for the long-term simulations of scenarios compared to scenario 0.

Simulation	Reduction in peak outflow [%]			
	Combined infil. and det.	Only detention	Only infiltration	Half exfil. capacity
Without climate factor	45.6	37.1	0.1	43.9
With climate factor	37.4	15.6	0.0	33.0

Table 14: Percent reduction in hours simulating outflow for the long-term simulations of scenarios compared to scenario 0.

Simulation	Reduction in hours simulating outflow [%]			
	Combined infil. and det.	Only detention	Only infiltration	Half exfil. capacity
Without climate factor	99.96	0.02	99.97	99.88
With climate factor	99.91	0.26	99.93	99.61

The effect of the processes of both infiltration and detention is evident based on the simulated flow duration curves. Notice that the two scenarios without detention basins, scenario 0 and only infiltration, do not manage to reduce the peak outflow as much as the scenarios having detention basins. This trend is most evident for the simulations without climate factor where the scenario of only detention reduces the peak outflow by 37.1 % compared to the reduction of 15.6 % for simulation with climate factor. Consequently, the use of detention is shown to reduce the peak outflow, agreeing with the findings of Damodaram et al. (2010). However, the scenario of only detention together with scenario 0 are the ones generating outflow for the longest period of time. Without climate factor, the scenario of only detention simulated outflow for 68 360 hours, and with climate factor a number of 68 913 hours generated outflow throughout the 30 years. The use of detention basins is showed to delay the stormwater runoff, hence reducing the outflow peak, but the same volume is still released. As a result, outflow will occur at a lower rate for a longer period of time. Moreover, will the outflow take up a fraction of the downstream combined sewer capacity for a longer time. Further, as the stormwater is led to the treatment plant at Høvringen, the stormwater from the city square might take up treatment capacity needed for actual sewage for a longer time.

The effect of infiltration is visible as the two scenarios without infiltration, scenario 0 and only detention, have a significant higher number of hours simulating outflow compared to the ones with infiltration. The scenario of only infiltration has the lowest number of hours simulating outflow. Comparing the scenario of only infiltration with scenario 0, the number of simulated hours is reduced by 99.97 % and 99.93 % for respectively simulation without and with climate factor. Thus, the use of infiltration is showed to reduce the number of hours simulating outflow.

However, the scenario of only infiltration simulates low reduction of peak outflow. Simulation without and with climate factor gives peak outflow reduction of respectively 0.1 % and 0.0%.

Once system inflow exceeds the rate of infiltration, the scenario of only infiltration performs with a trend similar to scenario 0. Even though infiltration alone has a big impact on the number of hours generating outflow, the highest outflow peaks are not avoided. This finding agrees with Damodaram et al. (2010) and Xian et al. (2021) who also concluded that infiltration alone is not adequate for reducing the largest flood peaks. Further, as the outflow is discharged onto the downstream combined sewer system, high outflow peaks, even for short durations, can cause large damages downstream. Potential damages are CSO emissions and flooding of streets and basements.

Infiltration combined with detention shows a significant reduction in both the peak outflow and the number of hours simulating outflow. The combination of infiltration and detention is successful as it benefits from both processes. Lower peak outflows and shorter outflow duration relieves stress on the downstream combined sewer system. Comparing the scenario of the originally combined infiltration and detention to scenario 0, the reduction in peak outflow is 45.6% and 37.4% for respectively simulations without and with climate factor. The combined system gives the highest reduction in peak flow compared to the other scenarios for both simulations with and without climate factor. The reduction in the number of hours simulating outflow is for the simulation without climate factor equal to 99.96%, and for the simulation with climate factor equal to 99.91%. As climate factor is added, the incoming flow is intensified, hence is an increase in the peak outflow and the number of hours simulating outflow expected.

Notice that the number of hours simulating larger outflows for the scenarios of only infiltration and only detention significantly increases with climate factor applied. Further, that the most evident change after climate factor is applied is the increase in outflow peak for the scenario of only detention, where outflow peak reduction decreases from 37.1% to 15.6%. This weakens the evident effect of detention basins from the simulations without climate factor as the outflow peak now is in closer distance to peak outflow from the two scenarios without detention basins compared to the other two scenarios with detention basins. Looking at the scenarios combining infiltration with detention, a lower decrease in peak outflow reduction is simulated. Thus, the effect of combining infiltration with detention is showed to be highly efficient in creating resilience against climate change as the combined systems gives higher reduction of outflow peak compared to only detention.

The scenario of half exfiltration capacity is developed with the goal to evaluate performance due to possible clogging of the perforated pipes in the combined system. Figure 24 shows that it has the same outflow trend as the originally combined infiltration and detention solution. Comparing the two flow duration curves, the biggest deviation is the number of hours with simulated outflows. Without climate factor, the scenario with half exfiltration capacity does only have an outflow peak of 0.6 l/s higher than the originally combined detention and infiltration scenario, whereas the difference in hours simulating outflow is 40. As the process of infiltration is showed to influence the number of hours simulating outflow, the number of hours is expected to be the biggest deviation as the only difference between the two scenarios

is the exfiltration rate. The two flow duration curves deviate the most for outflows smaller than 13.35 l/s. As outflow decreases, the volume reduction due to infiltration gets increased impact on the generated outflow. When reducing the exfiltration to half, the infiltration capacity is reduced to half and further is the impact on volume reduction reduced to half. Consequently, is the deviation for smaller outflows explained as the difference in exfiltration capacity is most evident for smaller outflows. This is likely to occur either as detention basins empties after a high intensity precipitation event or during the more frequent precipitation events of lower intensity. Compared to the other scenarios, the outflow performance of clogged and unclogged combined infiltration and detention systems are similar. Clogging of perforations causes a slight increase in peak outflow, but the biggest change is in number of hours simulating outflow. Conley et al. (2020) found that clogging of infiltration systems increases over time and that accumulation of sediments in the infiltration systems reduces the infiltration process. The scenario of half exfiltration capacity has constantly equal clogging rate, causing limitation of the developed scenario as the true clogging development will increase over time.

The maximum possible outflow before flooding is 34.33 l/s. Throughout simulation of the 30 years without climate factor, flooding only occurred for scenario 0. Flooding of scenario 0 occurred once during a precipitation event on August 13th, 2007. The event lasted for 35 minutes and in total was 12.2 mm precipitation measured. According to the IDF-curves developed for Trondheim in 2020, this event corresponds to a 10 year return period precipitation event (Trondheim Municipality 2020). However, according to the previous IDF-curve for Trondheim (Moholt, Tyholt) from 2015 developed by Trondheim Municipality (Trondheim Municipality 2015), the precipitation event of August 13th 2007 corresponds to an event with return period in between 50 to 100 years. For the simulations with climate factor, flooding during the same event occurred for both scenario 0 and the scenario of only infiltration. All flooded water flooded through manhole O1. The combined systems do not flood during the simulations of the 30 years with or without climate factor. Hence, the capacity is sufficient for the simulated precipitation time series.

4.4.3 Threshold for system outflow

When evaluating the performance of the combined infiltration and detention system it was of interest to investigate the consequences of the generated outflows. This is especially relevant as the outflow from the system is discharged onto a combined sewer system. If the capacity of combined sewer systems exceeds, CSO emissions and flooding of streets and basements are potential outfalls. In communication with Trondheim Municipality, it was addressed that no specific outflow causing downstream damages if exceeded is known. Despite the lack of knowledge in regarding specific outflows, the generated outflows from the city square will affect the downstream combined sewer system.

Comparison with pre-developed surface runoff is a common method within stormwater management. The pre-developed surface runoff from the city square was computed for a precipitation event with return period of 20 years and duration of 30 min. Further, using the rational formula with the area of the generated sub-catchments and a runoff coefficient of 0.3, a pre-developed outflow of 15 l/s was computed. To get an indication of the consequences of the generated outflows, the computed pre-developed outflow was compared with the

continuous outflow simulations without and with climate factor, respectively plot a) and plot b) in Figure 25.

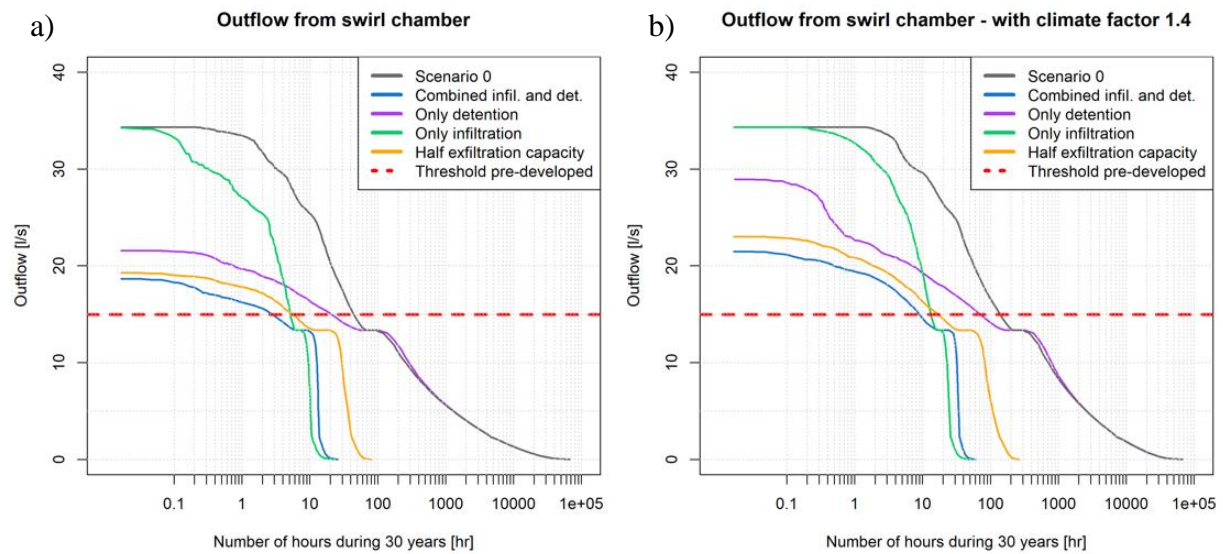


Figure 25: Continuous simulated outflows from the swirl chamber for the five scenarios presented as flow duration curves compared with a threshold for pre-developed surface runoff for simulation a) without climate factor and b) with climate factor.

Table 15: Percent reduction in the number of hours generating outflow above pre-developed threshold compared to scenario 0.

Simulation	Reduction in number of hours above pre-developed threshold [%]			
	Combined infil. and det.	Only detention	Only infiltration	Half exfil. capacity
Without climate factor	94.4	55.5	88.9	88.9
With climate factor	94.0	53.3	90.7	88.0

Scenario 0 has 45 hours with outflow higher than 15 l/s during the 30 years of simulation without climate factor and 150 hours with climate factor. In comparison, gives all other scenarios reduction in the number of hours where 15 l/s is exceeded. The percent reduction is shown in Table 15. The biggest reduction in hours is achieved by the original combined infiltration and detention solution during both the simulation with and without climate factor with respectively 94.0 % and 94.4 %.

As the threshold for outflows exceeding the capacity of the downstream sewer system is unknown, another potential threshold is addressed. The outflow from the combined infiltration and detention solution is through the combined sewer system led to a pumping station (PA34 Frostakaia) pumping sewage and stormwater to the treatment plant at Høvringen. Based on input from Trondheim Municipality, the pump has a capacity of 30 l/s. In total, the pumping station receives water from an area of 0.31 km², where about 0.21 km² is impermeable area.

The generated area in ArcMap draining water from the city square to the stormwater facility is 6319.189 m² impermeable area. This area is 3 % of the impermeable area the pump receives water from. Accounting for some water from the remaining permeable area of 0.01 km², the water from the city square is assumed to account for 2.8 % of the capacity of the pump. Further, it is assumed that if the 2.8 % is exceeded, the capacity of the pump is exceeded. However, there are some uncertainties to this assumption as local variations in precipitation patterns are expected, additionally that water draining to the pumping station from the upstream areas are likely to have different traveling time. Hence, the drained water might not reach the pumping station at the same time. Consequently, the assumption is conservative as water from all drainage areas are assumed to arrive at the same time with equal precipitation occurrences.

Figure 26 plot a) and b) shows the simulated flow duration curves in combination with the assumed maximum flow that the city square accounts for in the downstream pumping capacity for respectively simulation without and with climate factor. Assuming that the combined stormwater facility accounts for 2.8 % of the 30 l/s pumping capacity, maximum flow equals to 0.84 l/s.

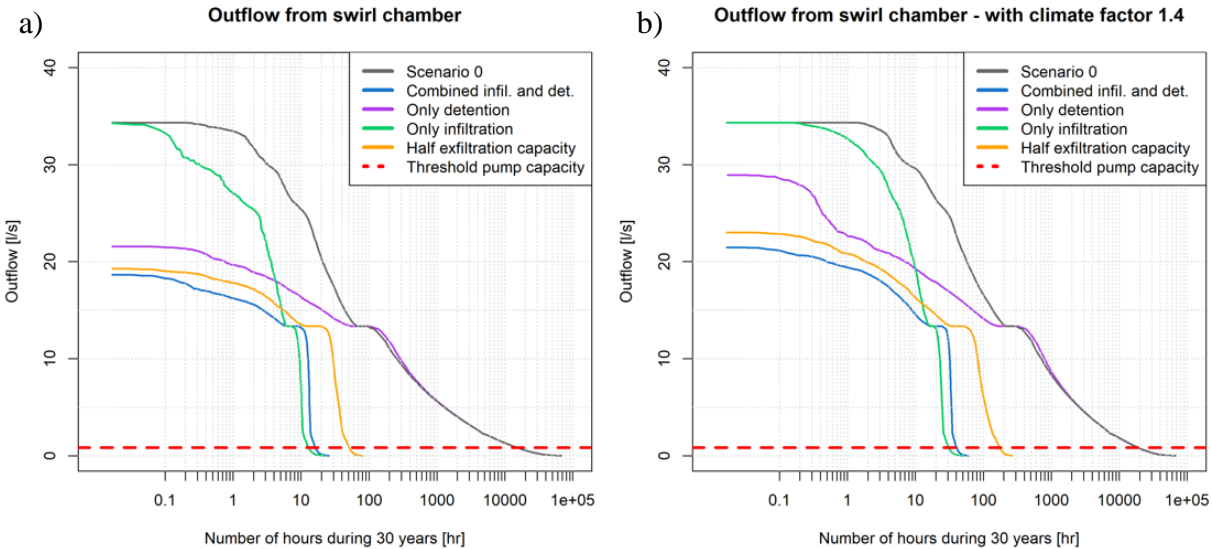


Figure 26: Continuous simulated outflows from the swirl chamber for the five scenarios presented as flow duration curves compared with a threshold for downstream pump capacity for simulation a) without climate factor and b) with climate factor.

Table 16: Percent reduction in the number of hours generating outflow above the pump capacity threshold compared to scenario 0.

Simulation	Reduction in number of hours above pump capacity threshold [%]			
	Combined infil. and det.	Only detention	Only infiltration	Half exfil. capacity
Without climate factor	99.9	0.0	99.9	99.7
With climate factor	99.8	0.0	99.9	99.1

An outflow of 0.84 l/s is a low system outflow where the number of hours simulating outflow varies widely depending on the model scenarios. Scenario 0 and the scenario of only detention does both have 15 000 and 20 000 hours with outflow above 0.84 l/s for respectively simulation without and with climate factor. Table 16 shows the percentages the different scenarios reduce the number of hours above outflow threshold. In the case of threshold to the downstream pumping station, the scenario of only infiltration gives be biggest reduction. However, it is tightly followed by the originally combined system and the combined system with half exfiltration capacity. The scenario of only detention does not reduce the time of exceedance at all compared to scenario 0. Even though the scenario of only infiltration gives the biggest reduction in time generating threshold exceedance, it does also generate large outflows. These large outflows cause bigger downstream floods compared to the peak outflows from the combined systems.

In regard of both the addressed outflow thresholds, the implementation of the combined infiltration and detention solution significantly reduces the number of hours exceeding outflow threshold in addition to reducing the magnitude of the downstream floods.

4.5 Design guideline for design exfiltration flow

With the assumption that the developed SWMM model mirrors the actual function of the combined infiltration and detention solution, it can be used for design guideline development. The use of exfiltration through infiltration pipes is not widely used in stormwater management, hence a guideline describing exfiltration rates are useful for both municipalities and consultants. To demonstrate how the result of the developed model can be used in future system designs, the relation between pipe length and the corresponding design flow for exfiltrated stormwater depending on the number of pipe perforations are found.

During model development, a conceptual value of saturated hydraulic conductivity in the trench was calibrated to 70 012 mm/hr. With the assumption that this is a value correctly describing the characteristics of the trench, it was used for guideline demonstration. The flow of exfiltrated water to the trench are computed using Equation (11):

$$Q_{Exfil} = K_{Sat,Trench} * A_{Wetted\ per\ meter} * L \quad (11)$$

Where,

$K_{Sat,Trench}$ = Saturated hydraulic conductivity of the trench [mm/hr]

$A_{Wetted\ per\ meter}$ = Total area of wetted perforations per meter [m^2/m]

L = Length of infiltration pipe [m]

For higher applicability, the relation is presented in a table for a collection of chosen lengths and numbers of perforations, Table 17.

Table 17: Developed design guideline relating design exfiltration flow to pipe lengths depending on the number of perforations per meter.

Pipe length [m]	Exfiltrated flow [l/s]		
	Number of perforations per meter		
	300	600	900
5	1.1	2.6	4.0
10	2.2	5.1	8.0
15	3.3	7.7	12.0
20	4.4	10.3	16.1
25	5.5	12.8	20.1
30	6.6	15.4	24.1
35	7.7	18.0	28.1
40	8.8	20.5	32.1
45	9.9	23.1	36.1
50	11.0	25.7	40.1
55	12.1	28.2	44.1
60	13.2	30.8	48.1

In the studied exfiltration system underneath Trondheim city square, the infiltration pipes have 300 perforations per meter. There are four perforations in one cross section which are located top, bottom, and both sides resulting in four rows of perforations along the pipe. Per meter, one row has 75 perforations. As this is a constructed and built system, the number of 75 perforations per row per meter is assumed to not reduce the strength of the pipe. Thus, the design guideline development is based on 75 perforations per row per meter pipe length. Three perforation alternatives are suggested varying the number of perforation rows, hence the number of perforations per cross-section. The cross-sections of the perforation alternatives are shown in Figure 27. Alternative 1 is identical to the one in the studied system with 300 perforations per meter and four perforations per cross-section. Next, alternative 2 has a cross-section with eight perforations, resulting in 600 perforations per meter. Lastly, alternative 3 is a cross-section with 12 perforations, hence a total of 900 perforation per meter.

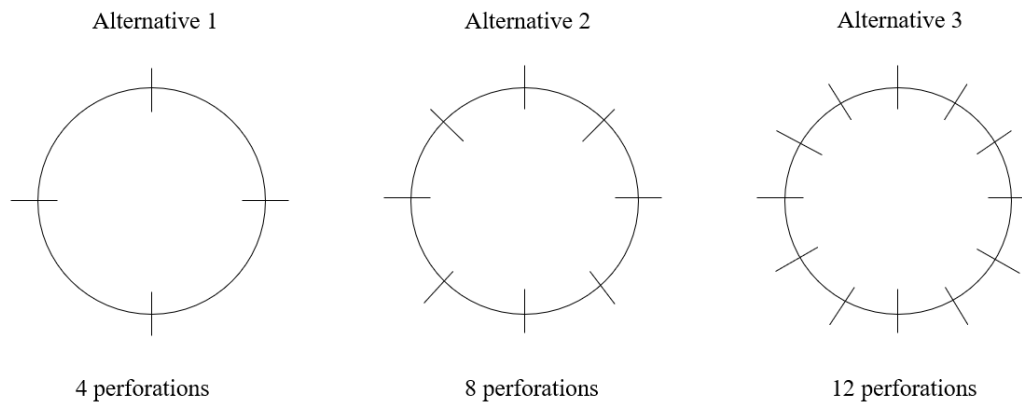


Figure 27: Illustration of the three developed perforations alternatives used for guideline development.

The table does only account for pipes with diameter equal to 0.16 m, which are the dimension the SWMM model was developed for. The very top perforation in each cross-section alternative is assumed to be less effective compared to the rest. Calculation of the design exfiltration flow does not account for exfiltration through the very top perforation. Hence, the design exfiltration flow for alternative 1 is generated for 75 % of the perforations, 87.5 % for alternative 2, and 91.2 % for alternative 3. A limitation of the guideline is that it does not address for exfiltration dependent on water pressure. A simplification of neglecting water pressure was done during model building, hence it is also a simplification in the guideline demonstration. However, the water pressure is to some degree indirectly included in the calibrated value for saturated hydraulic conductivity. The developed design guideline can be used by developers evaluating whether an exfiltration system is suitable for specific sites. As the developers know the stormwater amount needed to retain on site, the needed pipe length can be addressed, and evaluated whether it can be implemented on site in regard of local spatial limitations. Further, if the available trench length is limited, a cross-section with increased number of perforations can be considered.

5 Conclusion

A model of a full-scale combined infiltration and detention solution was developed in SWMM, and further calibrated and validated against available data. The modelled stormwater facility was located in the city center of Trondheim, Norway. SWMM was the chosen stormwater model for model development. It is a widely used stormwater model that can combine stormwater draining from catchments to stormwater structures, in addition to be an open-source software. However, there was no explicit function to model perforated pipes in SWMM. Pumps were used to simulate exfiltration from the perforated pipes to the voids of the trench. Further, were the voids of the trench modelled as a storage unit with a seepage rate simulating infiltration to the native soil. Calibration and validation of the developed SWMM model against the available data resulted in NSE of respectively 0.41 and -0.64. Limitations regarding calibration and validation were lack of available local precipitation data, lack of several measured detention basin activations, and errors in sensor measurements.

The performance of the combined system agrees with the expected behavior. Based on simulations, the combination of infiltration and detention solution showed to benefit from both processes and outperformed infiltration and detention as separate stormwater measures. The event-based simulations showed that the combined system included step one and step two of the 3-step-approach of modern stormwater management. Infiltration showed to delay the start of outflow generation through retaining stormwater. When infiltration capacity exceeded, the detention basins were activated and reduced the outflow rate. Comparison of event-based simulations for dry and wet soil showed that wet soil reduced the ability of infiltration to delay the start of outflow generation. Long-term continuous simulations of the combined infiltration and detention solution resulted in an average number of 2.1 and 3.0 detention basin activations per year for simulations respectively without and with climate factor. The results indicated a well-functioning infiltration system that managed all precipitation events except 2-3 events per year. The FDCs showed that the separate process of detention was efficient in reducing the peak outflow, whereas the separate process of infiltration showed to reduce the number of hours generating outflow. The FDC for the combined system showed a reduction of peak outflow equal to 45.6% and 37.4% for respectively without and with climate factor. Further, the duration of outflow generation was reduced with 99.96% and 99.91% for simulations, respectively, without and with climate factor. Simulations with climate factor showed that combining infiltration with detention increased resilience against climate change significantly more than the performance of the separate process of detention.

A design table addressing exfiltration design flows was developed to demonstrate the applicability of combined systems. Combined systems are not yet widely implemented, especially combinations using infiltration pipes. Consequently, a design table for designing infiltration pipes has been developed. The calibrated SWMM model was used as a baseline for guideline development. The design table presents exfiltration design flow as a function of pipe length and the number of perforations on the pipe. Developers can use the created design

guideline to evaluate whether an exfiltration system is suitable for specific sites and in combination with other stormwater measures.

5.1 Further work

Further research on the combined infiltration and detention solution is still highly relevant as combined stormwater solutions are not commonly installed. Consequently, further performance evaluations will be of interest to municipalities and consultants. Additionally, it is of interest for the sake of progress in modern stormwater management research to develop stormwater management solutions with high resilience against climate change and urbanization.

Improved calibration of developed SWMM model

Calibration of the developed model can further be improved as more data becomes available. As time goes by, the time series of local precipitation measurements is increasing, in addition to several detention basin activation being monitored. Further, by reducing the errors of sensor measurements, a better calibrated model can be achieved. To avoid uncertainty in the measured outflow data, installing a sensor directly measuring the system outflow can reduce the sources of uncertainty.

Identification of outflow threshold

The threshold for system outflow causing downstream exceedance is currently unknown. In order to conclude to what degree the combined system is adequate for stormwater management from the city square in Trondheim, comparison to an outflow threshold is crucial.

Further evaluations of system performance through modelling

Based on the developed model, further system performance investigations are of interest. Topics outside of the scope of this thesis that are relevant for evaluation are the challenges regarding stormwater pollution, clogging of perforations, and sediment accumulation in the infiltration pipes. Further to evaluate what measures that can reduce these challenges. For example, evaluation of the needed frequency of maintenance in terms of flushing and street sweeping to reduce clogging and sedimentation accumulation. Further, using the model to implement an upstream LID to investigate whether the pollution load in the incoming stormwater to the combined system can be reduced, potentially further reducing the frequency of clogging and sedimentation accumulation. Finally, evaluating the optimal locations of the perforations in the pipe cross-section regarding the impact of sedimentation accumulation are of interest to obtain the most efficient combined infiltration and detention system.

References

- Beven, Keith. 1993. 'Prophecy, Reality and Uncertainty in Distributed Hydrological Modelling'. *Advances in Water Resources* 16(1):41–51. doi: 10.1016/0309-1708(93)90028-E.
- Butler, David, and John Davies. 2010. *Urban Drainage*. Third edition. Abingdon, Oxon: CRC Press.
- Chen, Yujiao, Holly W. Samuelson, and Zheming Tong. 2016. 'Integrated Design Workflow and a New Tool for Urban Rainwater Management'. *Journal of Environmental Management* 180:45–51. doi: 10.1016/j.jenvman.2016.04.059.
- Chow, Ven Te, David R. Maidment, and Larry W. Mays. 1988. *Applied Hydrology*. McGraw-Hill, Inc.
- Conley, Gary, Nicole Beck, Catherine A. Riihimaki, and Michelle Tanner. 2020. 'Quantifying Clogging Patterns of Infiltration Systems to Improve Urban Stormwater Pollution Reduction Estimates'. *Water Research X* 7:100049. doi: 10.1016/j.wroa.2020.100049.
- Damodaram, Chandana, Marcio H. Giacomoni, C. Prakash Khedun, Hillary Holmes, Andrea Ryan, William Saour, and Emily M. Zechman. 2010. 'Simulation of Combined Best Management Practices and Low Impact Development for Sustainable Stormwater Management1'. *JAWRA Journal of the American Water Resources Association* 46(5):907–18. doi: <https://doi.org/10.1111/j.1752-1688.2010.00462.x>.
- DHI Inc. 2017a. 'MIKE URBAN Model Manager'. Retrieved (<https://manuals.mikepoweredbydhi.help/2017/Cities/ModelManager.pdf>).
- DHI Inc. 2017b. 'MOUSE Runoff Reference Manual'. Retrieved (<https://manuals.mikepoweredbydhi.help/2017/Cities/MOUSERunoffReference.pdf>).
- Dongquan, Zhao, Chen Jining, Wang Haozheng, Tong Qingyuan, Cao Shangbing, and Sheng Zheng. 2009. 'GIS-Based Urban Rainfall-Runoff Modeling Using an Automatic Catchment-Discretization Approach: A Case Study in Macau'. *Environmental Earth Sciences* 59(2):465. doi: 10.1007/s12665-009-0045-1.
- Eckart, Kyle, Zach McPhee, and Tirupati Boliseti. 2017. 'Performance and Implementation of Low Impact Development – A Review'. *Science of The Total Environment* 607–608:413–32. doi: 10.1016/j.scitotenv.2017.06.254.
- Elliott, A. H., and S. A. Trowsdale. 2007. 'A Review of Models for Low Impact Urban Stormwater Drainage'. *Environmental Modelling & Software* 22(3):394–405. doi: 10.1016/j.envsoft.2005.12.005.
- ESRI. 2011. 'Arc Hydro Geoprocessing Tools - Tutorial'. Retrieved 18 March 2021 (<http://downloads.esri.com/archydro/archydro/Tutorial/Doc/Arc%20Hydro%20GP%20Tools%202.0%20-%20Tutorial.pdf>).

- Fletcher, Tim D., William Shuster, William F. Hunt, Richard Ashley, David Butler, Scott Arthur, Sam Trowsdale, Sylvie Barraud, Annette Semadeni-Davies, Jean-Luc Bertrand-Krajewski, Peter Steen Mikkelsen, Gilles Rivard, Mathias Uhl, Danielle Dagenais, and Maria Viklander. 2015. 'SUDS, LID, BMPs, WSUD and More – The Evolution and Application of Terminology Surrounding Urban Drainage'. *Urban Water Journal* 12(7):525–42. doi: 10.1080/1573062X.2014.916314.
- Hirabayashi, Yukiko, Roobavannan Mahendran, Sujan Koirala, Lisako Konoshima, Dai Yamazaki, Satoshi Watanabe, Hyungjun Kim, and Shinjiro Kanae. 2013. 'Global Flood Risk under Climate Change'. *Nature Climate Change* 3(9):816–21. doi: 10.1038/nclimate1911.
- Hosseiny, Hossein, Michael Crimmins, Virginia Smith, and Peleg Kremer. 2020. 'A Generalized Automated Framework for Urban Runoff Modeling and Its Application at a Citywide Landscape'. *Water* 12:357. doi: 10.3390/w12020357.
- Kartverket. 2021. 'Air Photo'. Retrieved (<https://norgeskart.no/#!?project=Tilgjengelighet&sok=Trondheim%20kommune&layers=1003&zoom=13&lat=7041726.55&lon=270314.59&markerLat=7041527.682287141&markerLon=270405.5590443162&panel=searchOptionsPanel>).
- Killingtveit, Ånund, Nils Roar Sælthun, Norges tekniske høgskole: Institutt for vassbygging, and Norges teknisk-naturvitenskapelige universitet: Institutt for vassbygging. 1995. *Hydrology*. Trondheim: Trondheim : Norwegian Institute of Technology. Department of Hydraulic Engineering, 1992-2003.
- Klima 2050. n.d. 'Klima2050'. *Klima2050*. Retrieved 24 May 2021 (<http://www.klima2050.no>).
- Krause, P., D. P. Boyle, and F. Bäse. 2005. 'Comparison of Different Efficiency Criteria for Hydrological Model Assessment'. *Advances in Geosciences* 5:89–97.
- Kristvik, Erle, Birgitte Gisvold Johannessen, and Tone Merete Muthanna. 2019. 'Temporal Downscaling of IDF Curves Applied to Future Performance of Local Stormwater Measures'. *Sustainability* 11(5):1231. doi: 10.3390/su11051231.
- Legates, David, and Gregory McCabe. 1999. 'Evaluating the Use Of "Goodness-of-Fit" Measures in Hydrologic and Hydroclimatic Model Validation'. *Water Resources Research* 35:233–41. doi: 10.1029/1998WR900018.
- Li, Hui, Liuqian Ding, Minglei Ren, Changzhi Li, and Hong Wang. 2017. 'Sponge City Construction in China: A Survey of the Challenges and Opportunities'. *Water* 9(9):594. doi: 10.3390/w9090594.
- Li, James, Darko Joksimovic, and John Tran. 2015. 'A Right-of-Way Stormwater Low Impact Development Practice'. *Journal of Water Management Modeling*. doi: 10.14796/JWMM.C390.
- Lim, Oseong, Young Hwan Choi, and Joong Hoon Kim. 2020. 'Storm Water Management Model Parameter Optimization in Urban Watershed Using Sewer Level Data'. Pp. 367–76 in *Advances in Hydroinformatics, Springer Water*, edited by P. Gourbesville and G. Caignaert. Singapore: Springer.

- Lindholm, Oddvar, Svein Endresen, Sveinn Thorolfsson, Sveinung Sægrov, Guttorm Jakobsen, and Lars Aaby. 2008. *Veiledning i Klimatilpasset Overvannshåndtering*. 162/2008. Hamar: Norsk Vann.
- Liu, Haiyue. 2016. 'LONG-TERM PERFORMANCE MODELLING OF ETOBICOKE EXFILTRATION SYSTEM'. MSc Thesis, Ryerson University, Toronto, Ontario, Canada.
- McBean, Edward, Gordon Huang, Aili Yang, Huiyan Cheng, Yicheng Wu, Zheng Liu, Zhineng Dai, Haiyan Fu, and Munir Bhatti. 2019. 'The Effectiveness of Exfiltration Technology to Support Sponge City Objectives'. *Water* 11:723. doi: 10.3390/w11040723.
- MFT. 2018. *Teknisk Beskrivelse Og Dokumentasjon*.
- Multiconsult. 2018. 'Infiltrasjon Av Overflatevann Fra Torggata'.
- Nash, J. E., and J. V. Sutcliffe. 1970. 'River Flow Forecasting through Conceptual Models Part I — A Discussion of Principles'. *Journal of Hydrology* 10(3):282–90. doi: 10.1016/0022-1694(70)90255-6.
- Norsk Klimaservicesenter. 2021a. 'Klimaprofil Sør-Trøndelag'. *Klimaprofil Sør-Trøndelag*. Retrieved 19 March 2021 (<https://klimaservicesenter.no/kss/klimaprofiler/sor-trondelag>).
- Norsk Klimaservicesenter. 2021b. 'Seklima. Stasjonsinformasjon'. *Seklima.Met.No*. Retrieved 2 June 2021 (<https://seklime.met.no/stations/>).
- Ødegaard, Hallvard, Oddvar Lindholm, Sveinn T. Thorolfsson, Arve Heistad, Gunnar Mosevoll, Sveinung Sægrov, and Stein Wold Østerhus. 2014. *Vann- Og Avløpsteknikk*. 2. edn. Hamar: Norsk Vann.
- Qin, Hua-peng, Zhuo-xi Li, and Guangtao Fu. 2013. 'The Effects of Low Impact Development on Urban Flooding under Different Rainfall Characteristics'. *Journal of Environmental Management* 129:577–85. doi: 10.1016/j.jenvman.2013.08.026.
- Rosa, David J., John C. Clausen, and Michael E. Dietz. 2015. 'Calibration and Verification of SWMM for Low Impact Development'. *JAWRA Journal of the American Water Resources Association* 51(3):746–57. doi: <https://doi.org/10.1111/jawr.12272>.
- Rossman, Lewis A. 2015. 'Storm Water Management Model User's Manual Version 5.1'. *US EPA Office of Research and Development*. Retrieved 18 March 2021 (https://www.epa.gov/sites/production/files/2019-02/documents/epaswmm5_1_manual_master_8-2-15.pdf).
- Rossman, Lewis A. 2017. 'Storm Water Management Model Reference Manual Volume II – Hydraulics'. *US EPA Office of Research and Development*. Retrieved (<https://nepis.epa.gov/Exe/ZyPDF.cgi?Dockkey=P100S9AS.pdf>).
- Rossman, Lewis A., and Wayne C. Huber. 2016. 'Storm Water Management Model Reference Manual Volume I – Hydrology (Revised)'. *US EPA Office of Research and*

- Development*. Retrieved
(<https://nepis.epa.gov/Exe/ZyPDF.cgi?Dockey=P100NYRA.txt>).
- Sagli, Pernille Moe. 2020. 'Infiltration Based Systems for Stormwater Management with Multipurpose Use'. Master's thesis, Norwegian University of Science and Technology, NTNU, Trondheim, Norway.
- Seametrics. n.d. 'PT12'. Retrieved 2 December 2020
(https://www.fondriest.com/pdf/seametrics_pt12_spec.pdf).
- Semadeni-Davies, Annette, Claes Hernebring, Gilbert Svensson, and Lars-Göran Gustafsson. 2008. 'The Impacts of Climate Change and Urbanisation on Drainage in Helsingborg, Sweden: Combined Sewer System'. *Journal of Hydrology* 350(1):100–113. doi: 10.1016/j.jhydrol.2007.05.028.
- Statistics Norway. 2020. 'Kommunefakta'. SSB. Retrieved 18 May 2021
(<https://www.ssb.no/kommunefakta/kommune>).
- Stovin, Virginia R., Sarah L. Moore, Matthew Wall, and Richard M. Ashley. 2012. 'The Potential to Retrofit Sustainable Drainage Systems to Address Combined Sewer Overflow Discharges in the Thames Tideway Catchment'. *Water and Environment Journal* 27(2):216–28. doi: <https://doi.org/10.1111/j.1747-6593.2012.00353.x>.
- Trondheim Municipality. n.d. 'Dekke - det store bygolvet | Torvet i Trondheim'. Retrieved 13 June 2021 (<https://torvetitrondheim.no/tema/gulv-2/>).
- Trondheim Municipality. 2015. *VA-Norm. Beregning Av Overvannsmengde. Dimensjonering Av Ledning Og Fordrøyningsvolum. Vedlegg 5*.
- Trondheim Municipality. 2020. *VA-Norm. Beregning Av Overvannsmengde. Dimensjonering Av Ledning Og Fordrøyningsvolum. Vedlegg 5*. Trondheim, Norway: Trondheim Municipality.
- Van Essen Instruments. 2016a. 'Diver Product Manual'. Retrieved 2 December 2020
(https://www.fondriest.com/pdf/van_essen_td-diver_manual.pdf).
- Van Essen Instruments. 2016b. 'Working with Divers'. Retrieved (https://aqualab.com.au/wp-content/uploads/2017/05/Diver-Office_WorkingWithDivers.pdf).
- Vartdal, Anette. 2020. *Performance of Combined Infiltration and Detention Solution with Measurement Uncertainty Analysis. Project thesis*.
- Viatronics. n.d. 'Pipeline AVSS'. Retrieved 2 December 2020
(<http://www.viatronics.fi/uploads/Brochures/Viatronics-Pipeline-SVR-AVSS.pdf>).
- Wong, T. H. F., and Malcolm L. Eadie. 2000. 'Water Sensitive Urban Design: A Paradigm Shift in Urban Design'. Retrieved 19 March 2021
(https://www.researchgate.net/profile/Tony-Wong-18/publication/267822087_WATER_SENSITIVE_URBAN_DESIGN_-_A_PARADIGM_SHIFT_IN_URBAN_DESIGN/links/55e6c3f908ae1696972e164d/WATER-SENSITIVE-URBAN-DESIGN-A-PARADIGM-SHIFT-IN-URBAN-DESIGN.pdf).

Xian, Bryant Chong Choy, Choong Wee Kang, Mahyun Ab Wahab, Mohd Remy Rozaini Mohd Arif Zainol, and Fauzi Baharudin. 2021. 'Evaluation of Low Impact Development and Best Management Practices on Peak Flow Reduction Using SWMM'. *IOP Conference Series: Earth and Environmental Science* 646(1):012045. doi: 10.1088/1755-1315/646/1/012045.

Appendices

Appendix 1: Planer overview of the pipe network underneath the city square

Appendix 2: Detailed constructional design of the combined infiltration and detention solution

Appendix 3: Sub-catchments input parameters

Appendix 4: Storage units input parameters

Appendix 5: Conduits input parameters

Appendix 6: Junctions input parameters

Appendix 7: Orifices inlet parameters

Appendix 8: Storage curve calculation - Detention basins

Appendix 9: Storage curve – detention basin

Appendix 10: Storage curve calculation - Infiltration pipes

Appendix 11: Storage curve – infiltration pipes (length = 20 m)

Appendix 12: Calibrated pump curve ($K_{sat,trench} = 70\ 012\ \text{mm/hr}$)

Appendix 13: Storage curve – Trench

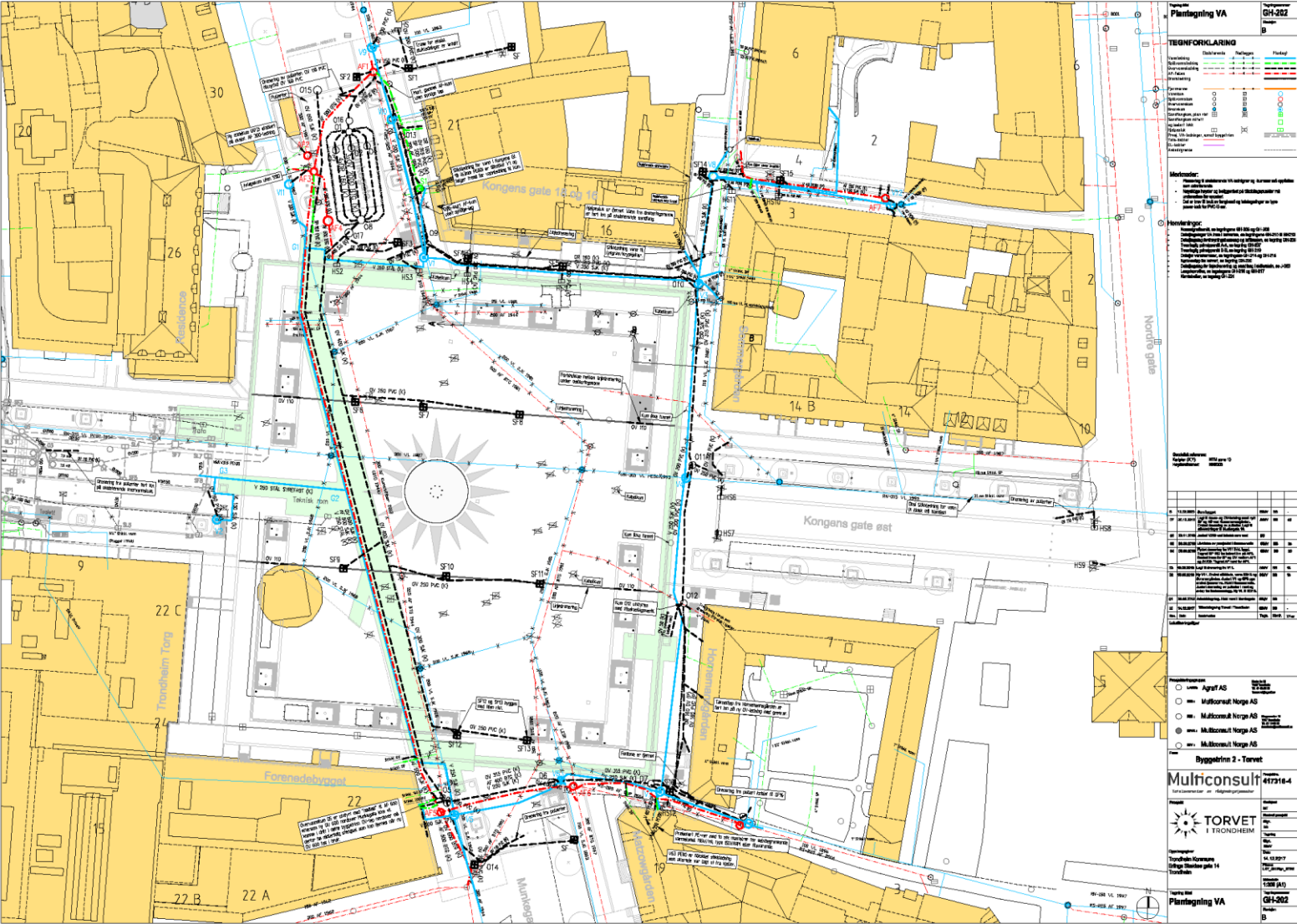
Appendix 14: Rating curve - hydraulic characteristics for swirl chamber

Appendix 15: Control rules in SWMM model

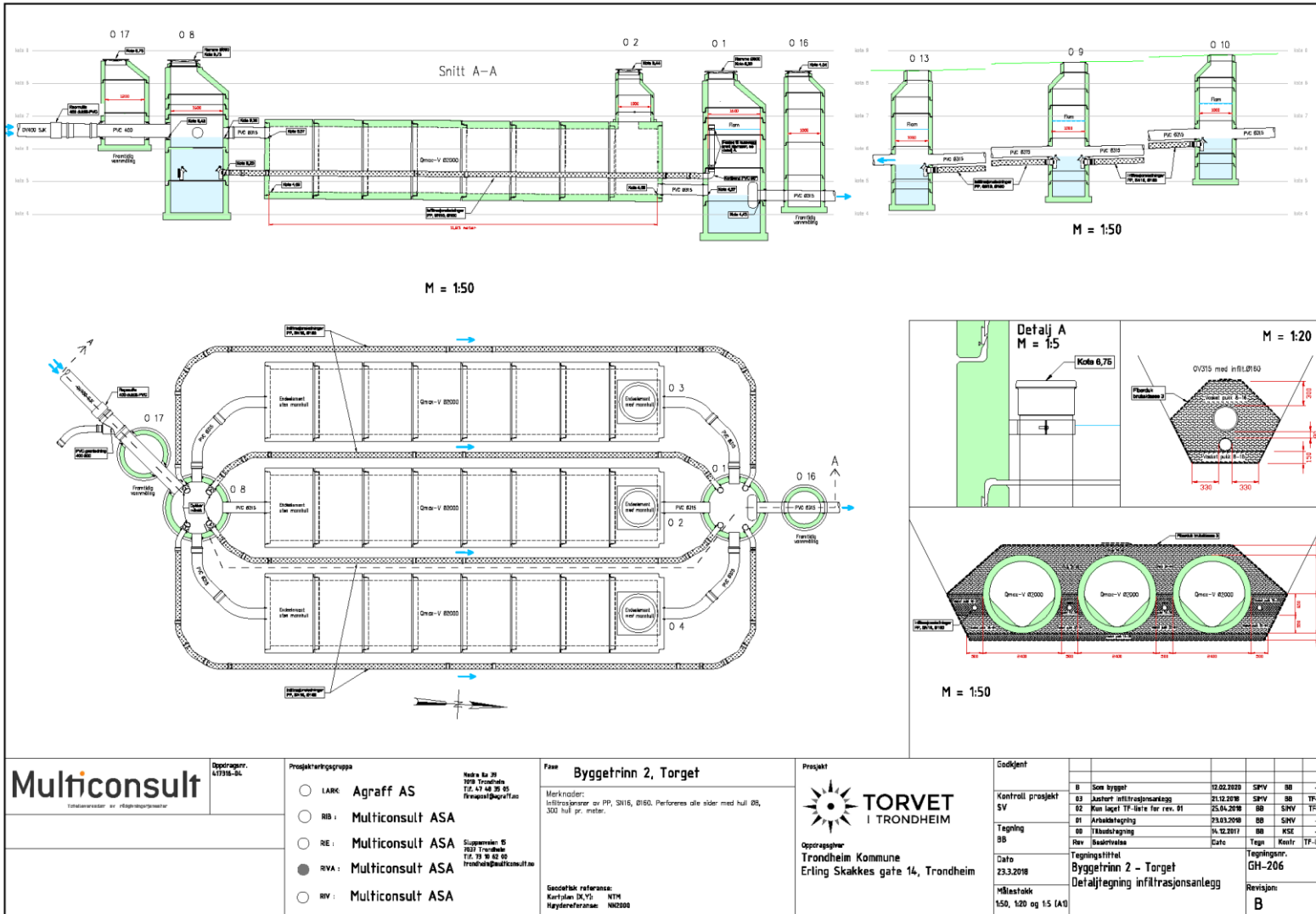
Appendix 16: Developed design precipitation events

Appendix 17: Precipitation time series from Risvollan used for long-term simulations

Appendix 1: Planer overview of the pipe network underneath the city square



Appendix 2: Detailed constructional design of the combined infiltration and detention solution



Multiconsult
Totalrådgiver og rådgiverorganisasjon

Oppdragsgiver:
437316-04

Prosjektutviklingsgruppe

- LARK : Agraff AS
- RIB : Multiconsult ASA
- RE : Multiconsult ASA
- RVA : Multiconsult ASA
- RVV : Multiconsult ASA

Medle av JH
109 Trondheim
Tlf. 37 48 26 35
E-post: jh@agruff.no

Superviser: S
R33 Trondheim
Tlf. 37 48 42 40
E-post: s@multiconsult.no

Fase: **Byggetrinn 2, Torget**

Merknader:
Infiltrasjonsanlegg av PP, SN16, Ø160. Perforerte alle sider med hull Ø8, 300 hull pr. meter.

Gesjebok referanse:
Kartfilen: IK_19 - N17M
Nyttårsreferanse: NM2000

Prosjekt

TORVET
I TRONDHEIM

Oppdragsgiver:
Trondheim Kommune
Erling Skakkes gate 14, Trondheim

Godkjent

B	Som bygget	12.02.2020	SHV	BB	-
Kontroll prosjekt					
SV	Justert infiltrasjonsanlegg	21.12.2018	SHV	BB	TF-44
	Ren layout TF-liste for rev. 01	25.04.2018	BB	SHV	TF-10
Tagning					
01	Arbeids tegning	23.03.2018	BB	SHV	-
02	Ikkearbeids tegning	14.02.2011	BB	KSE	-
Rev:	Revisjon	Dato	Tegn	Rev	TF-liste
Dato	Tegningsstiftet		Tegningsnr.		
23.3.2018	Byggetrinn 2 - Torget		GH-206		
Målestokk	Detaljtegning infiltrasjonsanlegg		Revisjon:		
1:50, 1:20 og 1:5 (A1)			B		

Appendix 3: Sub-catchments input parameters

Parameters																
Name	Outlet	Area	Width	%Slope	%Imperv	n-imperv	n-perv	Dstore-Imperv	Dstore-Perv	%Zero-Imperv	Subarea Routing	Percent Routed	Infiltration Data	Suction head	Conductivity	Initial deficit
		[ha]	[m]	[%]	[%]	[-]	[-]	[mm]	[mm]	[%]	[-]	[%]	[-]	[mm]	[mm/hr]	[mm]
1	SF3	0.1018	19.15	3.84	95	0.015	0.042	0.05	0.05	52.32	OUTLET	100	GREEN-AMPT	28.43	2.57	0.29
2	SF7	0.2336	66.44	3.52	95	0.015	0.042	0.05	0.05	52.32	OUTLET	100	GREEN-AMPT	28.43	2.57	0.29
3	SF7	0.0038	3.94	3.31	95	0.015	0.042	0.05	0.05	52.32	OUTLET	100	GREEN-AMPT	28.43	2.57	0.29
4	SF7	0.0094	5.28	3.5	95	0.015	0.042	0.05	0.05	52.32	OUTLET	100	GREEN-AMPT	28.43	2.57	0.29
5	SF10	0.2378	56.45	3.39	95	0.015	0.042	0.05	0.05	52.32	OUTLET	100	GREEN-AMPT	28.43	2.57	0.29
6	SF10	0.0129	3.33	4.35	95	0.015	0.042	0.05	0.05	52.32	OUTLET	100	GREEN-AMPT	28.43	2.57	0.29
7	SF10	0.0174	4.65	3.7	95	0.015	0.042	0.05	0.05	52.32	OUTLET	100	GREEN-AMPT	28.43	2.57	0.29
8	SF12	0.0035	3.43	4.45	95	0.015	0.042	0.05	0.05	52.32	OUTLET	100	GREEN-AMPT	28.43	2.57	0.29
9	SF13	0.0116	9.95	4.1	95	0.015	0.042	0.05	0.05	52.32	OUTLET	100	GREEN-AMPT	28.43	2.57	0.29

Source	Color code
Data from Trondheim Municipality	
DEM analysis	
Dimensions - Multiconsult	
Calibrated	
Assumed	

Appendix 4: Storage units input parameters

Parameters									
Name	Invert El.	Max. Depth	Initial Depth	Surcharge Depth	Suction head	Conductivity	Initial deficit	Functional curve	Tabular curve
	[m]	[m]	[m]	[m]	[mm]	[mm/hr]	[-]	[m ²]	[m ²]
O17	6.145	2.663	0.305	0	0	0	0	1.13	-
O8	4.05	4.682	1.15	0	0	0	0	2.01	-
Infil1	5.05	0.16	0	4	0	0	0	-	Storage_infil
Infil2	5.05	0.16	0	4	0	0	0	-	Storage_infil
Infil3	5.05	0.16	0	4	0	0	0	-	Storage_infil
Infil4	5.05	0.16	0	4	0	0	0	-	Storage_infil
Trench	4.05	2.9	0	4	223.63	3600	0.32	-	Storage_trench
Storage1	4.59	2	0	3	0	0	0	-	Storage_basin
Storage2	4.59	2	0	3	0	0	0	-	Storage_basin
Storage3	4.59	2	0	3	0	0	0	-	Storage_basin
O1	3.406	5.082	1.024	0	0	0	0	2.01	-

Source	Color code
Data from Trondheim Municipality	
DEM analysis	
Dimensions - Multiconsult	
Calibrated	
Assumed	

Appendix 5: Conduits input parameters

Parameters							
Name	Inlet Node	Outlet Node	Max. Depth	Length	Roughness	Inlet Offset	Outlet Offset
	[-]	[-]	[m]	[m]	[-]	[m]	[m]
C1	SF3	Bend1	0.25	14.42	0.01	0	0
CSF12	SF12	Bend1	0.2	1.66	0.01	0	0
C2	Bend1	SF10	0.3	34	0.01	0	0
C3	SF10	SF7	0.4	34	0.01	0	0
C4	SF7	O17	0.4	33	0.01	0	0.335
C5	SF3	O17	0.2	9.7	0.01	0	1
C6	O17	O8	0.4	1.8	0.01	0.305	2.37
C7	O8	Storage1	0.315	4	0.01	2.34	1.68
C8	O8	Storage2	0.315	3	0.01	2.34	1.68
C9	O8	Storage3	0.315	4	0.01	2.34	1.68
C10	O8	Infil1	0.16	0.5	0.01	1.15	0
C11	O8	Infil2	0.16	0.5	0.01	1.15	0
C12	O8	Infil3	0.16	0.5	0.01	1.15	0
C13	O8	Infil4	0.16	0.5	0.01	1.15	0
C14	Storage1	O1	0.315	0.5	0.01	0	1.164
C15	Storage2	O1	0.315	0.5	0.01	0	1.164
C16	Storage3	O1	0.315	0.5	0.01	0	1.164
C17	O16	OUT1	0.315	15	0.01	0	0

Source	Color code
Data from Trondheim Municipality	
DEM analysis	
Dimensions - Multiconsult	
Calibrated	
Assumed	

Appendix 6: Junctions input parameters

Parameters		
Name	Invert El.	Max. Depth
	[masl]	[m]
SF13	9	1
SF12	9	1
Bend1	8.8	1
SF10	8.1	1.5
SF7	7.3	2
SF3	7.75	1
O16	4.25	4.193

Source	Color code
Data from Trondheim Municipality	
DEM analysis	
Dimensions - Multiconsult	
Calibrated	
Assumed	

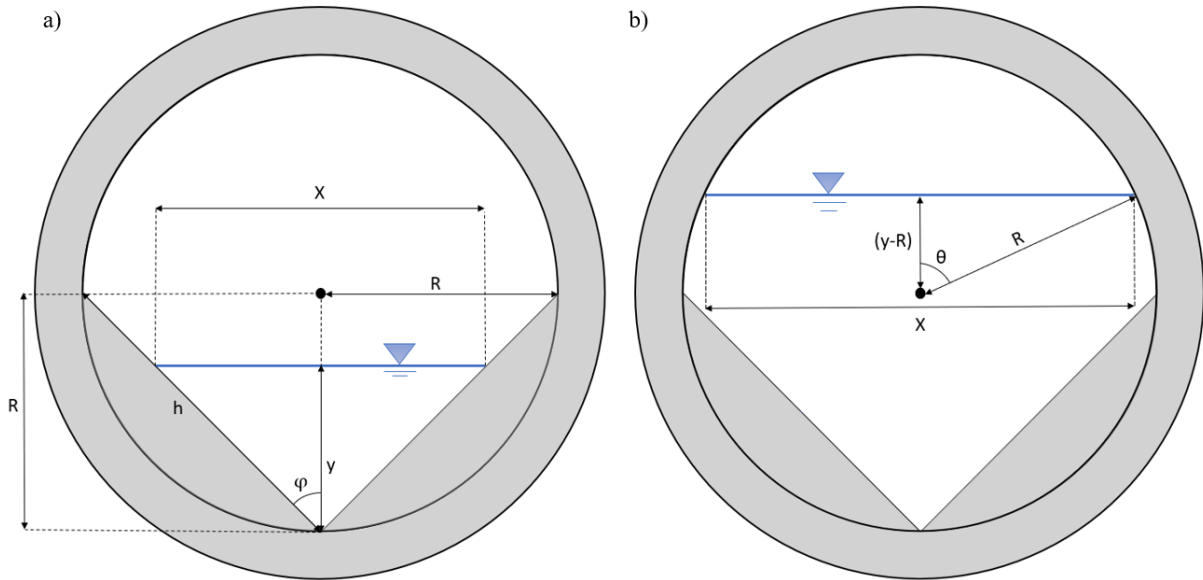
Appendix 7: Orifices inlet parameters

Parameters					
Name	Shape	Height	Inlet Offset	Discharge Coeff.	Flap Gate
Ori4	CIRCULAR	0.16	0	0.65	YES
Ori5	CIRCULAR	0.16	0	0.65	YES
Ori6	CIRCULAR	0.16	0	0.65	YES
Ori7	CIRCULAR	0.16	0	0.65	YES

Source	Color code
Data from Trondheim Municipality	
DEM analysis	
Dimensions - Multiconsult	
Calibrated	
Assumed	

Appendix 8: Storage curve calculation - Detention basins

The storage curves in SWMM relates water depth in storage unit to the corresponding water surface area. Based on the geometry of the cross-section of the detention basins, the corresponding surface areas for different water depths were calculated. The water surface areas were calculated differently for water levels below and above center of the circular cross-section. The parameters included in the calculation are visualized in the following figure for a) below center and b) above center:



For water depth below center, $y \leq R$, the angle φ and water surface width was found using the following equations:

$$h = \sqrt{R^2 + R^2}$$

$$\varphi = \sin^{-1}\left(\frac{R}{h}\right)$$

$$X = 2 * y * \tan (\varphi)$$

Where,

h = The length of the slope side (chord) [m]

R = Radius of detention basin [m]

φ = The angle between the length slope side and center line of measured water depth

y = Measured water depth [m]

X = Width of water surface [m]

For water depth above center, $y > R$, the angle θ and water surface width was found using the following equations:

$$\theta = \cos^{-1}\left(\frac{y}{R} - 1\right)$$

$$X = 2 * R * (\sin (\theta))$$

Where,

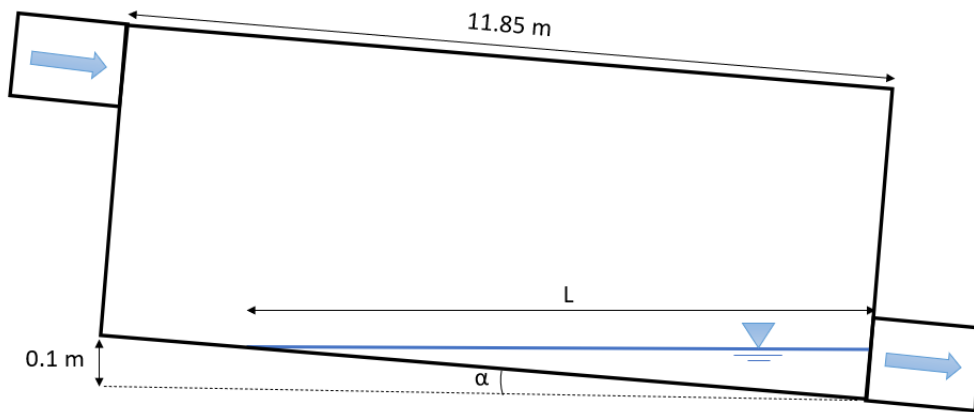
θ = Angle between the line of measured water depth and the distance to where water surface touches basin wall.

y = Measured water depth [m]

R = Radius of detention basin [m]

X = Width of water surface [m]

The slope of the detention basins was necessary to address as it effected the computation of water surface area. The elevation difference between bottom inlet and bottom outlet of the basins was 0.1 m. The sensor measuring water depth in the basin was located close to the bottom on outlet side. Consequently, the measured water depth needed to exceed 0.1 m in order for the water surface area to cover the full length of the basin. The following is an illustration of the detention basin visualizing the parameters used in calculation:



The water surface length was computed using the following set of equations:

$$\alpha = \sin^{-1}\left(\frac{0.1 \text{ m}}{11.85 \text{ m}}\right) = 0.00844 \text{ Rad}$$

$$L = \left\{ \begin{array}{ll} \frac{y}{\sin(\alpha)}, & \text{for } y \leq 0.1 \text{ m} \\ \cos(\alpha) * 11.85, & \text{for } y > 0.1 \text{ m} \end{array} \right\}$$

Where,

α = The angle due to the slope

L = Water surface length [m]

Based on the water surface widths calculated for water depths below and above center and the water surface lengths dependent on water depth, the water surface area was computed using the following equation:

$$A_{Surface} = L * X$$

Where,

L = Length of water surface [m]

X = Width of water surface [m]

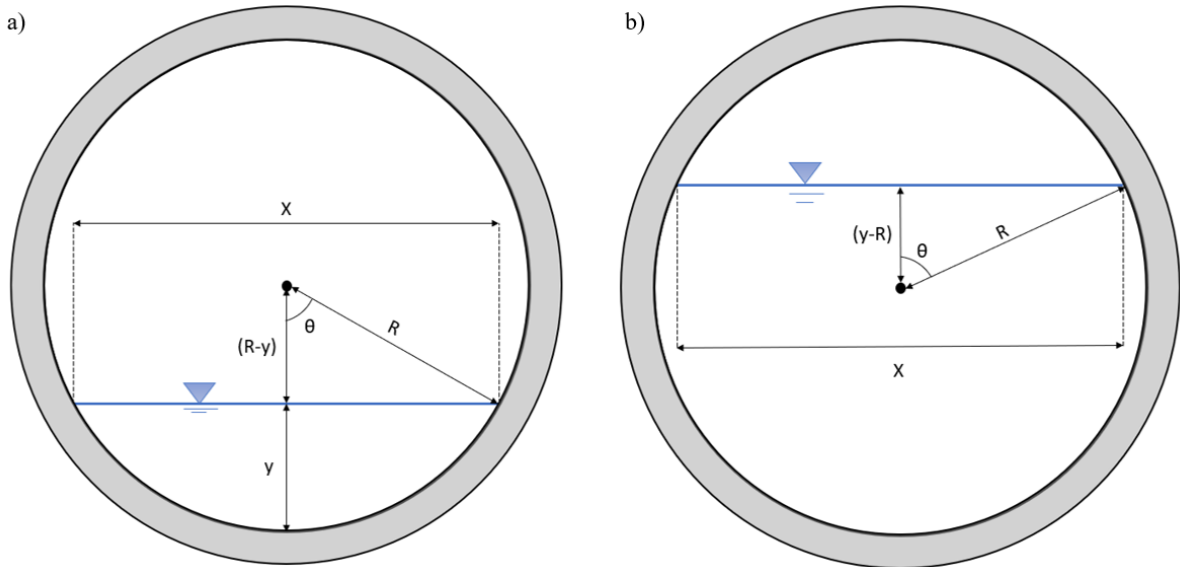
$A_{Surface}$ = Water surface area [m²]

Appendix 9: Storage curve – detention basin

Depth [m]	Surface area[m²]	Depth [m]	Surface area[m²]
0.000	0.000	1.100	23.581
0.025	0.148	1.125	23.514
0.050	0.593	1.150	23.432
0.075	1.333	1.175	23.334
0.100	2.370	1.200	23.221
0.125	2.963	1.225	23.092
0.150	3.555	1.250	22.947
0.175	4.148	1.275	22.786
0.200	4.740	1.300	22.608
0.225	5.333	1.325	22.413
0.250	5.925	1.350	22.201
0.275	6.518	1.375	21.970
0.300	7.110	1.400	21.721
0.325	7.703	1.425	21.453
0.350	8.295	1.450	21.165
0.375	8.888	1.475	20.856
0.400	9.480	1.500	20.525
0.425	10.073	1.525	20.171
0.450	10.665	1.550	19.793
0.475	11.258	1.575	19.390
0.500	11.850	1.600	18.960
0.525	12.443	1.625	18.501
0.550	13.035	1.650	18.010
0.575	13.628	1.675	17.486
0.600	14.220	1.700	16.925
0.625	14.813	1.725	16.323
0.650	15.405	1.750	15.676
0.675	15.998	1.775	14.977
0.700	16.590	1.800	14.220
0.725	17.183	1.825	13.394
0.750	17.775	1.850	12.485
0.775	18.368	1.875	11.474
0.800	18.960	1.900	10.331
0.825	19.553	1.925	9.005
0.850	20.145	1.950	7.400
0.875	20.738	1.975	5.266
0.900	21.330	2.000	0.000
0.925	21.923		
0.950	22.515		
0.975	23.108		
1.000	23.700		
1.025	23.693		
1.050	23.670		
1.075	23.633		

Appendix 10: Storage curve calculation - Infiltration pipes

The storage curves in SWMM relates water depth in storage unit to the corresponding water surface area. Based on the geometry of the cross-section of the infiltration pipes, the corresponding surface areas for different water depths were calculated. The water surface areas were calculated differently for water levels below and above center of the circular cross-section. The parameters included in the calculation are visualized in the following figure for a) below center and b) above center:



Calculation of the angle θ was calculated for different water depths together with the corresponding water width and water surface area showed in the following equations:

$$\theta = \begin{cases} \cos^{-1} \left(1 - \frac{y}{R} \right), & \text{for } y \leq R \\ \cos^{-1} \left(\frac{y}{R} - 1 \right), & \text{for } y > R \end{cases}$$

$$X = 2 * R * \sin (\theta)$$

$$A_{Surface} = X * L$$

Where,

θ = Angle between the line of measured water depth and the distance to where water surface touches pipe wall.

y = Measured water depth [m]

R = Radius of detention basin [m]

X = Width of water surface [m]

L = Length of water surface [m]

$A_{Surface}$ = Water surface area [m²]

Appendix 11: Storage curve – infiltration pipes (length = 20 m)

Depth [m]	Surface area [m²]	Depth [m]	Surface area [m²]
0.0000	0.00	0.1100	2.97
0.0025	0.79	0.1125	2.92
0.0050	1.11	0.1150	2.88
0.0075	1.35	0.1175	2.83
0.0100	1.55	0.1200	2.77
0.0125	1.72	0.1225	2.71
0.0150	1.87	0.1250	2.65
0.0175	2.00	0.1275	2.57
0.0200	2.12	0.1300	2.50
0.0225	2.22	0.1325	2.41
0.0250	2.32	0.1350	2.32
0.0275	2.41	0.1375	2.22
0.0300	2.50	0.1400	2.12
0.0325	2.57	0.1425	2.00
0.0350	2.65	0.1450	1.87
0.0375	2.71	0.1475	1.72
0.0400	2.77	0.1500	1.55
0.0425	2.83	0.1525	1.35
0.0450	2.88	0.1550	1.11
0.0475	2.92	0.1575	0.79
0.0500	2.97	0.1600	0.00
0.0525	3.00		
0.0550	3.04		
0.0575	3.07		
0.0600	3.10		
0.0625	3.12		
0.0650	3.14		
0.0675	3.16		
0.0700	3.17		
0.0725	3.19		
0.0750	3.19		
0.0775	3.20		
0.0800	3.20		
0.0825	3.20		
0.0850	3.19		
0.0875	3.19		
0.0900	3.17		
0.0925	3.16		
0.0950	3.14		
0.0975	3.12		
0.1000	3.10		
0.1025	3.07		
0.1050	3.04		
0.1075	3.00		

Appendix 12: Calibrated pump curve (Ksat,trench = 70 012 mm/hr)

Depth [m]	Surface area [m²]	Depth [m]	Surface area [m²]
0.0000	0.00	0.1100	4.40
0.0025	1.47	0.1125	4.40
0.0050	1.47	0.1150	4.40
0.0075	1.47	0.1175	4.40
0.0100	1.47	0.1200	4.40
0.0125	1.47	0.1225	4.40
0.0150	1.47	0.1250	4.40
0.0175	1.47	0.1275	4.40
0.0200	1.47	0.1300	4.40
0.0225	1.47	0.1325	4.40
0.0250	1.47	0.1350	4.40
0.0275	1.47	0.1375	4.40
0.0300	1.47	0.1400	4.40
0.0325	1.47	0.1425	4.40
0.0350	1.47	0.1450	4.40
0.0375	1.47	0.1475	4.40
0.0400	1.47	0.1500	4.40
0.0425	1.47	0.1525	4.40
0.0450	1.47	0.1550	4.40
0.0475	1.47	0.1575	4.40
0.0500	1.47	0.1600	5.87
0.0525	1.47		
0.0550	1.47		
0.0575	1.47		
0.0600	1.47		
0.0625	1.47		
0.0650	1.47		
0.0675	1.47		
0.0700	1.47		
0.0725	1.47		
0.0750	1.47		
0.0775	1.47		
0.0800	4.40		
0.0825	4.40		
0.0850	4.40		
0.0875	4.40		
0.0900	4.40		
0.0925	4.40		
0.0950	4.40		
0.0975	4.40		
0.1000	4.40		
0.1025	4.40		
0.1050	4.40		
0.1075	4.40		

Appendix 13: Storage curve – Trench

Depth [m]	Surface area [m ²]
0.0	59.43
0.1	60.26
0.2	61.09
0.3	58.80
0.4	56.51
0.5	54.22
0.6	51.93
0.7	49.63
0.8	47.34
0.9	45.05
1.0	42.76
1.1	40.47
1.2	38.18
1.3	35.89
1.4	33.60
1.5	35.31
1.6	37.02
1.7	38.73
1.8	40.43
1.9	42.14
2.0	43.85
2.1	45.56
2.2	47.27
2.3	48.98
2.4	50.69
2.5	52.39
2.6	54.45
2.7	52.23
2.8	50.02
2.9	47.81

Appendix 14: Rating curve - hydraulic characteristics for swirl chamber

y [m]	Q [l/s]	y [m]	Q [l/s]	y [m]	Q [l/s]
0.000	0.000	0.306	13.120	0.662	13.950
0.103	2.260	0.325	13.160	0.700	14.240
0.109	3.930	0.344	13.250	0.775	14.910
0.115	5.040	0.363	13.340	0.850	15.630
0.127	6.630	0.381	13.350	1.038	17.360
0.137	7.710	0.400	13.350	1.225	18.960
0.156	9.130	0.419	13.350	1.412	20.430
0.175	10.260	0.438	13.350	1.600	21.790
0.194	11.130	0.456	13.350	2.400	26.720
0.213	11.760	0.475	13.350	3.288	31.160
0.231	12.200	0.512	13.350	4.787	37.330
0.250	12.530	0.550	13.360	6.662	43.760
0.269	12.820	0.587	13.480	7.600	46.620
0.288	13.050	0.625	13.690		

Appendix 15: Control rules in SWMM model

Control rule controlling operation of the pumps:

RULE PUMPS

IF NODE Trench DEPTH \geq NODE O8 DEPTH

THEN PUMP P1 STATUS = OFF

AND PUMP P2 STATUS = OFF

AND PUMP P3 STATUS = OFF

AND PUMP P4 STATUS = OFF

ELSE PUMP P1 STATUS = ON

AND PUMP P2 STATUS = ON

AND PUMP P3 STATUS = ON

AND PUMP P4 STATUS = ON

Control rule controlling operation of the orifices from the infiltration pipes:

RULE INFILS

IF NODE O8 DEPTH $>$ 2.7

THEN ORIFICE Ori4 SETTING = 1

AND ORIFICE Ori5 SETTING = 1

AND ORIFICE Ori6 SETTING = 1

AND ORIFICE Ori7 SETTING = 1

ELSE ORIFICE Ori4 SETTING = 0

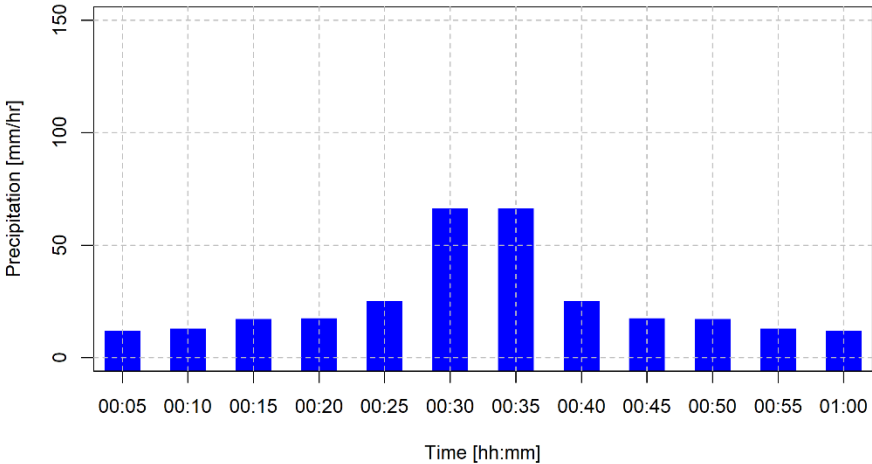
AND ORIFICE Ori5 SETTING = 0

AND ORIFICE Ori6 SETTING = 0

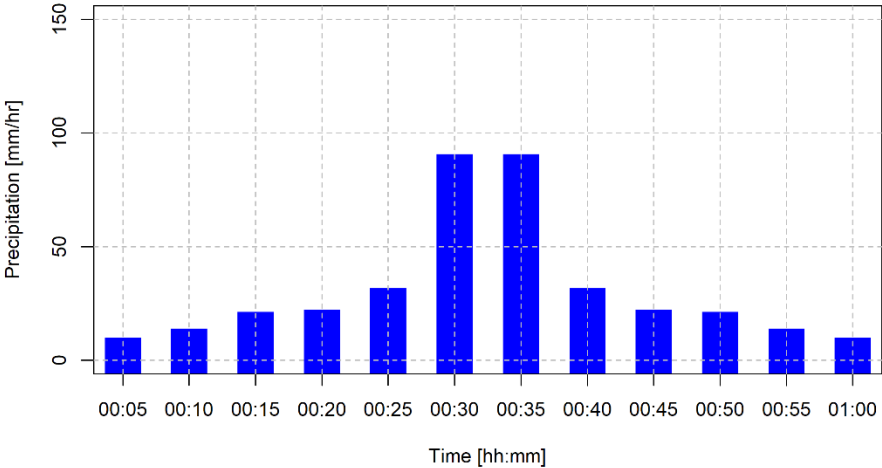
AND ORIFICE Ori7 SETTING = 0

Appendix 16: Developed design precipitation events

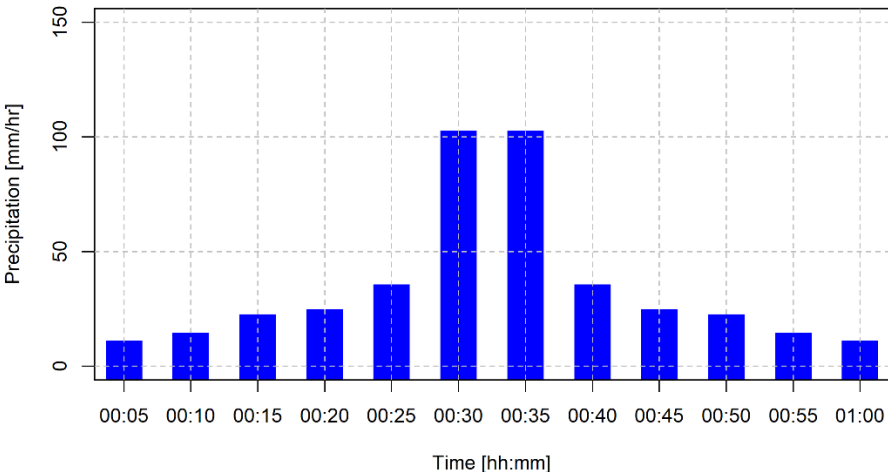
Design event 20-year return period



Design event 100-year return period

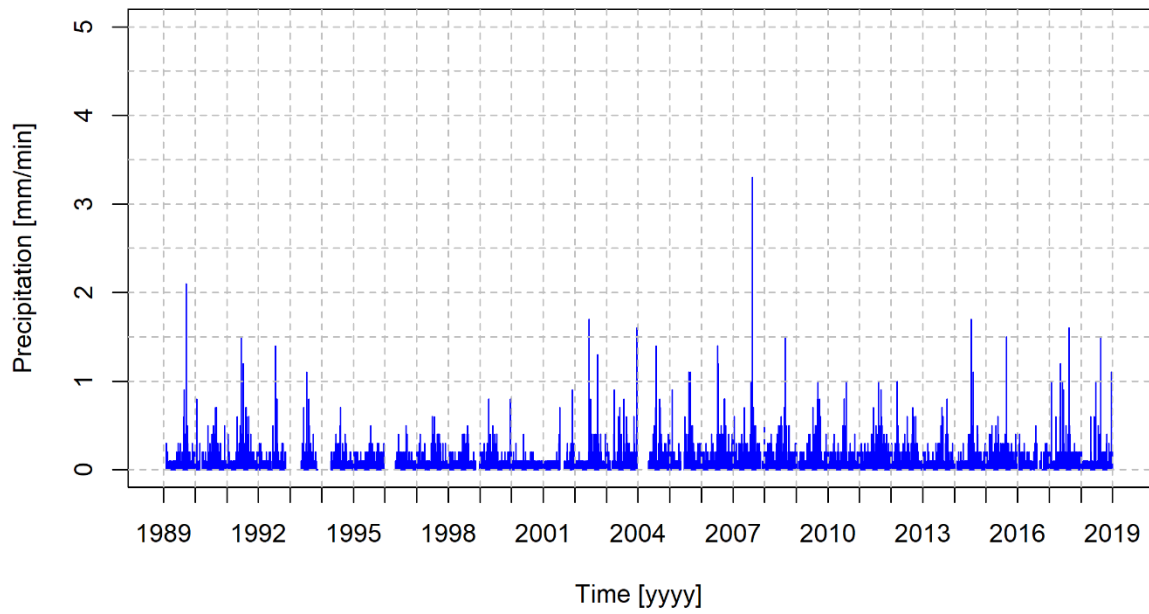


Design event 200-year return period



Appendix 17: Precipitation time series from Risvollan used for long-term simulations

Precipitation Risvollan 1989-2019



Precipitation Risvollan 1989-2019 with climate factor 1.4

